Polarized light vision in the eye of the desert locust, *Schistocerca gregaria*

- An electrophysiological and histological approach -

Polarisationssehen im Auge der Wüstenheuschrecke, *Schistocerca gregaria*

- Ein elektrophysiologischer und histologischer Ansatz -

Dissertation zur Erlangung des
Doktorgrades der Naturwissenschaften
(Dr. rer. nat.)

dem Fachbereich Biologie
der Philipps-Universität Marburg
vorgelegt von

Fabian Schmeling
aus Berlin
Marburg/Lahn 2015

Polarized light vision in the eye of the desert locust, *Schistocerca gregaria*

- An electrophysiological and histological approach -

Polarisationssehen im Auge der Wüstenheuschrecke, *Schistocerca gregaria*

- Ein elektrophysiologischer und histologischer Ansatz -

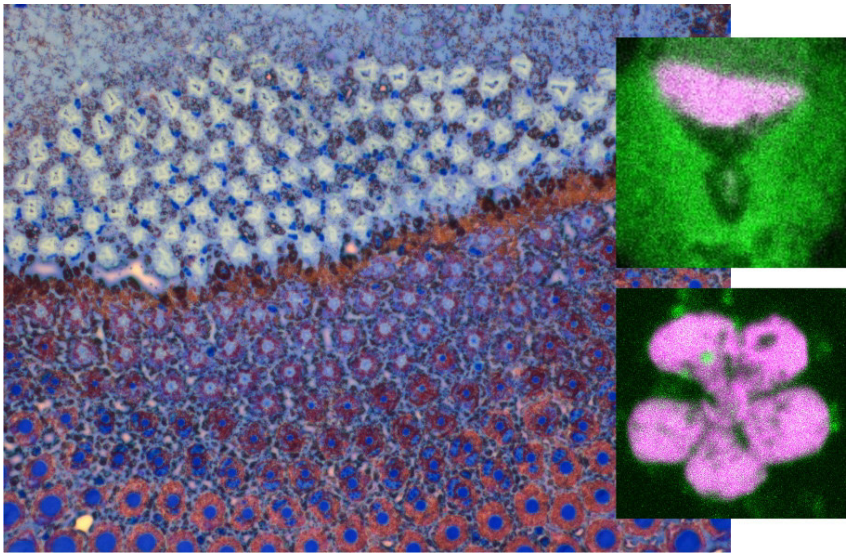

Dissertation zur Erlangung des
Doktorgrades der Naturwissenschaften
(Dr. rer. nat.)

dem Fachbereich Biologie
der Philipps-Universität Marburg
vorgelegt von

Fabian Schmeling
aus Berlin
Marburg/Lahn 2015

Vom Fachbereich Biologie der Philipps-Universität Marburg als Dissertation angenommen am 24.09.2015

Erstgutachter: Prof. Dr. Uwe Homberg
Zweitgutachter: Prof. Dr. Monika Hassel

Tag der Disputation 25.09.2015

Erklärung: Eigene Beiträge und veröffentlichte Teile der Arbeit

Laut §8, Absatz 3 der Promotionsordnung der Philipps-Universität Marburg (Fassung vom 28.4.1993) müssen bei den Teilen der Dissertation, die aus gemeinsamer Forschungsarbeit entstanden sind, „die individuellen Leistungen des Doktoranden deutlich abgrenzbar und bewertbar sein." Diese Leistungen sollen im Folgenden erläutert werden.

allgemeiner Versuchsaufbau:

- Aufbau einer elektrophysiologischen Versuchsapparatur (Beschaffung, Installation und Inbetriebnahme der notwendigen Geräte), in Zusammenarbeit mit den feinmechanischen und elektronischen Werkstätten der Philipps-Universität Marburg.
- Etablierung einer elektrophysiologischen Standardmethode zur Ableitung an Fotorezeptoren von Insekten.
- Etablierung einer histologischen Färbemethode für Fotorezeptorprojektionen (Massenfärbungen).

Kapitel 1:

Opsin expression, physiological characterization and identification of photoreceptor cells in the dorsal rim area and main retina of the desert locust, *Schistocerca gregaria*

- Durchführung aller elektrophysiologischen Experimente (Vorpräparation der Tiere, Ableitungen, Injektionen des Farbstoffes, Nachpräparation zur Entfernung der optischen Loben aus der Kopfkapsel und erste Fixierung des Präparats).
- Durchführung der folgenden histologischen Bearbeitung (bei ca. 70% aller Präparate).
- Scannen der Präparate am konfokalen Laserscanmikroskop (bei ca. 70% aller Präparate).
- Bearbeitung und Auswertung aller Daten, mit Ausnahme der Berechnung der visual-pigment absorbance templates.
- Anfertigung aller Abbildungen und Tabellen, mit Ausnahme des Abschnitts zur *in-situ* Hybridisierung.
- Anfertigung des Manuskripts, mit Ausnahme des Methoden- und Ergebnisteils für die *in-situ* Hybridisierung, in Zusammenarbeit (Korrektur) mit Dr. Michiyo Kinoshita, Prof. Dr. Kentaro Arikawa und Prof. Dr. Uwe Homberg.
- Das Kapitel wurde in seiner hier vorliegenden Form im Journal of Experimental Biology veröffentlicht. (Schmeling F, Tegtmeier J, Kinoshita M, Homberg U [2015] Photoreceptor projections and receptive fields in the dorsal rim area and main retina of the locust eye. J. comp. Physiol. A 201:427-440)

Kapitel 2:

Photoreceptor projections and receptive fields in the dorsal rim area and main retina of the locust eye

- Durchführung aller elektrophysiologischen Experimente (Vorpräparation der Tiere, Ableitungen, Injektionen des Farbstoffes, Nachpräparation zur Entfernung der optischen Loben aus der Kopfkapsel und erste Fixierung des Präparats).
- Durchführung der histologischen Bearbeitungen (bei ca. 70% aller Präparate).
- Scannen der Präparate am konfokalen Laserscanmikroskop (bei ca. 80% aller Präparate).
- Anfertigung aller Abbildungen und Tabellen.
- Anfertigung des Manuskripts in Zusammenarbeit (Korrektur) mit Dr. Michiyo Kinoshita und Prof. Dr. Uwe Homberg.
- Das Kapitel wurde in seiner hier vorliegenden Form im Journal of Comparative Physiology A veröffentlicht. (Schmeling F, Wakakuwa M, Tegtmeier J, Kinoshita M, Bockhorst T, Arikawa K, Homberg U [2014] Opsin expression, physiological characterization and identification of photoreceptor cells in the dorsal rim area and main retina of the desert locust, *Schistocerca gregaria*. J. exp. Biol. 217:3557-3568)

DANKSAGUNG

Als allererstes möchte ich Prof. Dr. Uwe Homberg danken, der mir die Möglichkeit gab, an diesem interessanten Projekt zu arbeiten und mich auf dem gesamten Weg begleitete.

Liebe Menschen wie Martina Kern, Martin Kollmann, Evelyn Rieber, Jerome Beetz, Joss von Hadeln, Anna Reifenrath, Dr. Ronny Rosner, Dr. Keram Pfeiffer und Dr. Stanley Heinze haben mir bei der praktischen Laborarbeit und auch später beim Verfassen meiner Dissertationsschrift mit Rat und Tat geholfen. Auch dafür bin ich sehr dankbar. Ihnen und allen anderen Mitgliedern der Neurobio-Arbeitsgruppen in Marburg außerdem vielen Dank für das angenehme Arbeitsklima.

Vielen Dank auch an Dr. Michiyo Kinoshita, die mich nach Japan einlud und sich dort viel Zeit nahm, mich in die grundlegenden Techniken der Elektrophysiologie am Insektenauge einzuarbeiten. Dort durfte ich in der Arbeitsgruppe von Prof. Dr. Kentaro Arikawa die Bekanntschaft mit Yuri Ogawa und Hironobu Uchiyama machen. Ihnen beiden will ich für regelmäßige Unterstützung im Labor danken und auch für die tolle Zeit außerhalb des Labors.

Last but not least möchte ich von ganzem Herzen meinen Eltern danken. Sie haben mir das Biologiestudium ermöglicht und waren auch in schwierigen Zeiten immer für mich da.

TABLE OF CONTENTS

ZUSAMMENFASSUNG

Verschiedene Arten von Insekten sind in der Lage Muster von polarisiertem Licht am Himmel zu erkennen und diese als Kompass zur räumlichen Orientierung zu nutzen. Bei Insekten wie der Wüstenheuschrecke *Schistocerca gregaria* wird das polarisierte Himmelsmuster über eine spezialisierte Region des Komplexauges, der dorsalen Randregion (dorsal rim area: DRA), detektiert. Dort befindet sich ein bestimmter Typ von Fotorezeptoren, der morphologisch und physiologisch spezialisiert ist, polarisiertes Licht zu detektieren. Obwohl die Sehbahn des polarisierten Lichts im Heuschreckengehirn bereits intensiv untersucht wurde, ist nur wenig über ihren rezeptiven Eingang, die DRA-Rezeptoren bekannt. Ziel dieser Arbeit war es die Physiologie und die Projektionsmuster dieser Rezeptoren zu untersuchen und neue Erkenntnisse über die ersten Verrechnungsschritte polarisierten Lichts zu erhalten. Zu diesem Zweck wurden elektrophysiologische und immunhistologische Methoden angewendet. *Schistocerca gregaria* tritt in zwei Erscheinungsformen (Phasen) auf, die sich morphologisch, physiologisch und in ihrem Verhalten stark unterscheiden. Zur Aufdeckung möglicher Unterschiede zwischen diesen Phasen, wurden sowohl gregäre als auch solitäre Tiere untersucht.

In Kapitel I der vorliegenden Arbeit wurde mit Glasmikroelektroden in einzelne Fotorezeptorzellen der DRA und des hauptsächlichen Komplexauges eingestochen, um Rezeptorantworten auf verschiedene Lichtreize aufzuzeichnen. Durch Lichtreize mit unterschiedlichen, Wellenlängen, Intensitäten und *E*-Vektororientierungen, wurden die spektrale Sensitivität, die absolute Lichtsensitivität und die Polarisationssensitivität dieser Zellen bestimmt. Tracer-Injektionen direkt nach der Ableitung markierten die Position der Zelle in der Retina der DRA oder des Hauptauges. Einen Überblick über die allgemeine spektrale Sensitivität in DRA, der dorsalen und ventralen Hälfte des Hauptauges gaben ERG Ableitungen. Diese Messungen wurden durchgeführt mit Silberdrähten, eingeführt in die jeweilige Augenregion. Alle Fotorezeptoren in der DRA reagierten am sensitivsten auf blaues Licht, während im Hauptauge unterschiedliche spektrale Rezeptortypen gefunden wurden. Dort lag die höchste Sensitivität entweder im UV, blauen oder im grünen Spektrum. Insbesondere die Rezeptoren die primär auf blaues Licht reagierten, variierten in ihrer sekundären Sensitivität zu längeren Wellenlängen. *In-situ* Hybridisierungsexperimente legen nahe, dass dies durch Koexpression von blau und grün absorbierenden Opsinen in fünf der insgesamt acht Fotorezeptoren eines Ommatidiums verursacht wird. Die verbleibenden drei Rezeptorzellen beinhalteten jeweils nur ein Sehpigment. Mit den vorliegenden Daten wurde somit die Existenz von fünf Rezeptortypen im Heuschreckenauge bestätigt: Blaurezeptoren in der DRA, UV, Blau- und Grünrezeptoren, sowie Blau/Grün-Breitbandrezeptoren im Hauptauge. Diese Typen wurden sowohl bei gregären, als auch bei solitären Tieren gefunden. Obwohl diese Rezeptortypen gleichmäßig im Hauptauge verteilt sind, konnte mit ERG-Ableitungen gezeigt werden, dass eine Verschiebung der spektralen Sensitivität hin zu längeren Wellenlängen von dorsal zu ventral vorhanden ist. Diese Verschiebung trat vor allem bei solitären Tieren auf und lässt auf eine unterschiedliche Spezialisierung des dorsalen und ventralen Auges schließen. DRA und Hauptauge unterschieden sich in der Form ihrer Rezeptorkennlinien und ihrer absoluten

Lichtsensitivität. Kennlinien der DRA-Rezeptoren hatten eine signifikant höhere Steigung als die des Hauptauges. Dies könnte bedeuten, dass sie weniger geeignet sind, um Helligkeitsunterschiede zu erkennen. DRA-Rezeptoren benötigten stärkere Lichtreize, um physiologische Antworten zu zeigen, als Rezeptoren im Hauptauge. Das suggeriert, dass sie im Vergleich weniger lichtsensitiv sind. Wenn allerdings die großen rezeptiven Felder der DRA-Rezeptoren berücksichtig werden (siehe Kapitel II), dann mag das unter natürlichen Bedingungen unter freiem Himmel nicht zutreffen. Dort sammeln DRA-Rezeptoren wahrscheinlich bedeutend mehr Photonen, als unter Laborbedingungen, wodurch ihre absolute Lichtsensitivität erhöht wird. Die Polarisationssensitivität (PS) ist hoch in der DRA (PS gewöhnlich >4). Alle acht Rezeptoren eines DRA-Ommatidiums scheinen zum Polarisationssehen beizutragen. Die Polarisationssensitivität im Hauptauge liegt unterhalb einer Schwelle (PS <4) die als notwendig für Polarisationssehen betrachtet wird. Durch Markierung der abgeleiteten Zellen mit einem Tracer, wurde ihre Identität innerhalb des entsprechenden Ommatidiums bestimmt (Rezeptoren wurden mit R1-8 nummeriert).

In Kapitel II der vorliegenden Arbeit wurden anterograde und retrograde Massenzellfärbungen, wie auch weitere Einzelzellableitungen durchgeführt, um Projektionsmuster der Fotorezeptoraxone auf die nachgeschalteten Neuropile Lamina und Medulla zu bestimmen. Um den physiologischen Datensatz zu vervollständigen, wurden die rezeptiven Felder einzelner Rezeptoren in der DRA und im Hauptauge gemessen. Dies geschah durch Bewegung des Perimeters und somit durch Veränderung des Einfallwinkels des Lichtreizes, während von der jeweiligen Zelle elektrophysiologisch abgeleitet wurde. Massen- und Einzelzellfärbungen bestätigten, dass die Position eines DRA-Rezeptors in der DRA-Retina mit der Position der Axonterminierungen in den dorsalen Randregionen von Lamina und Medulla (DRLA, DRME) korreliert. Dieses als Retinotopie bezeichnete Prinzip wurde bereits für das Hauptauge bestätigt. Retinotopie in DRA, DRLA und DRME ist überraschend, da bisher keinerlei strukturelle Organisation in DRLA und DRME bestätigt werden konnte. Das Chiasma zwischen Lamina und Medulla invertiert zwar den Verlauf der Axonbündel, zerstört aber die retinotope Ordnung nicht. Jedes Ommatidium beinhaltet sieben Rezeptoren, welche nach den Ergebnissen aus Kapitel I als R1-6 und R8 identifiziert wurden, deren kurze Axone in der DRLA terminieren. Das längere Axon von Rezeptor R7 läuft durch die DRLA und terminiert in der DRME. Die Morphologie dieser kurzen und langen visuellen Fasern unterscheidet sich stark. Bis hin zur DRLA sind lange visuelle Fasern deutlich dicker im Durchmesser, als kurze Fasern. Innerhalb der DRLA sind sie mit kurzen feinen Verästelungen bedeckt, was Informationsaustausch mit anderen Neuronen nahe legt. Kurze visuelle Fasern dringen tief in die DRLA ein, reichen aber scheinbar nicht durch ihre volle Tiefe. Verzweigungen ihrer Endigungen treten ausschließlich in der inneren proximalen Hälfte des Neuropils auf, haben unterschiedliche Längen und kontaktieren eventuell andere Neurone über größere Distanz. Nach Verlassen der DRLA nimmt der Durchmesser von langen visuellen Fasern abrupt ab und ist vergleichbar mit dem Durchmesser der kurzen Fasern. Das hat wahrscheinlich Einfluss auf die Weiterleitungsgeschwindigkeit von durch Lichtreiz verursachten Depolarisationen. Die Endigungen der langen Fasern in der DRME zeigen Ähnlichkeiten zu denen der kurzen Fasern in der DRLA. Auch im Hauptauge hat ausschließlich R7 eine lange Faser als Axon. Die Axone aller anderen Rezeptoren terminieren bereits in der Lamina. Wenn Blau/Grün-Breitbandrezeptoren markiert

wurden, waren immer R2-3, R5-6 und R8 gemeinsam angefärbt. Dies könnte durch elektrischer Kopplung erklärt werden. Diese Kopplung lässt zusammen mit der Breitbandsensitivität dieser Rezeptoren eine erhöhte absolute Lichtsensitivität vermuten und auf eine Rolle beim Sehen unter schwachen Lichtbedingungen schließen. Die visuellen Felder von DRA-Rezeptoren sind groß (durchschnittlicher Akzeptanzwinkel: 33°) und decken zusammen fast die gesamte visuelle Hemisphäre oberhalb des Horizontes der Tiere ab. Vorherige Untersuchungen konnten zeigen, dass die Polarisationssehbahn auch auf polarisiertes Licht reagiert, das von unterhalb dieses Horizonts präsentiert wurde. Als logische Schlussfolgerung muss man davon ausgehen, dass auch das Hauptauge am Polarisationssehen beteiligt ist. Rezeptoren im Hauptauge haben deutlich kleinere rezeptive Felder (durchschnittlicher Akzeptanzwinkel: 2°), was notwendig für eine höhere räumliche Auflösung ist.

SUMMARY

Several insect species are able to detect the pattern of polarized light in the sky and use it as a compass cue for spatial orientation. In insects like the desert locust *Schistocerca gregaria* the sky polarization pattern is detected by a specific area of the compound eye, the dorsal rim area (DRA). A certain type of photoreceptor cells, which is morphologically and physiologically specialized to detect polarized light, is located here. Although the polarization vision pathway in the locust brain has been investigated intensively, little is known about its receptive site, the DRA photoreceptors. The scope of this work was to examine the physiology and projection patterns of these receptors and to illuminate the first processing steps of polarized light vision. To do so electrophysiological and immunohistological methods were applied. *Schistocerca gregaria* occurs in two forms of appearance (phases), which differ strongly in morphology, physiology and behavior. To clarify possible differences between those phases, gregarious and solitarious animals were examined.

In chapter I of this work, single photoreceptor cells in the DRA and the main eye of the locust were penetrated with glass microelectrodes to record receptor responses to different light stimuli. By applying light stimuli of different wavelengths, intensities and *E*-vector orientations spectral sensitivity, absolute sensitivity and polarization sensitivity of these cells was determined. A tracer injection immediately after recording marked the position of the cell in the retina of the DRA and the main eye. An overview of overall spectral sensitivity in the DRA and the dorsal and ventral half of the main eye is contributed by ERG recordings using silver wires inserted in the respective eye region. All photoreceptors of the DRA are most sensitive to blue light. In the main eye, receptor peak sensitivities were either in the UV, blue or green spectrum. Often the blue peaking receptors showed a secondary sensitivity to green light. *In-situ* hybridization experiments suggest that this is caused by coexpression of blue and green sensitive opsins in five out of eight photoreceptors per ommatidium. Two of the remaining three receptor cells contained only green absorbing pigments and one either UV or blue absorbing pigments. So, the existence of five receptor types in the desert locust eye was confirmed: blue receptors in the DRA, and UV, blue, green, and blue/green broadband receptors in the main eye. These types occurred in gregarious as well as in solitarious animals. Even though these receptor types were distributed evenly in the main eye, ERG recordings measured a shift in spectral sensitivity toward longer wavelengths from dorsal to ventral. This shift occurred predominantly in solitarious locusts, suggesting different adaptations of the dorsal and ventral main eye. Photoreceptors of DRA and the main eye differed in the shape of their intensity response curves and in their absolute sensitivity. Response curves of absolute sensitivity in DRA receptors were significantly steeper than those in main eye receptors and might be less suited to detect differences in brightness levels. Furthermore, DRA receptors seemed to have a higher threshold to respond to light stimuli than receptors of the main eye, implying that they have a lower absolute sensitivity. However, when considering the wide receptive fields of DRA receptors (see chapter II), this might not be the case under the free sky. Under this free sky conditions, DRA receptors can be considered to collect more photons than under laboratory conditions. This would enhance their absolute sensitivity. Polarization sensitivity (PS) is high (PS values usually >4) in the DRA and all eight receptors of an ommatidium seem

to contribute to polarization vision. In contrast, polarization sensitivity in the main eye is below a level that is considered to be sufficient for polarization vision (PS <4), but the results in chapter II actually imply the contribution of the main eye to polarization vision. By marking the recorded cells with tracer, their identity within an ommatidium was clarified (receptors were numbered as R1-8), and it was confirmed that all DRA receptors have similar characteristics considering spectral, absolute and polarization sensitivity.

In chapter II of this work anterograde and retrograde mass stainings, as well as further single cell stainings revealed certain projection patterns of photoreceptor axons into the underlying lamina and medulla of the optic lobe. To complement the set of physiological data receptive fields of single receptors in DRA and the main eye were measured by changing the angle of the light stimulus while recording from the cell. Mass and single cell stainings confirmed that the position of a DRA receptor in the DRA retina corresponds to the location of its axonal target in the lamina and medulla. Retinotopic projections, previously demonstrated for the main eye, are also present in DRA receptors terminating in dorsal rims of the lamina and medulla (DRLA, DRME). This was surprising, because hitherto no structural organization had been reported for these neuropils. The chiasma of fiber projections between the DRLA and DRME inverts this pattern but maintains it. In each DRA ommatidium the photoreceptors identified as R1-6 and R8 in chapter I show axonal projections which terminate in the DRLA. The axon of receptor R7 projects through the DRLA and continues to terminate in the DRME. The morphology of these short and long visual fibers differs considerably. Before reaching the DRLA, long visual fibers are considerably larger in diameter than short visual fibers. Inside the DRLA they are covered with short side branches indicating the exchange of information with other neurons. Short visual fibers reach deeply into the DRLA but apparently never through its full depth. Arborizations of their terminations occur exclusively in the inner proximal half of the neuropil with various lengths, perhaps contacting neurons over a greater distance. After leaving the DRLA and proceeding to the DRME, long visual fibers abruptly decrease in diameter to a similar level as short visual fibers. This has likely consequences for conduction velocity of light induced depolarizations within the neuron. Termination sites of the long visual fibers in the DRME appear similar to those of short visual fibers in the DRLA. In the main eye, as in the DRA, only R7 is a long visual fiber. All other receptors have short visual fibers terminating in the lamina. When marking blue/green broadband receptors, R2-3, R5-6 and R8 were always stained together, possibly due to electrical coupling. This coupling in combination with the broad spectral sensitivity of these receptors might enhance absolute sensitivity of these receptors, suggesting a role in vision under low light conditions. Visual fields of DRA receptors are large (average acceptance angle 33°), altogether covering almost the whole visual hemisphere above the horizon of the individual locust. Other investigations reported responses to polarized light presented from below this horizon. It must be assumed that the main eye contribute to polarization vision as well. Main eye receptors have much smaller receptive fields (average acceptance angle 2°), which are more typical for insect eyes and are essential for a high spatial resolution of the eye.

SUMMARY

GENERAL INTRODUCTION

ORIENTATION AND COMPASS CUES

In the animal kingdom, a large variety of strategies for spatial orientation has evolved. One of the more complex navigational mechanisms is the ability to align the direction of movement in a certain vector to a specific cue. This is the prerequisite for behavior like compass orientation and path integration (Collett and Collett 2000). Such cues can be environmental landmarks, wind, the earth's magnetic field, the light gradients in the sky, the position of the stars, the sun, or the moon. Many insect species are known to use a selection of these cues (reviews: Collett 1996, Giurfa and Capaldi 1999, Frost and Mouritsen 2006, Merlin et al. 2012). However, insects which are known to use the suns position as navigational cue, had been proven to show elaborate orientation behavior, even if the sun is out of sight. The only prerequisite was that a small patch of blue sky was still visible (Santschi 1923, von Frisch 1949), and von Frisch (1949) concluded that those insects are able to navigate by using a specific celestial light pattern: the pattern of polarized light.

POLARIZED LIGHT OF THE SKY AS A CELESTIAL COMPASS

In addition to intensity (photon number) and color (wavelength of photons) a ray of light is also characterized by its polarization (oscillation plane of the photons electric field vector; *E*-vector). Direct sunlight contains *E*-vectors which are oscillating in all possible orientations perpendicular to the direction of light propagation. When entering the atmosphere, sun light is scattered by particles in the air. This results in partially linear polarized light in which some *E*-vectors occur more often than others. The degree of polarization in a light ray depends on the scattering angle, the angle between the incoming and outcoming light rays (Fig.1A).

Measuring the *E*-vector distribution in the sky shows a pattern which may not be as accurate as theoretically calculated (Strutt 1871), but is still clearly structured (Brines and Gould 1982, Pomozi et al. 2001). This pattern consists of concentric circles of *E*-vector orientations, with the sun in the center (Fig.1B). The degree of polarization in the sky is low near the sun and increases till a maximum of up to about 75 % at 90° distance from the sun (Coulson 1988). In the antisolar half of the sky, the degree of polarization decreases again. At night similar celestial *E*-vector patterns can be measured in the moonlight (Gál et al. 2001). By using polarized light information, even a small patch of the sky with a fraction of the whole *E*-vector pattern is sufficient to extrapolate for the complete circle, its center and therefore the position of the sun or moon.

The polarized light pattern of the sky has been proven to serve as compass cue not only for bees and ants, but for several insect species, other invertebrates and some vertebrates (reviews: Horváth and Varjú 2003, Wehner and Labhart 2006, Horváth 2014). Polarized light is detected by insects either in the UV, blue or green spectrum (review: Labhart and Meyer 1999). Which light spectrum is used, seems to correlate with

the life style of the insect (UV: diurnal; blue: nocturnal; green: living under the green light of forest canopies). It has been discussed that there might be specific reasons for an insect to choose between UV and blue light for polarized light orientation (Herzmann and Labhart 1989, Barta and Horváth 2004). UV light is considered to be more reliable for orientation. In this part of the light spectrum, polarization patterns are less likely to scatter due to atmospheric irregularities like clouds. A disadvantage is the low intensity of UV light in the sky, but this might not be a limiting factor during bright daylight. In contrast, polarized light patterns in the blue spectrum are easier disturbed, but light levels are relatively high during the night. This could enable polarized light orientation at crepuscular and nocturnal conditions, when UV levels are too low to be detected by the insect. Often the polarized light compass is combined with other strategies to integrate in a reliable orientation system, but it is considered to be the main compass cue in at least some insect species like the desert ant (Wehner and Müller 2006). To detect polarized light patterns considerable specializations of the insect visual system have evolved.

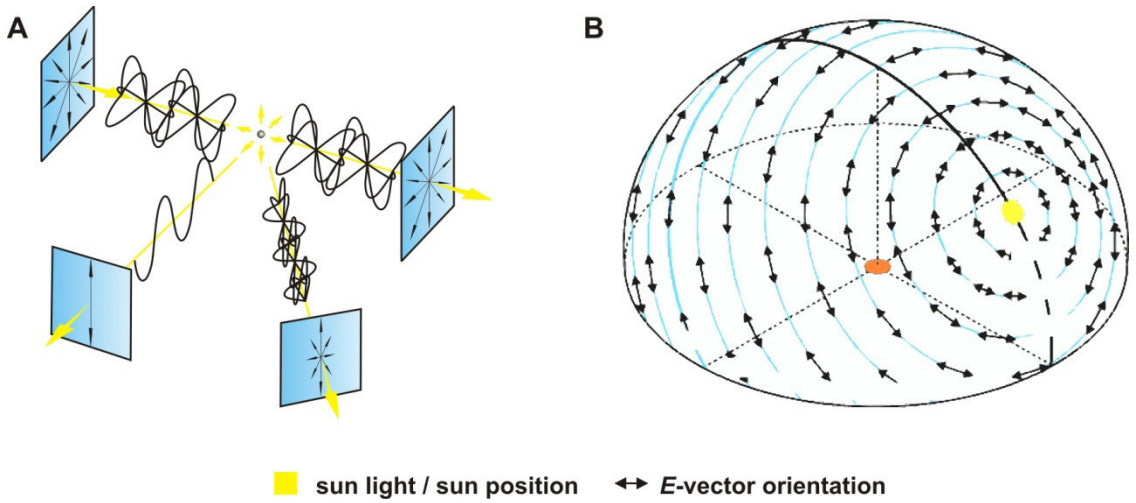

Fig.1: Polarization of light in the atmosphere and celestial polarization patterns. A: Sun light entering the atmosphere contains photons with randomly distributed orientations of *E*-vectors. When scattered by particles in the atmosphere, some orientations become more frequent. All photons scattered at 90° from a particle have the same *E*-vector orientation (100% linear polarized). The smaller the scatter angle, the smaller is the degree of polarization. Without any reflection, the light stays unpolarized. B: The pattern of *E*-vector distribution in the sky. *E*-vector orientations form concentric circles in the sky, with the sun in the center. The degree of polarization increases with increasing distance from the sun with a maximum at 90° and decreases with further distance. Adapted from Wehner (2001) and Homberg et al. (2011).

COMPOUND EYES, PHOTORECEPTORS AND *E*-VECTOR DETECTION

ANATOMY

Compound eyes of insects are an arrangement of numerous single eyes, ommatidia, each consisting of the same main structures: a distal crystalline cone collecting light, several pigment cells for protection from scattered light and eight to nine retinula cells, which are the actual photoreceptors (review: Nilsson and Kelber 2007, see also Fig.2). The photosensitive sites of the retinula cells are densely packed finger shaped extensions of the cell membrane, the microvilli, which together are called rhabdomere. Often, as in locusts (Wilson et al. 1978), the rhabdomeres of the retinula cells touch each other in the center of the ommatidium, forming a closed rhabdom, which serves as a light guide.

PHYSIOLOGY

Photoreceptors are photon counters. Photons are detected if they interact with the photosensitive molecules in the membrane of the microvilli, the rhodopsins. These are highly selective to certain wavelengths and *E*-vector orientations. Insect rhodopsins consist of a UV sensitive chromophore, which is retinal in locusts (Towner et al. 1997), and an opsin protein that can shift the absorption band to longer wavelengths (Vogt 1987, Chang et al. 1995, Briscoe and Chittka 2001). To what extend the spectral sensitivity is shifted depends on the opsin's amino acid sequence, but can also be influenced by the presence of screening pigments of the ommatidium. Absorption of a photon by a rhodopsin molecule starts a transduction cascade causing an increased membrane conductivity for certain ions, and eventually a neuronal photoreceptor response (review: Fain et al. 2010).

Insect retinula cells code information of a light stimulus with graded potential changes (Fig.3). The physiological response is a depolarization of the generally negative intracellular potential, called receptor potential. The amount of absorbed photons directly influences the amplitudes of depolarization. The response to a longer lasting light stimulus is a rapid and strong depolarization caused by an inward current of sodium and calcium ions, directly followed by fast repolarization due to a delayed outward current of potassium (as demonstrated in fruit flies and honey bees: Hardie 1991, Weckström et al. 1991, Becker and Backhaus 2000). If the light stimulus lasts long enough, a potential plateau is achieved when ions currents are even. The relation between the number of absorbed photons and the receptor potential amplitudes is not linear. In fact, photoreceptor response curves are shaped sigmoidally. This is the result of a mechanism that maximizes the receptors ability to discriminate brightness levels of a wide range of light intensities.

ADAPTATIONS FOR THE DETECTION OF POLARIZED LIGHT

Insect compound eyes are well known to develop specialized regions for a variety of tasks. In behavioral experiments, in which certain parts of the eye were occluded, a distinct area at the dorsal rim of the eyes has been found to be essential for the detection

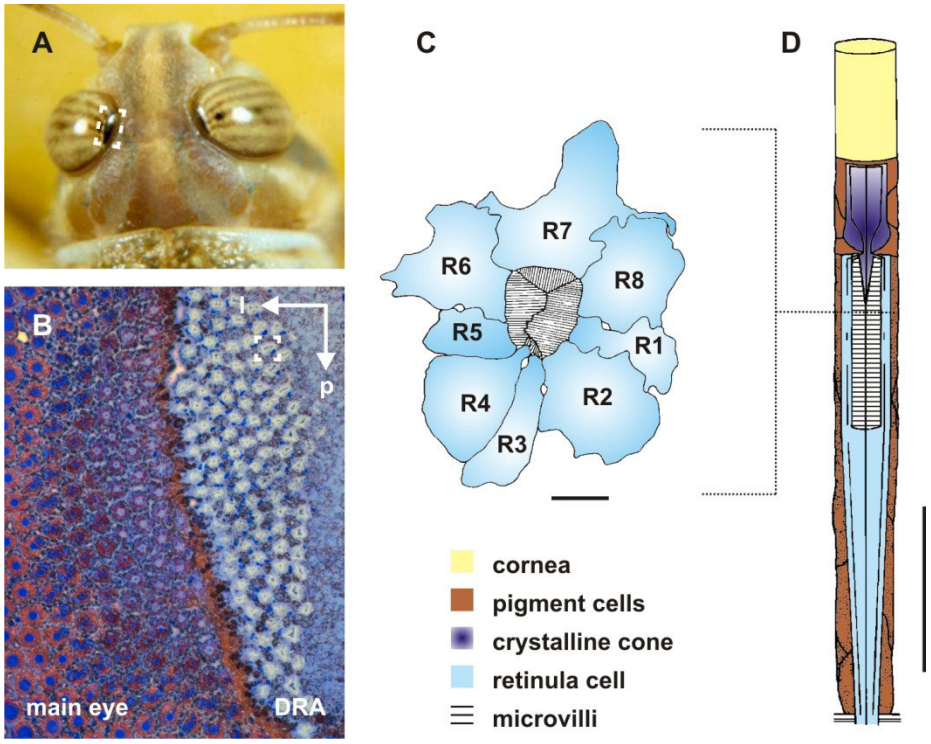

Fig.2: Structure and anatomy of the dorsal rim area of the desert locust and its ommatidia. A: Dorsal view on the locust's head. The dark brown elliptical regions of cornea (marked with white dashed box in the left eye) are the specialized dorsal rim areas of the compound eyes. B: Horizontal section through the locust's compound eye, in the region marked in A by the white dotted box. The dorsal rim area is located right to a wall of brownish screening pigment. The light blue, almost clear patches are the microvilli, surrounded by the slightly darker cell bodies of the corresponding retinula cells, forming the ommatidia (marked by white dashed box). Located left to the pigment wall is the main eye. Blue patches are the retinula cells. Microvilli regions are so small that they are hardly recognizable at this magnification. Dark blue patches are the crystalline cones of the ommatidia. C: Transverse drawing of a dorsal rim area ommatidium as marked in B by the white dashed square. The microvilli of the eight retinula cells build the rhabdom. The retinula cells can be divided in two groups, each with blocks of microvilli orientations orthogonal to each other (indicated by black lines) One group consists of retinula cells numbered as R1-6 and R8. The other group consists of only R7. D: Longitudinal drawing of a dorsal rim ommatidium. Scale bar in C indicates 4 µm, in D 100 µm. Orientations indicated by arrows (l: lateral, p: posterior). C and D adapted from Homberg and Paech (2002).

of polarized skylight (bee: Wehner and Strasser 1985, fly: von Philipsborn and Labhart 1990, ant: Fent 1985, locust: Mappes and Homberg 2004). Similar dorsal rim areas (DRA) occur in several other insect species (review: Labhart and Meyer 1999). Cornea structures and photoreceptor anatomy and physiology of these areas are highly specialized, contributing to the detection of polarized light.

Due to its dichroic character, a rhodopsin molecule preferably absorbs light with *E*-vectors oscillating parallel to the longitudinal axis of its retinal chromophore. Geometrical arguments cause the rhodopsins to be aligned in a relatively parallel manner, in the cylindrically shaped microvilli. This way a certain intrinsic polarization sensitivity is present in each single microvillus. However, microvilli of the main eye are arranged relatively random, thus weakening the detection of a certain *E*-vector by the receptor cell.

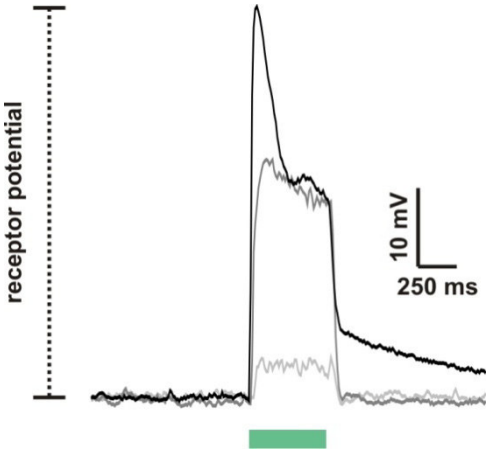

Fig.3: Electrophysiology of the insect photoreceptor. The photoreceptor responds to light stimuli with a graded depolarization of the receptor cell potential (receptor potential). The amplitude of the response increases with increasing light intensity. Above a certain light intensity and stimulus duration, the response changes from a tonic to a phasic tonic type. Lines show changes in membrane potential in a single desert locust photoreceptor of the main eye. The wavelength of the light stimuli is 530 nm, which matches the peak sensitivity of this receptor cell. Stimulus intensity: 3.59 x 10^{9} photons cm^{-2} s^{-1} (light gray), 3.59 x 10^{11} photons cm^{-2} s^{-1} (gray), 2.85 x 10^{13} photons cm^{-2} s^{-1} (black). The green bar indicates the stimulus duration.

In contrast, microvilli axes in dorsal rim area retinula cells are arranged parallel to each other (review: Roberts et al. 2011). Parallel alignment of rhodopsins and microvilli enables a receptor cell to preferably detect light of a specific *E*-vector.

Usually two blocks of retinula cells occur in a dorsal rim ommatidium, resulting in two perpendicular orientations of microvilli (Labhart and Meyer 1999, see also Fig.2). In accordance, two *E*-vector orientations are detected, which are orthogonal to each other (further explanation in the next paragraphs). Furthermore, the microvilli orientations are distributed in a fan shaped manner over the whole DRA, thus *E*-vectors of all orientations can be detected.

To minimize self screening, which stands for the scatter of *E*-vectors when light passes cellular tissue, rhabdoms in the dorsal rim area are often shorter compared to the main eye (e.g. Homberg and Peach 2002). In contrast, rhabdom diameters are larger, crystalline cones are not surrounded by pigment cells and in some cases the facets possess corneal pores, all of which are specializations to widen the receptive field and to maximize the number of collected photons. In the case of the locust, the cornea of the dorsal rim area is also flattened, indicating a relatively homogeneous visual field (Homberg and Peach 2002).

VISUAL PATHWAYS OF THE DESERT LOCUST, *SCHISTOCERCA GREGARIA*

Axons from photoreceptors of the main retina extend proximally through the optic lobe as so called short and long visual fibers. They target the two first main stations of visual processing: lamina and medulla. Both are neuropils of the insect optic lobe, predominantly consisting of neurites of interneurons. The corresponding cell bodies are located around the neuropils.

In the insect lamina retinula cell axons originating from the same ommatidia enter as bundles, thus forming so-called optic cartridges (Kirschfeld 1973). The position of such a cartridge in the lamina resembles the position of the associated ommatidium in the retina, a principle called retinotopy (Fig.4). Interneurons of the locust's lamina can be

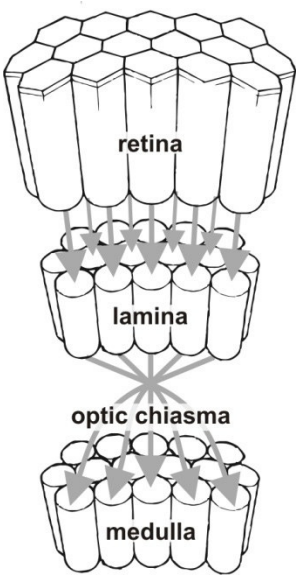

Fig.4: The principle of retinotopy. All photoreceptor visual fibers originating from one ommatidium project as a bundle (indicated by grey arrows) to a corresponding cartridge in the lamina and to columnar structures in the medulla. The result is that fiber location within the neuropils is strongly related to position of the corresponding ommatidum in the retina. This pattern is maintained, even though the bundles cross each other between lamina and medulla in an optic chiasma, reversing anterior and posterior positions. Adapted from Laughlin (1987).

either restricted to a single cartridge, connecting retinula axons from a single ommatidium, or arborize through neighboring cartridges, most likely gathering and processing information arriving from several ommatidia (Nowel and Shelton 1981, Wernitznig et al. 2015). Other interneuron types only branch in the proximal half of the lamina, implying further specific connection patterns. An important role for spatial and temporal resolution has been suggested for the insect lamina (Warrant 1999).

As in other insect species, the locust medulla is the termination site of the long visual fibers and is differentiated in ten distinct layers (Wendt and Homberg 1992, Gebhardt and Homberg 2004, Homberg et al. 2004). Several neuron types, originating in the lamina, send their axons into this neuropil (Nowel and Shelton 1981), and further connections between lamina and medulla have been confirmed as well (e.g. Homberg and Würden 1997). As the second visual neuropil, the medulla is quite complex with a high variety of different structures and cells (review: Homberg 1994). The lamina

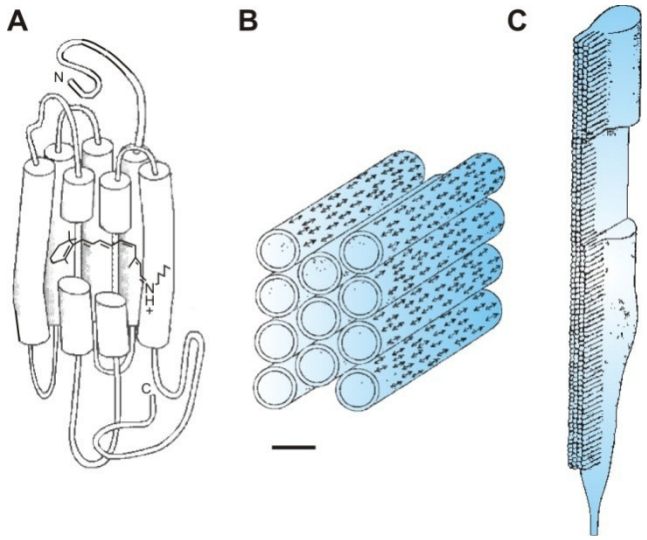

Fig.5: *E*-vector detection in an insect photoreceptor. A: A retinal molecule, embedded in the structure of an opsin, preferably absorbs photons with an *E*-vector oscillating in the same direction as the retinals longitudinal axis. B: In the microvilli of dorsal rim area photoreceptors, opsins are aligned parallel to each other (indicated by arrows). C: Parallel arrangement of all microvilli of a retinula cell sustains this orientation. Thus, the photoreceptor cell detects predominantly light with one specific *E*-vector orientation parallel to the microvilli. Scale bar in B: 50 nm. Adapted from Wehner (1976) and Hargrave (2001).

cartridge structure and therefore retinotopy is continued in columnar units, even though a chiasma is inverting the projecting sites in horizontal orientation (review: Strausfeld 2005). A considerable convergence of visual information was shown in certain interneurons of this neuropil (O'Carroll et al. 1992), and the medulla has been considered to be the first station for movement detection (Osorio 1986a, 1987, 1991) and color coding (Osorio 1986b).

THE POLARIZATION VISION PATHWAY

Like bees, ants and crickets, desert locusts have evolved a highly specialized neuronal pathway for the processing of polarized light information (review: Homberg 2004, Homberg et al. 2011, el Jundi et al. 2014, see Fig.6). Short and long visual fibers from the DRA target the dorsal rim regions of the lamina and medulla (DRLA, DRME; Homberg and Paech 2002). These neuropil regions strongly differ from the main lamina and medulla, showing no obvious layer structure (Gebhardt and Homberg 2004, Homberg et al. 2004). A particular neuronal pathway, running from the DRLA and DRME toward the central brain, is involved in polarized light signaling (red neuropils in Fig.6). Important elements of this pathway are line tangential interneurons, also called transmedulla neurons. These neurons connect the DRME with the lower unit of the

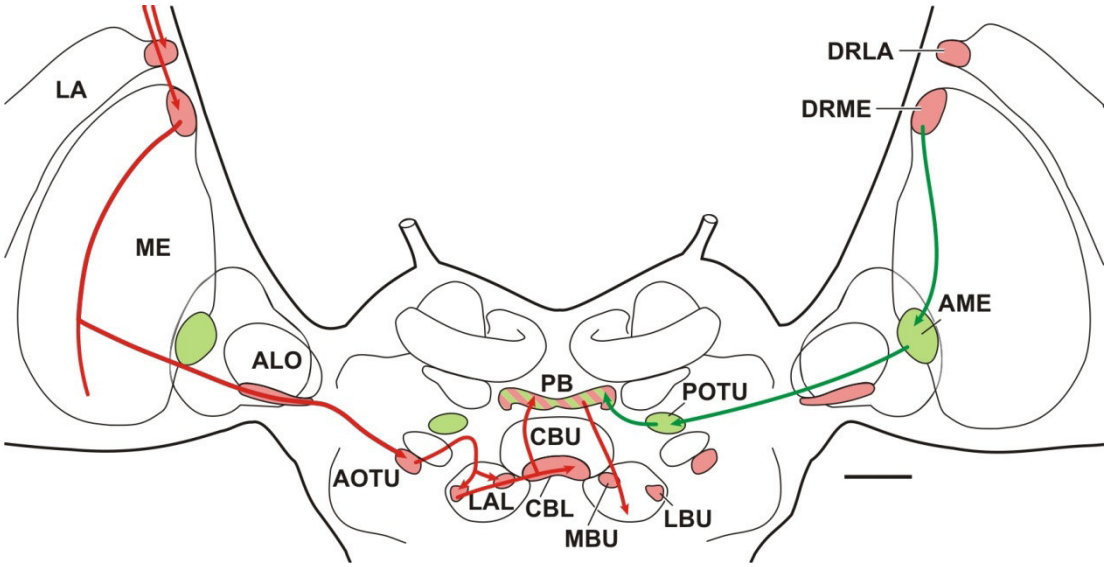

Fig.6: Neuronal pathways for the process of polarized light information in the brain of the desert locust. Schematic drawing of a desert locust brain. Marked are two different pathways (red and green arrows) contributing either to the processing of polarized or unpolarized light information, or to time compensation of such information. An anterior polarization pathway (red) consists of short and long visual fibers, entering the dorsal rim areas of lamina and medulla (DRLA, DRME) in the optic lobe. From there, line tangential / transmedulla neurons target the anterior lobes ventral layer in the lobula (ALO). Further connections include the lower unit of the anterior optic tubercle (AOTU), the medial (MBU) and lateral (LBU) bulb and the lower division of the central body (CBL). The pathway proceeds to the protocerebral bridge (PB) and again into the lateral accessory lobe (LAL). A second proposed pathway (green) connects the accessory medulla (AME) to the posterior optic tubercle (POTU) and protocerebral bridge (PB). It most likely contributes to time compensation of visual information. Scale bar: 200 µm. Adapted and modified from Pfeiffer and Homberg (2014).

anterior optic tubercle, run vertically through the medulla and also have small arborizations in the ventral layer of the lobula (Homberg et al. 2003). From the anterior optic tubercle polarized light signals are transferred to the lateral accessory lobe via interneurons and, finally, to the central body and protocerebral bridge, both major neuropils in the central brain (Homberg 1994, Müller et al. 1997, Homberg et al. 2003). The central body is part of the central complex, a set of central brain neuropils, which play an important role in locomotor control, spatial orientation, visual memory and polarization vision (review: Pfeiffer and Homberg 2014). In addition, a second more posterior located polarized light pathway to the central complex has been suggested (el Jundi and Homberg 2010, green neuropils in Fig.6). The optic tubercles from both brain hemispheres are connected with each other (Homberg et al. 2003), implying integration of information from both compound eyes.

NEURONAL *E*-VECTOR CODING

Like photoreceptors of the DRA, polarized-light sensitive interneurons in the optic lobe respond with different strength to certain *E*-vector orientations. There are two types of interneuronal responses to different *E*-vectors. A neuron can be excited strongly by a certain *E*-vector and excited weakly by an *E*-vector in perpendicular orientation (Fig.7 upper panel), or the neuron is excited by one *E*-vector and inhibited by the perpendicular one (Fig.7 lower panel). Both mechanisms result in a sinusoidal modulation of the neurons activity, when the *E*-vector orientation rotates, and there is 90° distance between the maximum and minimum activity.

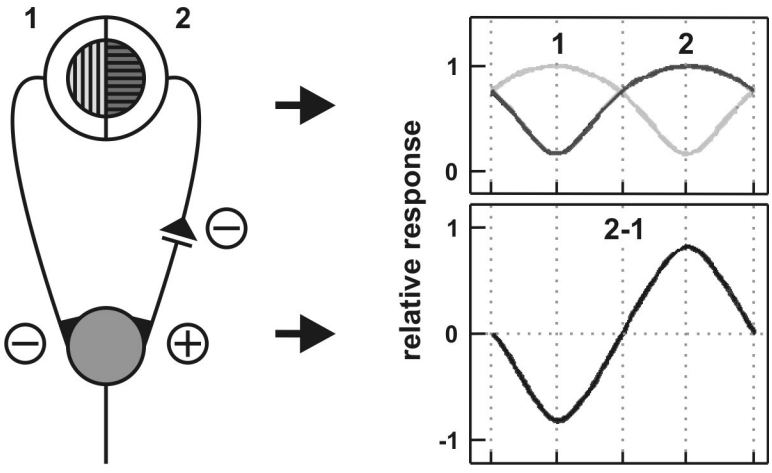

Fig.7: The principle of polarization opponency. The dorsal rim area photoreceptors and interneurons of the polarization vision pathway respond to a gradually rotating *E*-vector with sinusoidal modulation of their response strength. In the case of photoreceptors and several interneurons, only excitation occurs (upper graph). In many other interneurons of the polarization vision pathway, phases of excitation and inhibition occur (lower graph, polarization opponency). Considered as the basis of polarization opponency is the antagonistic input from the two orthogonal microvilli blocks in the dorsal rim area ommatida (left drawing). If excited by adequate polarized light, one block (block 1) inhibits the following interneuron. Orthogonal polarized light excites the other block (block 2), with the effect that the interneuron is excited as well. In the latter case, an additional interneuron has to be postulated, which reverses the actual inhibitory effect of the photoreceptor's transmitter to an excitatory effect. Adapted from Labhart (1988).

The latter mechanism is called polarization opponency (review: Labhart et al. 2001). Orthogonal microvilli orientation in the DRA ommatidia is considered to be the basis of polarization opponency. Two groups of photoreceptors provide either inhibitory or excitatory input to the subsequent interneurons (Fig.7 left). Summed up, two major advantages arise through this coding of information: (1) the interneuron's sensitivity to a specific *E*-vector is enhanced, and (2) the interneuron is hereby responding solely to changes in *E*-vector orientation and not to light intensities, as on photoreceptors level. The two mechanisms of simple modulation of neuron activity and of polarization opponency occur in locust interneurons of the medulla, optic tubercle and central complex (Homberg and Würden 1997, Pfeiffer et al. 2005, Vitzthum et al. 2002). Interestingly, in the desert locust central complex a population of neurons has been identified with a variety of preferred *E*-vectors, covering orientations from 0° to 180°. Thereby a neuronal map of celestial polarization patterns might be provided (Vitzthum et al. 2002, Heinze and Homberg 2007, 2009, Bech et al. 2014).

Finally, it should be mentioned that the celestial *E*-vector patterns change gradually over the day due to the moving sun. A temporal compensation of these changes is suspected to happen in the accessory medulla, a neuropil considered to be associated to insect circadian rhythms (reviews Helfrich-Förster et al. 1998, Homberg et al. 2003b). In the desert locust, the accessory medulla is connected to stations of the polarized light pathway, strongly implying its significance for polarization vision (Würden and Homberg 1997, el Jundi and Homberg 2010).

MIGRATORY BEHAVIOR IN THE DESERT LOCUST AND THE RELEVANCE OF POLARIZED LIGHT VISION

Swarms of the desert locust *Schistocerca gregaria* are a well known, large scale phenomenon in North Africa and the Middle East (review van Huis 1995). Usually, migrating swarms consist of several million individuals of animals in their gregarious phase. This gregarious phase develops from a normally solitarious phase when environmental conditions cause stronger spatial concentration of existing locust populations (Pener 1983, 1991, Collett et al. 1998) via pheromones, mechanical and even visual stimuli (Deng et al. 1996, Roessingh et al. 1998, Hägele and Simpson 2000, Simpson et al. 2001).

Solitarious locusts are larger and have a more cryptic appearance than gregarious individuals (Sword 1999, Wilson 2000, De Loof et al. 2010, see also Fig.8). Further differences concern numerous physiological factors (Pener and Yerushalim 1998, Rogers et al. 2004, Pener and Simpson 2009). Phase dependent differences include substantially larger brains (Ott and Rogers 2010) but smaller eyes (Dirsh 1953, Rogers et al. 2010) in gregarious compared to solitarious animals. An altered physiology of visual interneurons has been demonstrated as well (Matheson 2004, Gaten 2012). However, most striking are the differences in the behavioral activity patterns.

Fig.8: The two phases of the desert locust. The diurnal gregarious phase is easily recognized by its relatively bright brownish-yellowish body color, while the nocturnal solitarious phase is darker with a brownish-greenish shade. Gregarious locusts are also smaller in body size than their solitarious counterparts. Both animals shown are males. Adapted from De Loof et al. (2010).

The gregarious phase is mainly diurnal and shows strong flight activity during the second half of the day (overview in Symmons and Cressman 2001). This, combined with the crowding behavior of gregarious locusts, leads to large flying swarms. In contrast, solitarious locusts are generally nocturnal (Rao 1960, Roffey 1963, Roffey and Popov 1968, Ely et al. 2011). They react repulsively to other locusts (Wiesel et al. 1996) and spend most time of the day resting isolated on the ground or in bushes (Steedman 1988).

Swarms of gregarious locusts perform long-range migration of up to 100 km per day (Symmons 1992) and even marching bands on the ground walk in a definite direction (Uvarov 1977). Swarming behavior and long range migration of solitarious locusts during the night has been reported as well, but has been studied only sparsely (Rao 1936, Rao 1942, Rao 1960, Waloff 1963, Roffey 1963).

The direction of swarm migration often follows seasonal winds downstream (Rainey 1976), thus causing the nickname “teeth of wind”. Furthermore, it has been argued that wind is the main factor for swarm movements (Draper 1980). Nevertheless, compass cues like the sun, chromatic gradients in the sky, polarized sky light or even magnetic fields have been discussed as well (Kennedy 1945, 1951, Schaefer 1976, Baker 1978, Riley and Reynolds 1986, Pfeiffer and Homberg 2007, el Jundi et al. 2014). In particular the relevance of polarized light in orientation behavior has been demonstrated under laboratory conditions in flying adult locusts (Mappes and Homberg 2004) and in walking nymphs (Eggers and Weber 1993). DRAs occur in both phases and in their larval stages, and the highly differentiated polarization vision pathway (discussed above) seems not to differ between gregarious and solitarious animals (el Jundi and Homberg 2012).

REFERENCES

Baker RR (1978) The evolutionary ecology of animal migration. Hodder & Stoughton, London

Barta A, Horváth G (2004) Why is it advantageous for animals to detect celestial polarization in the ultraviolet? Skylight polarization under clouds and canopies is strongest in the UV. J. theor. Biol. 226:429-437

Bech M, Homberg U, Pfeiffer K (2014) Receptive fields of locust brain neurons are matched to polarization patterns of the sky. Curr. Biol. 24:2124-2129

Becker K, Backhaus W (2000) A physiological model of dark-adapted and light-adapted photoreceptors of the honeybee. Biol. Cybern. 82:153-160

Brines M (1982) Skylight polarization patterns and animal orientation. J. exp. Biol. 96:69-91

Briscoe AD, Chittka L (2001) The evolution of color vision in insects. Annu. Rev. Entomol. 46:471-510

Chang BSW, Crandall KA, Carulli JP, Hartl DL (1995) Opsin phylogeny and evolution: A model for blue shifts in wavelength regulation. Mol. Phylogenet. Evol. 4:31-43

Collett M, Despland E, Simpson SJ, Krakauer DC (1998) Spatial scales of desert locust gregarization. Proc. Natl. Acad. Sci. 95:13052-13055

Collett TS (1996) Insect navigation *en route* to the goal: Multiple strategies for the use of landmarks. J. exp. Biol. 199:227-235

Collett TS, Collett M (2000) Path integration in insects. Curr. Opin. Neurobiol. 10:757-762

Coulson KL (1988) Polarization and intensity of light in the atmosphere. Hampton VA, Deepak Publishing

De Loof A, Huybrechts J, Geens M, Vandersmissen T, Boerjan B, Schoofs L (2010) Sexual differentiation in adult insects: Male-specific cuticular yellowing in *Schistocerca gregaria* as a model for reevaluating some current (neuro)endocrine concepts. J. Insect Physiol. 56:919-925

Deng AL, Torto B, Hassanali A, Ali EE (1996) Effects of shifting to crowded or solitary conditions on pheromone release and morphometrics of the desert locust, *Schistocerca gregaria* (Forskål) (Orthoptera: Acrididae). J. Insect Physiol. 42:771-776

Despland E, Rosenberg J, Simpson SJ (2004) Landscape structure and locust swarming: a satellite's eye view. 27:381-391

Dirsh VM (1953) Morphometrical studies on phases of the desert locust. Anti-Locust Bull. 16: 1-34

Draper J (1980) The direction of desert locust migration. J. Animal Ecol. 49:959-974

Eggers A, Weber T (1993) Behavioral evidence for polarization vision in locusts. In: Elsner N, Heisenberg M (eds.) Gene-Brain-Behaviour. Thieme, Stuttgart p 336

el Jundi B, Homberg U (2010) Evidence for the possible existence of a second polarization-vision pathway in the locust brain. J. Insect Physiol. 56:971-979

el Jundi B, Homberg U (2012) Receptive field properties and intensity-response functions of polarization-sensitive neurons of the optic tubercle in gregarious and solitarious locusts. J. Neurophysiol. 108:1695-1710.

el Jundi B, Pfeiffer K, Heinze S, Homberg U (2014) Integration of polarization and chromatic cues in the insect sky compass. J. comp. Physiol. A 200:575-589

Ely SO, Njagi PGN, Bashir MO, El-Amin SET, Hassanali A (2011) Diel behavioral activity patterns in adult solitarious desert locust, *Schistocerca gregaria* (Forskål). Psyche 1-9

Fain GL, Hardie R, Laughlin SB (2010) Phototransduction and the evolution of photoreceptors. Curr. Biol. 20:R114-R124

Fent K (1985) Himmelsorientierung bei der Wüstenameise *Cataglyphis bicolor*: Bedeutung von Komplexaugen und Ocellen. Dissertation at the University Zürich

Frost BJ, Mouritsen H (2006) The neural mechanisms of long distance animal navigation. Curr. Opin. Neurobiol. 16:481-488

Gál J, Horvát G, Barta A, Wehner R (2001) Polarization of the moonlit clear night sky measured by full-sky imaging polarimetry at full moon: Comparison of the polarization of moonlit and sunlit skies. J. geophys. Res. 106:22647-22653

Gaten E, Huston SJ, Dowse HB, Matheson T (2012) Solitary and gregarious locusts differ in circadian rhythmicity of a visual output neuron. J. biol. Rhythms 27:196-205

Gebhardt S, Homberg U (2004) Immunocytochemistry of histamine in the brain of the locust *Schistocerca gregaria*. Cell Tissue Res. 317:195-205

Giurfa M, Capaldi EA (1999) Vectors, routes and maps: new discoveries about navigation in insects. TINS 22:237-242

Hägele BF, Simpson SJ (2000) The influence of mechanical, visual and contact chemical stimulation on the behavioural phase state of solitarious desert locusts (*Schistocerca gregaria*). J. Insect Physiol. 46:1295-1301

Hargrave PA (2001) Rhodopsin structure, function, and topography the Friedenwald lecture. Invest. Ophthalmol. Vis. Sci. 42:3-9

Hardie RC (1991) Voltage-sensitive potassium channels in *Drosophila* photoreceptors. J. Neurosci. 11:3079-3095

Heinze S, Homberg U (2007) Maplike representation of celestial *E*-vector orientations in the brain of an insect. Science 315:995-997

Heinze S, Homberg U (2009) Linking the input to the output: New sets of neurons complement the polarization vision network in the locust central complex. J Neurosci. 29:4911-4921

Helfrich-Förster C, Stengl M, Homberg U (1998) Organization of the circadian system in insects. Chronobiol. Internat. 15:567-594

Herzmann D, Labhart T (1989) Spectral sensitivity and absolute threshold of polarization vision in crickets. J. comp. Physiol. 165:315-319

Homberg U (1994) Distribution of neurotransmitters in the insect brain. Progress in Zoology 40. Gustav Fischer Verlag, Stuttgart, Jena, New York

Homberg U (2004) In search of the sky compass in the insect brain. Naturwissenschaften 91:199-208

Homberg U, Paech A (2002) Ultrastructure and orientation of ommatidia in the dorsal rim area of the locust compound eye. Arthopod Struct. Dev. 30:271-280

Homberg U, Würden S (1997) Movement-sensitive, polarization-sensitive, and light-sensitive neurons of the medulla and accessory medulla of the locust, *Schistocerca gregaria*. J. comp. Neurol. 386:329-346

Homberg U, Reischig T, Stengl M (2003) Neural organization of the circadian system of the cockroach *Leucophaea maderae*. Chronobiol. Int. 20:577-591

Homberg U, Hofer S, Pfeiffer K, Gebhardt S (2003) Organization and neural connections of the anterior optic tubercle in the brain of the locust, *Schistocerca gregaria*. J. comp. Neurol. 462:415-430

Homberg U, Brandl C, Clynen E, Schoofs L, Veenstra JA (2004) Mas-allatotropin/Lom-AG-myotropin I immunostaining in the brain of the locust, *Schistocerca gregaria*. Cell Tissue Res. 318:439-457

Homberg U, Heinze S, Pfeiffer K, Kinoshita M, el Jundi B (2011) Central neural coding of sky polarization in insects. Phil. Trans. R. Soc. B 366:680-687

Horváth G (2014) Polarized light and polarization vision in animal sciences. 2nd edition. Springer, Heidelberg, New York, Dordrecht, London

Horváth G, Varjú D(2003) Polarized Light in Animal Vision - Polarization Patterns in Nature. Springer, Heidelberg, Berlin, New York

Johnsen S, Kelber A, Warrant EJ, Sweeney AM, Widder EA, Lee Jr. RL, Hernández-Andrés J (2006) Crepuscular and nocturnal illumination and its effects on color perception by the nocturnal hawkmoth *Deilephila elpenor*. J. exp. Biol. 209:789-800

Kennedy JS (1939) The behavior of the desert locust *Schistocerca gregaria* (Forskål) (Orthoptera) in an outbreak centre. Trans. Entomol. Soc. Lon. 89:385-542

Kennedy JS (1945) Observations on the mass migration of desert locust hoppers. Trans. R. Entomol. Soc. Lond. 95:247-262

Kennedy JS (1951) The migration of the desert locust (*Schistocerca gregaria* Forsk.). I. Behaviour of swarms. II. A theory of long-range migrations. Phil. Trans. R. Soc. Lond. 235:163-290

Kirschfeld K (1973) Das neurale Superpositionsauge. Fortschr. Zool. 21:229-257

Labhart T (1988) Polarization-opponent interneurons in the insect visual system. Nature 331:435-437

Labhart T, Meyer EP (1999) Detectors for polarized skylight in insects: A survey of ommatidial specializations in the dorsal rim area of the compound eye. Microsc res. Tech. 47:368-379

Labhart T, Meyer EP, Schenker L (1992) Specialized ommatidia for polarization vision in the compound eye of cockchafers, *Melolontha melolontha* (Coleoptera, Scarabaeidae). Cell Tissue Res. 268:419-429

Labhart T, Petzold J, Helbling H (2001) Spatial integration in polarization-sensitive interneurons of crickets: A survey of evidence, mechanisms and benefits. J. exp. Biol. 204:2423-2430

Mappes M, Homberg U (2004) Behavioral analysis of polarization vision in tethered flying locusts. J. comp. Physiol. A 190:61-68

Matheson T, Rogers SM, Krapp HG (2004) Plasticity in the visual system is correlated with a change in lifestyle of solitarious and gregarious locusts. J. Neurophysiol. 91:1-12

Merlin C, Heinze S, Reppert S (2012) Unraveling navigational strategies in migratory insects. Curr. Opin. Neurobiol. 22:353-361

Müller M, Homberg U, Kühn A (1997) Neuroarchitecture of the lower division of the central body in the brain of the locust (*Schistocerca gregaria*). Cell Tissue Res. 288:159-176

Nilsson D-E, Kelber A (2007) A functional analysis of compound eye evolution. Arthropod Struct. Dev. 36: 373-385

Nowel MS, Shelton PMJ (1981) A Golgi-electron-microscopical study of the structure and development of the lamina ganglionaris of the locust optic lobe. Cell Tissue Res. 216:377-401

O'Carroll DC, Osorio D, James AC, Bush T (1992) Local feedback mediated via amacrine cellsin the insect optic lobe. J. comp. Physiol. A 171:447-455

Osorio D (1986a) Directionally selective cells in the locust medulla. J. comp. Physiol. A 159:841-847

Osorio D (1986b) Ultraviolet sensitivity and spectral opponency in the locust. J. exp. Biol. 122:193-208

Osorio D (1987) The temporal properties of nonlinear transient cells in the locust medulla. J. comp. Physiol. A 161:431:440

Osorio D (1991) Mechanisms of early visual processing in the medulla of the locust optic lobe: how self-inhibition, spatial pooling and signal rectification contribute to the properties of transient cells. Visual Neurosci. 7:345-355

Ott SR, Rogers SM (2010) Gregarious desert locusts have substantially larger brains with altered proportions compared with the solitarious phase. Proc. R. Soc. B 277:3087-3096

Pener MP (1983) Endocrine aspects of phase polymorphism in locusts. In: Downer RGH, Laufer, H (eds.) Invertebrate endocrinology Vol. 1, Endocrinology of insects. Alan R. Liss, Inc., New York pp 379-394

Pener MP (1991) Locust phase polymorphism and its endocrine relations. Adv. Insect Physiol. 23:1-79

Pener MP, Simpson SJ(2009) Locust phase polyphenism: an update. Adv. Insect Physiol. 36:1-272

Pener MP, Yerushalmi Y (1998) The physiology of locust phase polymorphism: an update. J. Insect Physiol. 44:365-377

Pfeiffer K, Homberg U (2007) Coding of azimuthal directions via time-compensated combination of celestial compass cues. Curr. Biol. 17:960-965

Pfeiffer K, Homberg U (2014) Organization and functional roles of the central complex in the insect brain. Annu Rev. Entomol. 59:165-184

Pfeiffer K, Kinoshita M, Homberg U (2005) Polarization-sensitive and light-sensitive neurons in two parallel pathways passing through the anterior optic tubercle in the locust brain. J. Neurophysiol. 94:3903-3915

Pomozi I, Horváth G, Wehner R (2001) How the clear-sky angle of polarization pattern continues underneath clouds: full-sky measurements and implications for animal orientation J. exp. Biol. 204:2933-29234

Rainey, R. C. 1976. Flight behaviour and features of the atmospheric environment. In Insect Flight Vol. 7. Symp. R. Entomol. Soc., London pp 75-112

Rao YR (1936) The locust incursion of 1935 in North-West India-its significance in the study of the locust problem. Indian J. agr. Sci. 6:1031-1053

Rao YR (1942) Some results of studies on the desert locust (*Schistocerca gregaria* Forsk.). Bull. Entomol. Res. 33:241-265

Rao YR (1960) The desert locust in India. Indian Coun. agric. Res. New Delhi

Riley JR, Reynolds DR (1986) Orientation at night by high-flying insects. In Danthanarayana W (ed.) Insect flight dispersal and migration. Springer, Berlin Heidelberg New York pp 71-87

Roberts NW, Porter ML, Cronin TW (2011) The molecular basis of mechanisms underlying polarization vision. Phil. Trans. R. Soc. B 366:627-637

Roessingh P, Bouaïchi A, Simpson SJ (1998) Effects of sensory stimuli on the behavioural phase state of the desert locust, *Schistocerca gregaria*. J. Insect Physiol 44:883-893

Roffey J (1963) Observation on night flight in the desert locust *Schistocerca gregaria* (Forskål). Anti-Locust Bull. 38:1-32, 1963

Roffey J, Popov G (1968) Environmental and behavioural processes in a desert locust outbreack. Nature 219:446-450

Rogers SM, Matheson T, Sasaki K, Kendrick K, Simpson SJ, Burrows M (2004) Substantial changes in central nervous system neurotransmitters and neuromodulators accompany phase change in the locust. J. exp. Biol. 3603-36-17

Rogers SM, Harston GWJ, Kilburn-Toppin F, Matheson T, Burrows M, Gabbiani F, Krapp HG (2010) Spatiotemporal receptive field properties of a looming-sensitive neuron in solitarious and gregarious phases of the desert locust. J. Neurophysiol. 103:779-792

Santschi F (1923) L'orientation siderale des fourmis, et quelques considerations sur leurs differentes possibilites d'orientation. Mem. Soc. Vaudoise Sci. Nat. 4:137-175

Schaefer GW (1976) Radar observations of insect flight. In Rainey RC (ed.) Insect flight Vol. 7. Symposium of the Royal Entomological Society. Blackwell, Oxford pp 157-197

Shashar N, Sabbah S, Aharoni N (2005) Migrating locusts can detect polarized reflections to avoid flying over the sea. Biol. Lett. 1:472-475

Simpson SJ, Despland E, Hägele BF, Dodgson T (2001) Gregarious behavior in desert locusts is evoked by touching their back legs. Proc. Natl. Acad. Sci. 98:3895-3897

Steedman A, (1988) Locust Handbook. Overseas Development Natural Resource Institute, London

Strausfeld NJ (2005) The evolution of crustacean and insect optic lobes and the origins of chiasmata. Arthropod Struct. Dev. 34:235-256

Strutt JW (1871) On the light from the sky, its polarization and colour. Phil. Mag. 41:274-279

Sword GA (1999) Density-dependent warning coloration. Nature 397:217

Symmons PM, Cressman K (2001) Desert locust guidelines 1. Biology and behaviour. Food and Agriculture Organization of the United Nations, Rome

Towner P, Harris P, Wolstenholme AJ, Hill C, Worm K, Gärtner W (1997) Primary structure of locust opsins: a speculative model which may account for ultraviolet wavelength light detection. Vision Res. 37:495-503

Uvarov B (1966) Grasshoppers and locusts. Vol. 1. Cambridge University Press, Cambridge

Uvarov B (1977) Grasshoppers and locusts. Vol. 2. Centre for overseas pest research, London

van Huis A (1995) Desert locust plagues. Endeavor 19:118-124

Vitzthum H, Müller M, Homberg U (2002) Neurons of the central complex of the locust *Schistocerca gregaria* are sensitive to polarized light. J. Neurosci. 22:1114-1125

Vogt K (1987) Chromophores of insect visual pigments. Photobioch. Photobiop. (Suppl.) pp 273-296

von Frisch K, (1949) Die Polarisation des Himmelslichtes als orientierender Faktor bei den Tänzen der Bienen. Experientia 5:142-148

von Philipsborn A, Labhart T (1990) A behavioural study of polarization vision in the fly, *Musca domestica*. J. comp. Physiol A 167:737-743

Waloff Z (1963) Field studies on solitarious and transient desert locusts in the red sea area. Anti-Locust Bull.40:1-93

Warrant EJ (1999) Seeing better at night: life style, eye design and the optimum strategy of spatial and temporal summation. Vision Res. 39:1611-1630

Weckström M, Hardie RC, Laughlin SB (1991) Voltage-activated potassium channels in blowfly photoreceptors and their role in light adaptation. J. Physiol. 440:635-657

Wehner R (1976) Polarized-light navigation by insects. Sci. Am. 235:106-115

Wehner R (2001) Polarization vision - A uniform sensory capacity? J. exp. Biol. 204:2589-2596

Wehner R, Labhart T (2006) Polarization vision. In Warrant EJ, Nilsson D-E (eds.) Invertebrate vision. Cambridge University Press, Cambridge pp 291-348

Wehner R, Müller M (2006) The significance of direct sunlight and polarized skylight in the ant's celestial system of navigation. Proc. Natl. Acad. Sci. 103:12575-12579

Wehner R, Strasser S. (1985) The POL area of the honey bee's eye: behavioural evidence. Physiol. Entomol. 10:337-349

Wendt B, Homberg U (1992) Immunocytochemistry of dopamine in the brain of the locust *Schistocerca gregaria*. J. comp. Neurol. 321:387-403

Wernitznig S, Rind FC, Pölt P, Zankel A, Pritz E, Kolb D, Bock E, Leitinger G (2015) Synaptic connections of first-stage visual neurons in the locust *Schistocerca gregaria* extend evolution of tetrad synapses back 200 million years. J. comp. Neurol. 523:298-312

Wiesel G, Tappermann S, Dorn A (1996) Effects of juvenile hormone and juvenile hormone analogues on the phase behaviour of *Schistocerca gregaria* and *Locusta migratoria*. J. Insect Physiol. 4:385-395

Wilson K (2000) How the locust got its stripes: the evolution of density-dependent aposematism. TREE 15:88-90

Wilson M, Garrard P, McGinness S (1978) The unit structure of the locust compound eye. Cell Tissue Res. 195:205-226

CHAPTER 1

Opsin expression, physiological characterization and identification of photoreceptor cells in the dorsal rim area and main retina of the desert locust, *Schistocerca gregaria*

© 2014. Published by The Company of Biologists Ltd | The Journal of Experimental Biology (2014) 217, 3557-3568 doi:10.1242/jeb.108514

RESEARCH ARTICLE

Opsin expression, physiological characterization and identification of photoreceptor cells in the dorsal rim area and main retina of the desert locust, *Schistocerca gregaria*

Fabian Schmeling[1], Motohiro Wakakuwa[2], Jennifer Tegtmeier[1], Michiyo Kinoshita[2], Tobias Bockhorst[1], Kentaro Arikawa[2] and Uwe Homberg[1,*]

ABSTRACT

For compass orientation many insects rely on the pattern of sky polarization, but some species also exploit the sky chromatic contrast. Desert locusts, *Schistocerca gregaria*, detect polarized light through a specialized dorsal rim area (DRA) in their compound eye. To better understand retinal mechanisms underlying visual navigation, we compared opsin expression, spectral and polarization sensitivities and response–stimulus intensity functions in the DRA and main retina of the locust. In addition to previously characterized opsins of long-wavelength-absorbing (Lo1) and blue-absorbing visual pigments (Lo2), we identified an opsin of an ultraviolet-absorbing visual pigment (LoUV). DRA photoreceptors exclusively expressed Lo2, had peak spectral sensitivities at 441 nm and showed high polarization sensitivity (PS 1.3–31.7). In contrast, ommatidia in the main eye co-expressed Lo1 and Lo2 in five photoreceptors, expressed Lo1 in two proximal photoreceptors, and Lo2 or LoUV in one distal photoreceptor. Correspondingly, we found broadband blue- and green-peaking spectral sensitivities in the main eye and one narrowly tuned UV peaking receptor. Polarization sensitivity in the main retina was low (PS 1.3–3.8). *V*–log *I* functions in the DRA were steeper than in the main retina, supporting a role in polarization vision. Desert locusts occur as two morphs, a day-active gregarious and a night-active solitarious form. In solitarious locusts, sensitivities in the main retina were generally shifted to longer wavelengths, particularly in ventral eye regions, supporting a nocturnal lifestyle at low light levels. The data support the role of the DRA in polarization vision and suggest trichromatic colour vision in the desert locust.

KEY WORDS: Compound eye, Dorsal rim area, Opsin expression, Spectral sensitivity, Polarization sensitivity, Phase change

INTRODUCTION

In addition to the position of the sun, many insects rely on the pattern of polarized light (POL) in the blue sky for spatial orientation (Horváth and Varjú, 2004; Wehner and Labhart, 2006; Homberg and el Jundi, 2014). Polarotactic orientation has been demonstrated in field experiments in the desert ant (Wehner and Müller, 2006), the honeybee (von Frisch, 1949), several species of dung beetles (Dacke et al., 2003; Dacke et al., 2011), the monarch butterfly (Reppert et al., 2004) and the fruitfly (Weir and Dickinson, 2012) and, in laboratory experiments, in the house fly (von Philipsborn and Labhart, 1990), the field cricket (Brunner and Labhart, 1987), and the desert locust (Mappes and Homberg, 2004). In all of these insects, POL detection is mediated by a small dorsal rim area (DRA) in the compound eye (Labhart and Meyer, 1999).

Ommatidia and photoreceptor cells in the DRA are highly specialized. DRA ommatidia contain homochromatic photoreceptors with high polarization sensitivity (PS) based on precisely aligned microvilli. In each ommatidium microvilli are oriented in two blocks orthogonal to each other (Labhart and Meyer, 1999). The DRA of the desert locust, *Schistocerca gregaria* (Forskål 1775), has about 400 ommatidia (Homberg and Paech, 2002). Each DRA ommatidium contains eight photoreceptor cells (R1–R8). The microvilli of R7 are oriented orthogonally to those of R1, R2, R5, R6 and R8, whereas the microvilli of R3 and R4 are small and less well oriented (Homberg and Paech, 2002).

Polarization vision pathways in the brain of *S. gregaria* have been studied particularly well (Homberg et al., 2011). Polarized light signals from the DRA are combined with chromatic contrast information from the sky in the anterior optic tubercle of the brain (Pfeiffer and Homberg, 2007), and signals from both eyes are integrated in the central complex, serving a probable role as an internal sky compass in the brain (Heinze and Homberg, 2007; Heinze et al., 2009).

Schistocerca gregaria occurs widely in North Africa and the Middle East, and exhibits two different morphological phases with strongly differing appearance and behaviour (Uvarov, 1966; Simpson et al., 1999). Swarm-building locusts of the gregarious phase perform long-distance migrations during the day, whereas the solitarious phase also migrates but is largely nocturnal (Roffey, 1963; Waloff, 1963; Roffey and Magor, 2003). While there is evidence for sky compass orientation in gregarious animals (Kennedy, 1951), the control of navigation in solitarious locusts is unknown.

In contrast to central processing of polarized light, the physiology of DRA photoreceptors in *S. gregaria* is poorly understood. Eggers and Gewecke (Eggers and Gewecke, 1993) reported blue-sensitive receptors with high PS values and UV receptors with low PS values in the DRA, but did not identify the photoreceptor cell types morphologically. Although two opsins, a long-wavelength opsin and a middle-wavelength opsin, have been identified in *S. gregaria* (Towner et al., 1997), no data exist on their distribution in the eye. We therefore reinvestigated the number and sequences of mRNAs encoding visual pigment opsins and their presence in the DRA of the locust. In addition, we studied spectral sensitivities, response–stimulus intensity (*V*–log *I*) functions and polarization sensitivity of DRA photoreceptors and identified the recorded cell type through dye injections. All data were compared with those from

[1]Fachbereich Biologie, Tierphysiologie, Philipps-Universität Marburg, 35032 Marburg, Germany. [2]Laboratory of Neuroethology, Sokendai (The Graduate University for Advanced Studies), Shonan Village, Hayama, Kanagawa 240-0193, Japan.

*Author for correspondence (homberg@biologie.uni-marburg.de)

Received 27 May 2014; Accepted 23 July 2014

RESEARCH ARTICLE The Journal of Experimental Biology (2014) doi:10.1242/jeb.108514

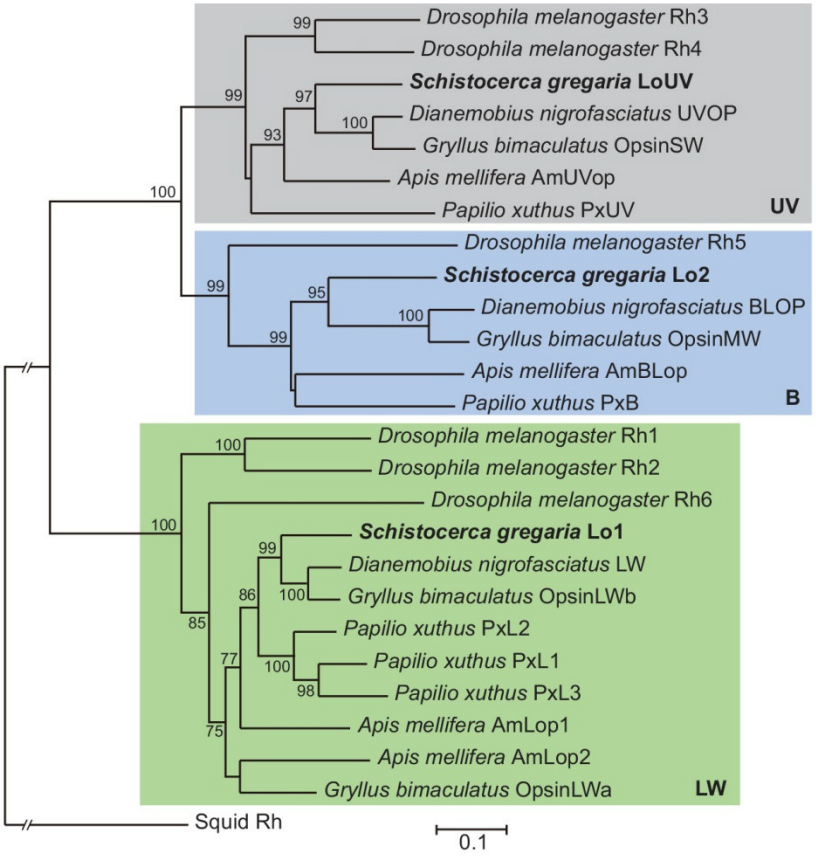

Fig. 1. Phylogenetic relationship of insect opsins of the UV, blue (B) and long wavelength (LW) type inferred by the neighbour joining method. Squid rhodopsin (Rh) was used as the outgroup. Numbers at the branches indicate bootstrap values based on 1000 replicate analyses. Values larger than 70% are shown. Accession numbers are as follows: *Drosophila melanogaster* Rh1, K02315; *D. melanogaster* Rh2, M12896; *D. melanogaster* Rh3, M17718; *D. melanogaster* Rh4, P08255; *D. melanogaster* Rh5, U67905; *D. melanogaster* Rh6, Z86118; *Schistocerca gregaria* LoUV, AB902953; *S. gregaria* Lo1, X80071; *S. gregaria* Lo2, X80072; *Dianemobius nigrofasciatus* UVOP, AB458852; *D. nigrofasciatus* BLOP, AB291232; *D. nigrofasciatus* LW, FJ232921; *Gryllus bimaculatus* OpsinSW, HM363623; *G. bimaculatus* OpsinMW, HM363622; *G. bimaculatus* OpsinLWa, HM363620; *G. bimaculatus* OpsinLWb, HM363621; *Apis mellifera* AmUVop, AF004169; *A. mellifera* AmBLop, AF004168; *A. mellifera* AmLop1, BK005514; *A. mellifera* AmLop2, BK005515; *Papilio xuthus* PxUV, AB028218; *P. xuthus* PxB, AB028217; *P. xuthus* PxL1, AB007423; *P. xuthus* PxL2, AB007424; *P. xuthus* PxL3, AB007425.

non-DRA regions, i.e. the main region of the eye. To uncover possible differences related to lifestyle, we compared data from gregarious and solitarious locusts.

RESULTS

Cloning of UV opsin cDNA

We cloned a cDNA encoding an opsin of an ultraviolet (UV)-absorbing visual pigment from poly-A RNA extracted from the compound eye. Phylogenetic analysis of the sequence we identified using the neighbour-joining method revealed that the cDNA sequence clusters in the UV wavelength-absorbing clade of insect opsins (Fig. 1). The desert locust, therefore, has at least three opsin genes, encoding a long wavelength (Lo1) and a blue-absorbing type (Lo2), which were identified previously (Towner et al., 1997), and a UV-absorbing type (LoUV).

Distribution of opsin mRNAs in the retina

We localized the LoUV, Lo1 and Lo2 mRNA in the retina by double-targeted *in situ* hybridization. We labelled transverse sections of distal and proximal tiers of the retina with probes specific to mRNAs encoding for the three opsins in all combinations (Fig. 2A–E). At the distal tier of the retina (Fig. 2A–C), R7 photoreceptors were labelled by either the LoUV (black arrowheads in Fig. 2A–C) or the Lo2 probe (white arrowheads). Labelling by the Lo2 probe in R7, which expressed solely Lo2, was stronger than that of the larger R2, R3, R5, R6 and R8 photoreceptors (white arrowheads in Fig. 2A). Interestingly, all other photoreceptor cells (R2, R3, R5, R6 and R8) in the distal tier were labelled by both the Lo1 and Lo2 probes in an overlapping manner (Fig. 2A,B). As a result, the appearance of double-labelled photoreceptors was dark red (Fig. 2C). R7 occurred at two different positions within the ommatidia (Fig. 2A–C) but its position was not related to mRNA expression in R7. In the proximal tier (Fig. 2D,E), two additional photoreceptors, R1 and R4 (proximal photoreceptor cells) appeared, whereas R7 disappeared. R1 and R4 were labelled by the Lo1 probe exclusively (Fig. 1D,E, arrowheads). As well as in the distal tier, R2, R3, R5, R6 and R8 were labelled by both the Lo1 and Lo2 probe.

Longitudinal sections showed that the DRA (Fig. 2F–I, surrounded by the interrupted line) was only labelled by the Lo2 probe throughout the entire length of ommatidia. We did not find any labelled cells in the DRA with the LoUV and the Lo1 probes. The labelling pattern in the rest of the eye was rather constant, suggesting that there is no clear regionalization. R7 photoreceptors labelled by the LoUV probe were identified only in the distal retina (Fig. 2F, inset arrows), whereas Lo1 and Lo2 probe labelled throughout the entire length of the ommatidia. The fluorescence image of double labelling with Lo1 and Lo2 probes showed that green opsin (Lo2) was expressed throughout the main retina: the green-induced red fluorescence is due to the dye FastRed (see Materials and methods) (Fig. 2I).

Fig. 2J summarizes the expression of opsin mRNAs on transverse sections. The DRA consisted of only one type of ommatidium expressing the blue opsin mRNA in all photoreceptors. In the main eye, two types of ommatidia were distinguished in accordance with R7 either expressing the UV (type I: solid circle) or blue opsin mRNA (type II: broken circle), respectively (Fig. 2A–C). In both types of ommatidia, receptors R2, R3 and R5–R8 co-expressed blue (Lo1) and green (Lo2) opsin mRNAs, whereas the proximal receptors (R1, R4) contained only green (Lo2) opsin mRNA. The appearance of labelled photoreceptors at different depths of the ommatidia indicates that R7 is a distal photoreceptor, and R1 and R4 are proximal

RESEARCH ARTICLE The Journal of Experimental Biology (2014) doi:10.1242/jeb.108514

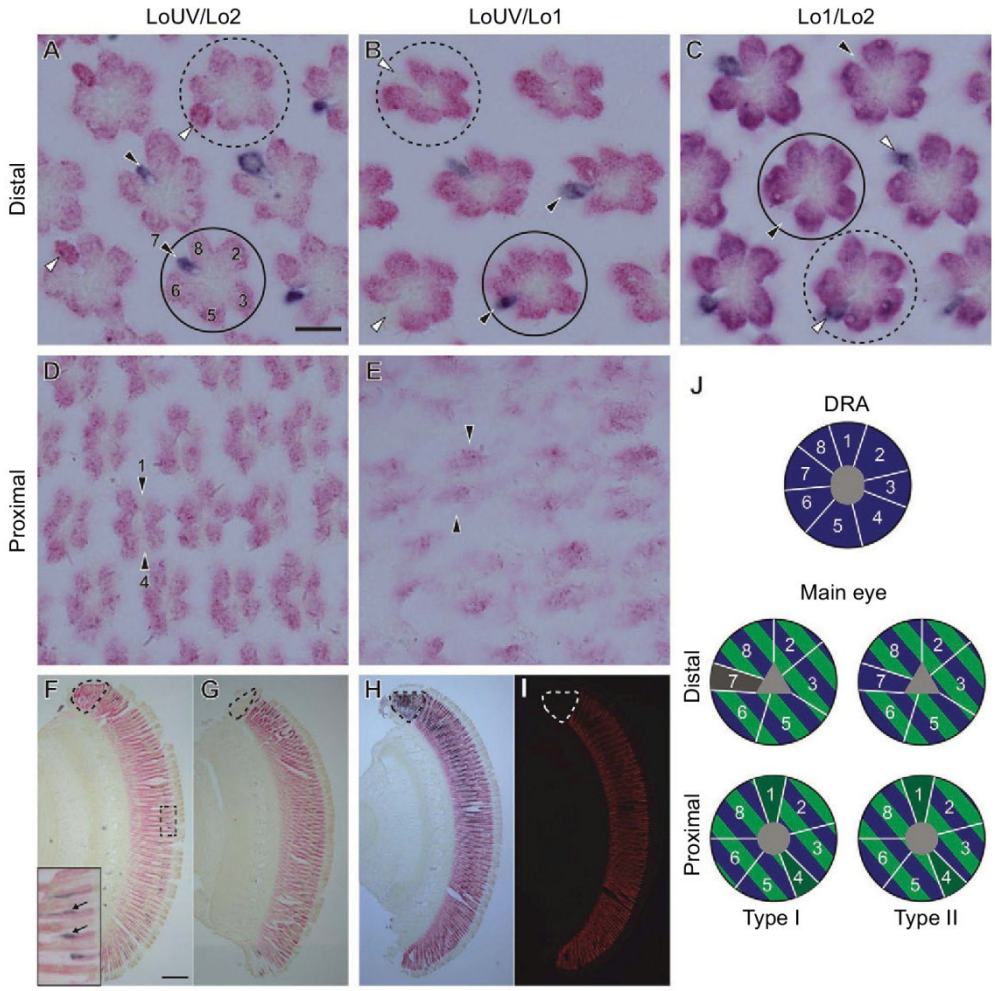

Fig. 2. Localization of opsin mRNAs by double label *in situ* hybridization. Transverse sections (A–E) and longitudinal sections (F–I) were labelled by probes specific to the LoUV (black) and the Lo2 (red) in A, D and F, the LoUV (black) and the Lo1 (red) in B, E and G, and Lo2 (black) and Lo1 (red) in C, H and I. H and I show the same section photographed under regular transmission light (H) and green epi-illumination (I). The distal transverse sections reveal two types of ommatidia indicated by solid circles (type I) and broken circles (type II) in A–C. Numbers in A and D indicate position of each photoreceptor. The distal photoreceptor R7 expresses either LoUV (black arrowheads in A–C) or Lo2 (white arrowheads in A–C). The proximal photoreceptors R1 and R4 (arrowheads in D,E) express only Lo1. The region surrounded by the broken line in transverse sections (F–I) is the DRA. Inset in F is the enlarged image of the distal tier (broken rectangle in F). The top and bottom of images in F–I are dorsal and ventral, respectively. (J) Diagram of *in situ* hybridization labelling patterns of ommatidia in the DRA and distal and proximal tiers of ommatidia in the main retina. In the DRA all photoreceptors express Lo2. In the main retina, the proximal photoreceptors R1 and R4 express Lo1, the distal photoreceptors R2, R3, R5, R6 and R8 co-express Lo1 and Lo2, whereas R7 expresses either LoUV (type I ommatidia) or Lo2 (type II ommatidia). Scale bars, 10 µm (A–E, shown in A) and 200 µm (F–I, shown in F).

photoreceptors. Type I and type II ommatidia were distributed randomly over the main retina in a ratio of 1.8:1.

Electroretinographic recordings

In electroretinographic (ERG) recordings from 28 locusts (13 gregarious and 15 solitarious animals) we investigated the spectral sensitivity of distinct eye regions (Fig. 3). Recordings from the DRA and the dorsal (DA) and ventral (VA) halves of the main retina in gregarious locusts supported the *in situ* hybridization results. The spectral sensitivity of the DRA showed a peak at 430 nm with a shoulder in the UV range at about 350 nm. At longer wavelengths beyond 430 nm, sensitivity decreased strongly, indicating the absence of long wavelength receptors. In the DA, the blue sensitivity peak remained the same, but the sensitivity bandwidth extended into longer wavelengths, indicating the presence of long wavelength-absorbing visual photopigments in the dorsal half of the main retina. Finally, in the VA peak sensitivities occurred broadly at around 350, 450 and 510 nm, indicating the presence of UV, blue and long wavelength-absorbing visual pigments.

The spectral sensitivity of the DRA did not differ between the two locust phases, but phase-dependent differences occurred in the DA and VA. In the DA of solitarious animals the peak sensitivity was slightly shifted to longer wavelengths (470 nm), suggesting a higher contribution of long wavelength receptors. In the VA of solitarious locusts the peak sensitivity was even further shifted into the green range (510–530 nm) and decreased strongly in the UV, suggesting low contribution of UV receptors.

Single-cell recordings

In intracellular recordings we investigated the spectral sensitivity, response–stimulus intensity functions, and polarization sensitivity of photoreceptors in the DRA (Fig. 4) and compared these data with recordings from the main eye (non-DRA receptors). Dye injection into the recorded cell allowed us to identify the photoreceptor within the DRA ommatidium (Fig. 4G).

Spectral sensitivity of single photoreceptors

Spectral sensitivity tested in recordings from over 100 gregarious and 24 solitarious locusts revealed three types of spectral receptors, peaking in the UV, blue or green region of the spectrum. Whereas only blue peaking cells were found in the DRAs of both phases, all three spectral types occurred in the main eye. In the main eye of gregarious locusts, peak sensitivities were found most frequently in the blue wavelength range around 410–450 nm and in the green spectrum at 530 nm. In solitarious locusts, likewise, peaks occurred in the long wavelength range around 530 nm but peaks in the blue spectrum were often shifted to longer wavelengths around 470 nm (Fig. 5).

Spectral recordings from the main retina were sorted into groups of 310–390 nm, 410–490 nm and 510–630 nm peak sensitivity. Averaged relative spectral sensitivities were calculated for those groups (Fig. 6). To estimate λ_{max} values and relative contributions of green and blue opsins in non-DRA photoreceptors, we fitted visual pigment absorption spectra to the absorbance spectra using the Govardovskii et al. (Govardovskii et al., 2000) template (Fig. 6).

RESEARCH ARTICLE The Journal of Experimental Biology (2014) doi:10.1242/jeb.108514

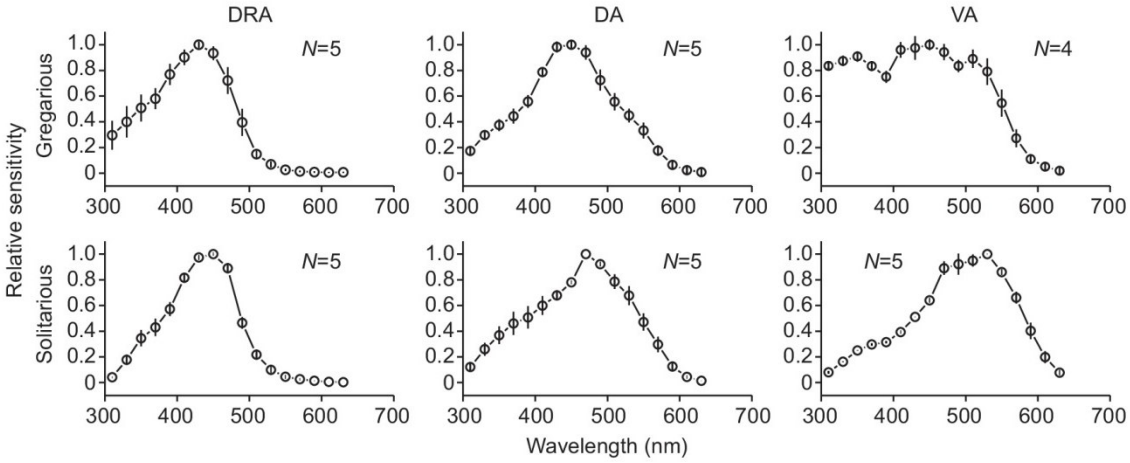

Fig. 3. ERG-determined spectral sensitivity curves from distinct eye regions in gregarious and solitarious locusts. Averaged data ± s.e.m. from ERG recordings in the DRA (*N*=5 animals, 23 and 21 recordings), and dorsal (DA; *N*=5 animals, 20 and 13 recordings) and ventral (VA; *N*=4 resp. 5 animals, 12 and 20 recordings) halves of the main eye. In both phases the DRA is mainly sensitive in the blue spectrum, whereas green sensitivity increases towards ventral eye regions. In the solitarious phase this green shift is more dominant than in the gregarious phase. In addition, the VA of gregarious animals shows high sensitivity in the UV.

The spectral sensitivities of the DRA blue receptors were best fitted by absorption spectra of a visual pigment with λ_{max} of 442 nm (Fig. 6A, gregarious locusts), resp. 437 nm (Fig. 6A′, solitarious locusts). Template fitting of the green peaking receptors yielded a λ_{max} of 516 nm (Fig. 6B, gregarious locusts), resp. 511 nm (Fig. 6B′, solitarious locusts), although with relatively low R^2 values. Poor matching with the template was especially obvious in the short wavelength range. Based on the *in situ* hybridization data suggesting co-expression of blue and green opsins in the main eye, we therefore fitted a mixture of blue and green templates based on the fitting results in Fig. 6A,B and 6A′,B′, respectively, to the green peaking spectra (Fig. 6C,C′). Best fits with improved R^2 values were obtained by a relative contribution of 16:84 (relative amplitude λ_{max} blue: λ_{max} green) for gregarious and 23:77 (blue:green) for solitarious locusts. Blue peaking receptors in the main eye region (Fig. 6D,D′) were best fitted by a ratio of 90:10 (blue:green) for gregarious, and 46:54 (blue:green) for solitarious locusts. The UV receptor was best fitted by an absorption spectrum with λ_{max} of 339 nm (Fig. 6F). Because the confidence intervals of λ_{max} values for green and blue visual pigments showed considerable overlap between gregarious and solitarious locusts, suggesting that their opsins are identical, we pooled the data of DRA blue and non-DRA green-peaking receptors from both phases and obtained best fits with peak absorbances at 441 nm (R^2=0.96) for the blue and 514 nm (R^2=0.83) for the green opsin (Fig. 6F).

V–log *I* functions

Mean V–log I curves were determined for DRA receptors and green and blue peaking receptors of the main eye of both locust phases. In both phases, the V–log I curves of DRA receptors were shifted to

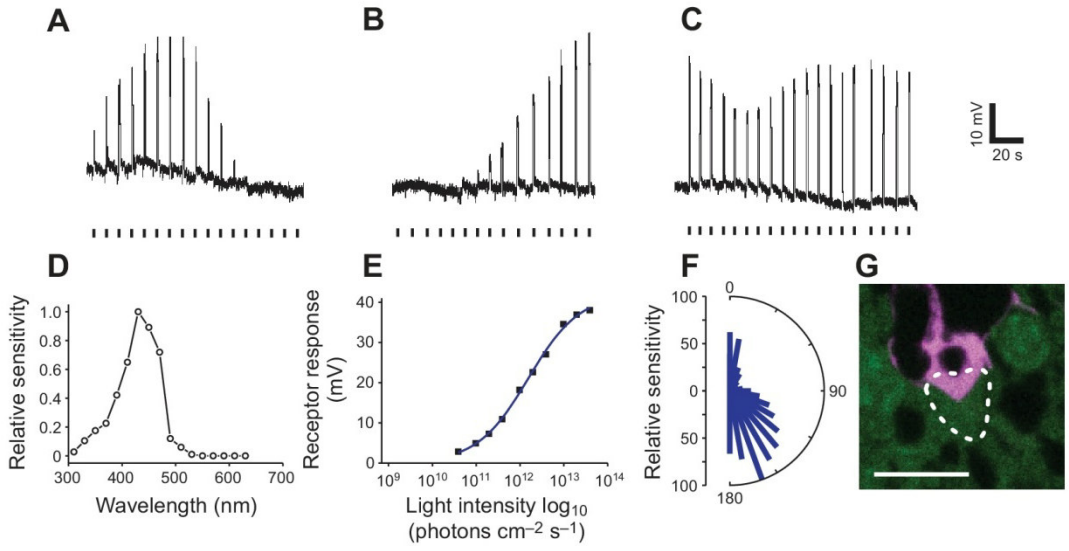

Fig. 4. Complete set of electrophysiological data from an R7 photoreceptor in the DRA. (A,D) Spectral sensitivity; (B,E) intensity response relationship; (C,F) polarization sensitivity. A–C show original recording traces and D–F the corresponding graphs. (A) Spectral testing was always the first step to determine receptor spectral type. (B) To calculate relative sensitivities the receptor response curve was measured with the wavelength causing the strongest receptor response (here 430 nm). (C) The same wavelength was used for POL testing. (G) Following tracer injection, the recorded photoreceptor was identified by fluorescence microscopy of ommatidial cross-sections. The white dotted line indicates the perimeter of the rhabdom (R). Scale bar, 5 µm.

RESEARCH ARTICLE The Journal of Experimental Biology (2014) doi:10.1242/jeb.108514

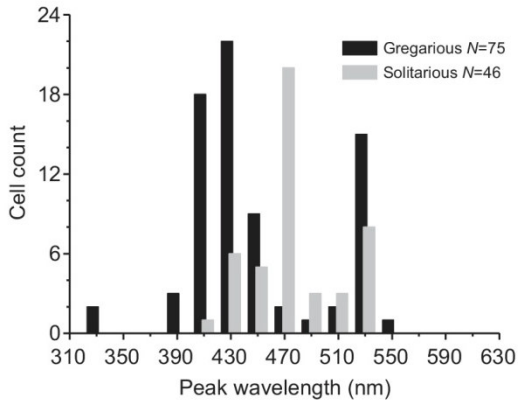

Fig. 5. Spectral sensitivity peaks in the main retina of gregarious and solitarious locusts. Data originate from single-cell recordings. Peak sensitivities occur around 430 and 530 nm in gregarious locusts. In solitarious animals peaks in the green are likewise around 530 nm, but in the blue are shifted towards longer wavelengths around 470 nm, indicating a difference in spectral sensitivity between the gregarious and solitarious phases.

higher light intensities (high K) and were steeper than the non-DRA curves (Fig. 7). To analyse possible differences in the relative sensitivities of DRA and non-DRA receptors, we compared two parameters of the V–log I functions: light intensity at half-maximal receptor excitation and the exponential slope (K and n in the Naka–Rushton equation). Blue peaking recordings from the DRA and blue- and green peaking recordings from the main retina (non-DRA) were grouped and compared with each other. Significant differences were found for K and n between the DRAs and main retinae, whereas the two locust phases did not differ from each other (Fig. 8).

K values did not differ statistically between DRA and non-DRA blue peaking receptors in gregarious and solitarious locusts, but in both phases they were significantly lower in non-DRA green peaking receptors than in DRA blue receptors. Values of n were significantly higher in both locust phases in DRA receptors compared with non-DRA receptors. No differences were found between blue peaking and green peaking cells in the main retina.

Polarization sensitivity

Polarization sensitivity was tested in 26 recordings from gregarious locusts and 43 recordings from solitarious locusts. During stepwise rotation of the polarizer, the amplitude of receptor responses was modulated sinusoidally as illustrated in the circular graphs in Fig. 9B,C,E. The strength of this modulation was calculated as the PS value. In gregarious locusts, PS values in the DRA ranged from 2.4 to 22.4 (N=16), confirming the role of DRA photoreceptors as detectors of polarized light (Fig. 9D). Dye injection showed that all eight receptors in DRA ommatidia had high PS values, despite differences in size and orientation of their rhabdomeres (Fig. 10). In contrast, PS values of non-DRA blue and green peaking receptors were well below 3 (non-DRA blue peaking receptors: PS=1.9–2.3, N=10; non-DRA green peaking receptors: PS=2–2.2, N=2; Fig. 9A).

In DRA photoreceptors of solitarious locusts, a higher number of PS values below 3 was found in addition to high values above 20 (DRA: range 1.3–31.7, N=9; Fig. 9D). The distribution of PS values in non-DRA photoreceptors was similar to that in gregarious locusts (non-DRA blue peaking receptors: PS=1.3–3.8, N=35; non-DRA green peaking receptors: PS=1.4–2.3, N=6; Fig. 9A). No test for polarization sensitivity was achieved for UV cells.

Cell identity

DRA photoreceptors of gregarious locusts were identified through neurobiotin injection. Cell numbering in DRA ommatidia of locusts is based on the position of crystalline cone threads (Homberg and Paech, 2002). Although these structures cannot be observed under confocal laser microscopy, another important landmark, photoreceptor R7, could be identified based on its position opposing the other photoreceptors in DRA ommatidia (Homberg and Paech, 2002). Data from right eyes were mirrored to fit to left eye conditions before cell numbering.

For further assurance that physiological responses originated from the actually stained cell, POL responses were compared with microvilli orientation, taking into account the position of the locust in the experimental setup. If E-vector orientation at maximum receptor response was identical with microvilli orientation of the labelled receptor cell, correct assignment of physiological and anatomical data was assumed. Further indicators for distinguishing receptors were position of the ommatidium in the DRA, size and orientation of cell body and rhabdomere and position of the stained cell within the ommatidium.

In the DRA of gregarious locusts, six of the eight photoreceptor cells could be identified by single-cell staining (R1=1, R2=6, R3=4, R6=2, R7=14, R8=2; Fig. 10). Staining of R4 (N=1) and R5 (N=1) included secondary fainter staining from other photoreceptor cells (for explanation, see Fig. 10).

DISCUSSION

We have characterized the functional organization of the DRA and the main retina in the desert locust through opsin gene expression, ERG and intracellular recordings. The data show that the DRA of the eye exclusively contains blue receptors with high polarization sensitivity. In the main retina of gregarious animals two types of ommatidia exist. Both types contain two proximal green receptors and five receptors that co-express blue and green opsins. The eighth receptor is a distal photoreceptor and expresses either blue or UV opsin. The two types of ommatidia are randomly distributed throughout the main retina. ERG and intracellular recordings revealed spectral sensitivities supporting the opsin gene expression data. Solitarious locusts differed from gregarious animals by a lower contribution of UV sensitivity in the ventral eye and an increase in green sensitivity throughout the eye.

Opsin expression and ommatidial organization

We identified a novel opsin of a UV-absorbing visual pigment (LoUV) in the retina of the desert locust, in addition to previously characterized (Towner et al., 1997) long wavelength (Lo1) and blue-absorbing types (Lo2). Desert locusts, therefore, have three distinct visual pigments like many other insect species (Briscoe and Chittka, 2001). We have predicted the possible absorbance spectra of these visual pigments based on the physiologically determined spectral sensitivities of photoreceptors. It thus appears that LoUV is a visual pigment (P) with an absorption peak at 339 nm (P339), Lo1 is a P514 and Lo2 is a P441. The distribution of opsin gene expression is strikingly different in the DRA and main retina. All photoreceptors of DRA ommatidia exclusively express the blue-sensitive Lo2, underscoring homochromacy throughout this polarization-sensitive eye region.

In contrast to the DRA, opsin gene expression in the main eye is not identical in all ommatidia. Ommatidial structure in the main eye is similar to that of the migratory locust *Locusta migratoria* (Wilson et al., 1978) with five photoreceptors (R2, R3, R5, R6, R8) contributing microvilli throughout the length of the rhabdom, a

RESEARCH ARTICLE The Journal of Experimental Biology (2014) doi:10.1242/jeb.108514

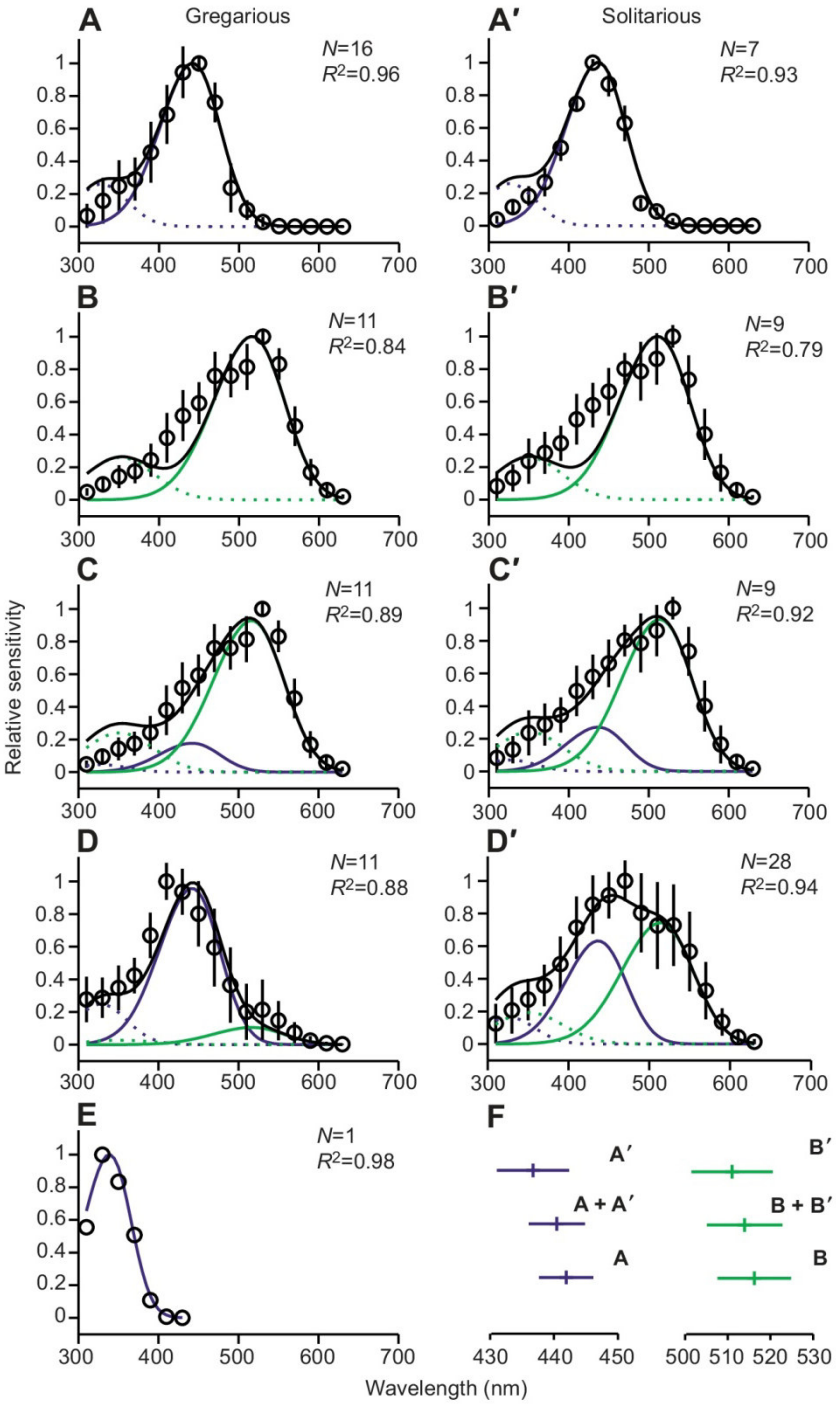

Fig. 6. Spectral sensitivity curves from different receptor types, based on intracellular recordings from gregarious and solitarious locusts. Data are sorted into DRA receptors (A,A′), non-DRA green (B,B′,C,C′) and non-DRA blue (D,D′) peaking receptors of gregarious (A–D) and solitarious (A′–D′) locusts. Open circles mark relative absorbances, averaged across *N* receptors and normalized to the value at the dominant peak wavelength (error bars: s.d.). The continuous black lines show fits of visual pigment-absorbance templates (see text). The goodness of fits is indicated by R^2 values. The continuous (dashed) lines in green and blue illustrate the fits' sub-templates for the α- (β-) bands of 'blue' and 'green' sensitive components, scaled to their relative contribution to the fit. Non-DRA green receptors are better described by inclusion of a blue component (C,C′) than by a green component alone (B,B′). (E) The relative sensitivity of a UV receptor could be measured only for one cell in a gregarious locust. (F) DRA blue and non-DRA green receptors do not differ between the two phases, as reflected by the 95% confidence intervals of their fitted dominant peak wavelengths. When pooling the data from gregarious and solitarious animals, peak absorbances of 441 nm (blue) and 514 nm (green) were obtained.

slightly smaller distal photoreceptor R7, and two proximal photoreceptors R1 and R4. This organization is reflected by opsin gene expression. In the main eye, receptors R2, R3, R5, R6 and R8 co-express Lo2 and Lo1, favouring a role in colour-blind motion detection, intensity coding and vision at low light levels. In contrast, the distal photoreceptor R7 expressing Lo2 or LoUV together with the two proximal photoreceptors R1 and R4 expressing Lo1 may constitute a trichromatic colour vision system operating at high light intensities. Behavioural studies supporting this hypothesis, however, are still missing. The two types of ommatidia differing in spectral types of R7 were stochastically distributed throughout the main eye without showing a dorsal–ventral gradient. Randomly distributed heterogeneous ommatidia were also found in the main retina of honeybees (Wakakuwa et al., 2005) and the Japanese yellow swallowtail and monarch butterflies (Arikawa, 2003; Sauman et al., 2005). However, in some other Lepidoptera (e.g. Sison-Mangus et al., 2006; Awata et al., 2010), Diptera (e.g. Hu et al., 2011) and the two-spotted cricket (Henze et al., 2012), a dorsal–ventral gradient or regionalization was found with higher expression of long-wavelength opsins in ventral eye regions.

Spectral sensitivity

The distribution of three opsins in the locust retina is matched by spectral sensitivity profiles of photoreceptors as determined in ERG and intracellular recordings. In addition to narrowly tuned blue receptors in the DRA, we found in the main retina a UV peaking cell,

RESEARCH ARTICLE The Journal of Experimental Biology (2014) doi:10.1242/jeb.108514

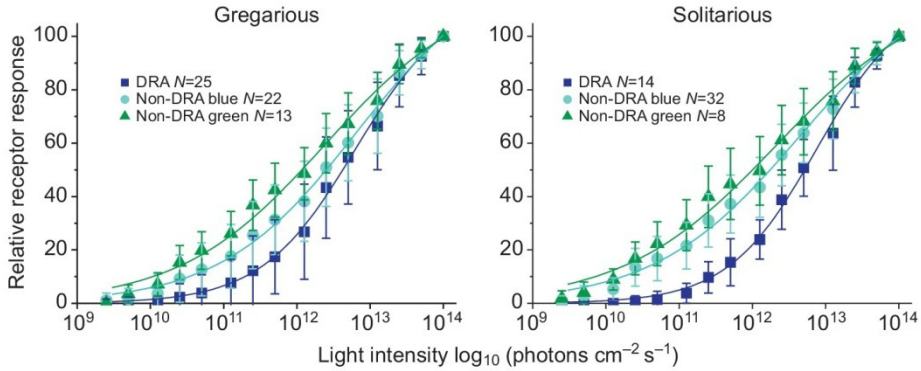

Fig. 7. Mean (±s.d.) relative *V*–log *I* curves from different receptor types of both locust phases. Data from DRA receptors (blue squares), non-DRA blue receptors (light blue circles), and non-DRA green receptors (green triangles) are compared. In both phases, the *V*–log *I* curves from DRA receptors are shifted to higher light intensities (high *K*) and are steeper than the non-DRA curves.

broadly sensitive blue peaking photoreceptors with shoulders of variable amplitude in the green, and photoreceptors with peak sensitivities in the green with a shoulder in the blue range (Fig. 6). Visual pigment template fits suggest that both the blue and green peaking photoreceptors contain a mixture of Lo1 and Lo2 opsins, albeit at different ratios. Narrowly tuned blue peaking receptors were not encountered in the main retina, suggesting that recordings from the Lo2 (blue opsin)-expressing photoreceptor R7 were not successful. Likewise, no narrowly tuned green receptors were found in the main retina, suggesting that recordings from the green opsin-expressing proximal photoreceptors were not successful. Broadband blue and green receptors have also been found in the compound eye of the migratory locust *L. migratoria* (Bennett et al., 1967; Vishnevskaya et al., 1986). Bennett et al. (Bennett et al., 1967) found considerable variation in the relative amplitude of green and blue peaks among different recorded cells and concluded that these locust receptors probably contain more than one opsin at different concentrations. This conclusion has long been obscured by the 'one cell-one pigment' dogma that has developed in recent years (Stavenga and Arikawa, 2008). The present study provides the first molecular as well as physiological evidence to support the conclusion of Bennett et al. (Bennett et al., 1967) after almost half a century.

A trichromatic set of UV, blue and green receptors is the most common state in insects (Briscoe and Chittka, 2001), whereas receptors containing more than one opsin have been reported only recently (Kitamoto et al., 1998; Arikawa et al., 2003; Mazzoni et al., 2008; Awata et al., 2010; Hu et al., 2011; Ogawa et al., 2012). Whereas in most cases two opsins of similar absorption spectra are co-expressed, combinations of UV and blue opsins have been reported in the mosquito *Aedes* and the butterfly *Parnassius* (Awata et al., 2010; Hu et al., 2011). The co-expression of blue and green opsins in five out of eight photoreceptors per ommatidium (which results in broad spectral sensitivity curves) may be an adaptation to low light conditions. Blue light around 460 nm, matching the ERG spectral peak sensitivity in the dorsal eye, is dominant in sky light at dusk (Lythgoe, 1979).

In many insect species ventral eye regions are more sensitive to longer wavelengths (Awata et al., 2010). ERG recordings indicate that this is also the case for *S. gregaria*, especially in solitarious animals. In contrast, a dorsal–ventral gradient was not found in the pattern of opsin gene expression, but because *in situ* hybridization may not precisely reflect quantitative gene expression levels, it is conceivable that a dorsal–ventral gradient of Lo1/Lo2 ratio in R2, R3, R5, R6 and R8 does exist. High green sensitivity in ventral eye regions is probably linked to the detection of vegetation that reflects more green than UV (Schwind, 1983) or to the detection of the horizon (Stange, 1981). Behavioural experiments on ants, likewise, imply a functional regionalization of the eye in the DRA, DA and VA related to orientation tasks (Wehner, 1982; Fent, 1985).

Explanations for the high UV sensitivity in the VA of gregarious animals (Fig. 3) remain speculative. The amount of expressed UV opsin as well as increased UV receptor length and cross-section might account for the high UV sensitivity, but none of these possible factors has been examined.

V–log *I* curves

Higher *K* values imply that DRA receptors require more photons to be equally excited than non-DRA receptors, which therefore makes

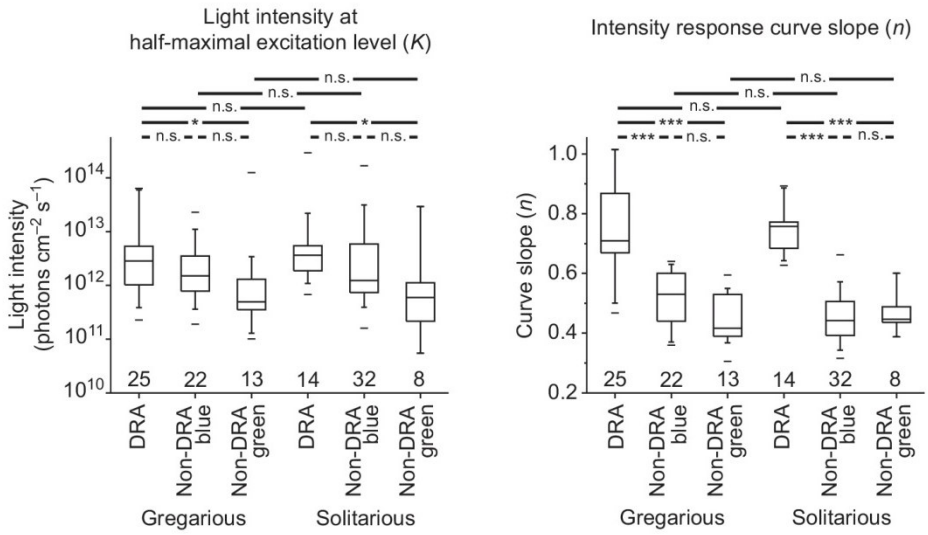

Fig. 8. Box plot diagrams comparing *K* and *n* values from different receptor types and eye regions in both locust phases. Significant differences were found for *K* values between DRA blue and non-DRA green receptors and for *n* values between DRA and non-DRA receptors (Kruskal–Wallis tests for *K* and one-way ANOVA with following Scheffé *post hoc* analysis for *n*; n.s., not significant; **P*<0.05, ****P*<0.001).

RESEARCH ARTICLE The Journal of Experimental Biology (2014) doi:10.1242/jeb.108514

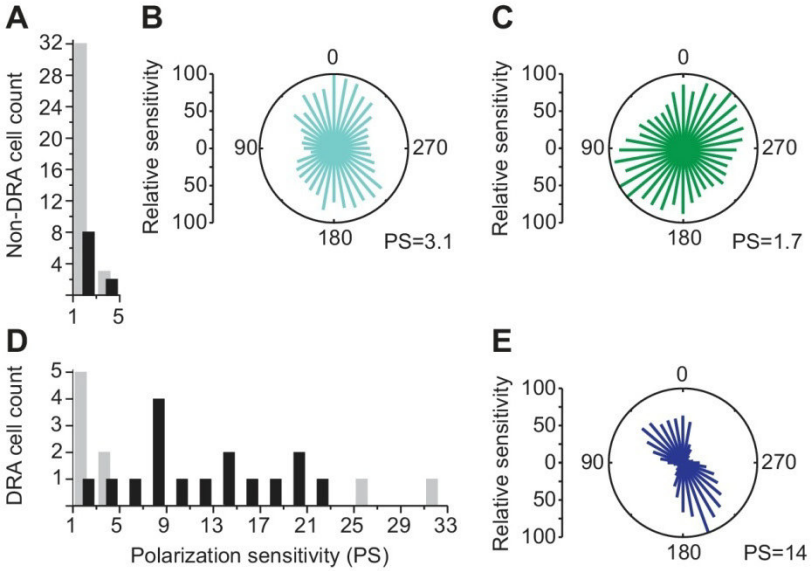

Fig. 9. Polarization sensitivities of photoreceptors in the DRA and main eye of gregarious and solitarious locusts. (A,D) Histograms of PS values. Data from gregarious locusts are shown in black, data from solitarious locusts in light grey. (B,C) Circular plots of POL responses of a non-DRA blue receptor (B) and a non-DRA green receptor (C). (E) Circular plot of POL responses of a blue receptor in the DRA.

them less sensitive. The reason for this condition might be the short rhabdom of DRA compared with non-DRA ommatidia (Wilson et al., 1978; Homberg and Paech, 2002). Two considerations, however, suggest that DRA receptors might actually be more sensitive. Firstly, owing to larger acceptance angles, DRA receptors are likely to collect more photons than non-DRA receptors with small visual fields (Zufall et al., 1989; Labhart et al., 1984). Thus DRA receptors may need more photons from a point light source to be excited than non-DRA receptors, but under a wide field stimulus, like the sky, they would actually collect more photons. Anatomical data suggest that this is the case in the locust (Homberg and Paech, 2002; Wilson et al., 1978). Secondly, DRA receptors have microvilli with parallel orientation, being more sensitive to E-vectors in parallel to the microvilli than to orthogonal E-vectors. V–log I curves were recorded while stimulating with unpolarized light. Because non parallel E-vector orientations are less effectively detected by DRA receptors they would appear to be less sensitive to unpolarized light than non-DRA receptors under otherwise similar conditions.

The exponential slope of the V–log I curve, n, determines the sensitivity of a photoreceptor to differences in light intensity. The steeper slope (larger n) in DRA versus non-DRA receptors indicates a smaller total response range in DRA receptors than in non-DRA

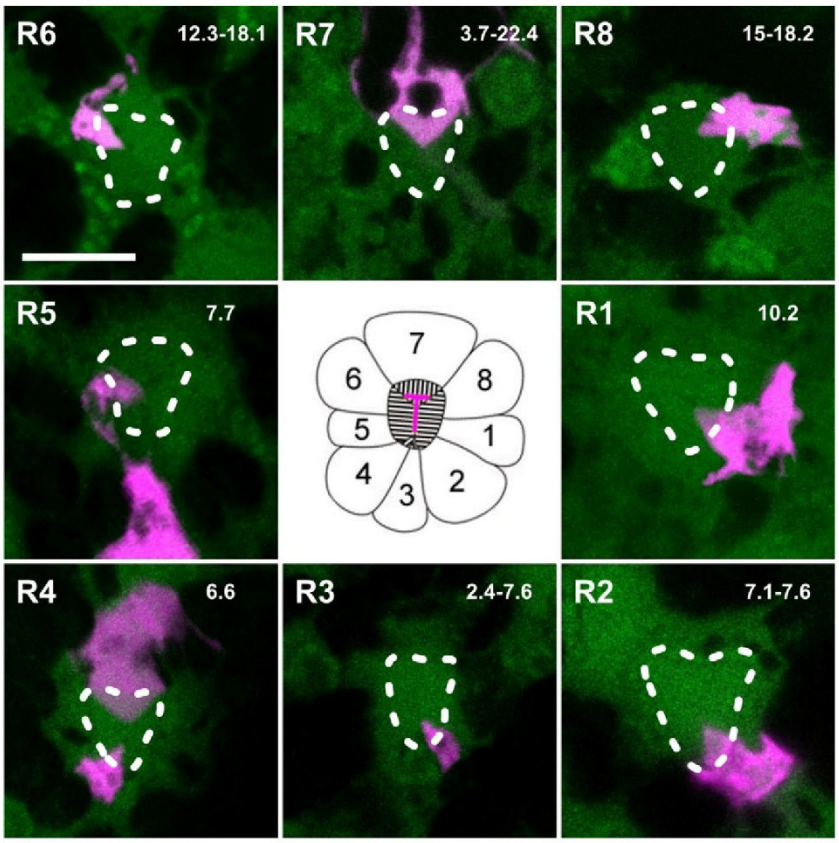

Fig. 10. Confocal laser scanning images of stained single DRA receptor cells of gregarious locusts. Stained cells (magenta) from the right eye (R3, R4, R7) are shown as mirror images to correspond to data from the left eye. Numbers in the upper right of the images indicate range of recorded PS values in this cell type. Only R4 could not be labelled individually. The Φ_{max} orientation of this recording showed best fit to the microvilli orientation of the R4 cell, hence this cell is considered to be recorded from. Additional staining in the image of R5 belongs to an R7 from a neighbouring ommatidium. Scale bar, 5 µm.

RESEARCH ARTICLE The Journal of Experimental Biology (2014) doi:10.1242/jeb.108514

receptors. This may contribute to the narrow intensity-dependent response range found in polarization-sensitive interneurons in crickets (Labhart, 1988) and locusts (Kinoshita et al., 2007), which above a certain light level signal E-vector orientation independent of light intensity.

Differences in the slope of V–log I curves have also been found between light- and dark-adapted photoreceptors in *L. migratoria* and other insects (Matić and Laughlin, 1981). *L. migratoria* receptor response curves were steeper in the light-adapted state with n up to 1, than in the dark-adapted state with n up to 0.6, which corresponds to values in the desert locust (Fig. 7).

Polarization sensitivity

High PS values (>4) were only found in the DRA, supporting ultrastructural (Homberg and Paech, 2002) and behavioural evidence (Mappes and Homberg, 2004) for the role of the DRA in celestial E-vector detection. Apparently all DRA photoreceptors contribute to high polarization sensitivity including receptors R3 and R4 which, based upon irregularities in microvillar alignment, were hitherto assumed to have low polarization sensitivity (Homberg and Paech, 2002). PS values below 3 measured in some recordings might, instead, result from damaged receptor cells during the experimental procedure. The expression of Lo2 (blue) opsin and peak sensitivity in the blue (441 nm) are consistent with data from Eggers and Gewecke (Eggers and Gewecke, 1993) but the presence of UV receptors in the DRA as reported by the same authors could not be confirmed.

The spectral sensitivity of polarization-sensitive photoreceptors differs considerably among different insect species. POL sensitivity in the green spectrum has been linked to greenish light conditions under tree canopies (Hegedüs et al., 2006). UV and blue POL sensitivity is more likely to be an adaptation to conditions under the free sky. Several authors have discussed that POL vision in the blue instead of the UV might be advantageous for insects active under crepuscular conditions (Labhart et al., 1984; Zufall et al., 1989; Horváth and Varjú, 2004). The sky polarization pattern is most stable in the UV and also reliable under cloudy conditions (Barta and Horváth, 2004). However, overall sky radiance is weaker in the UV than at longer wavelengths (Lythgoe, 1979; Johnsen et al., 2006), favouring blue receptors for animals that navigate at low light levels. POL vision of solitarious desert locusts follows this logic, and the phase change to the day-active gregarious phase might not have altered the spectral sensitivity of the DRA.

Phase-dependent differences in spectral sensitivity

Various differences in the visual system of solitarious and gregarious locusts have been reported, including differences in eye size, number of ommatidia and sensitivity to motion stimuli (Matheson et al., 2004; Ott and Rogers, 2010; Rogers et al., 2010; Gaten et al., 2012), while polarization-sensitive interneurons were not noticeably affected by locust phase (el Jundi and Homberg, 2012). Here we show differences in photoreceptor spectral sensitivities, particularly in the ventral eye as revealed by ERG recordings and in peak wavelength of blue peaking receptors found in intracellular recordings. Judged from the *in situ* hybridization data, the high UV sensitivity in the ventral eye of gregarious animals, measured by ERGs, cannot be explained by changing receptor occurrences but may result from differences in rhabdomere lengths and cross-sections in different eye regions which were not studied here. In addition, differences in the relative concentrations of Lo1/Lo2 opsins may underlie not only the sensitivity differences in the blue–green range between dorsal and ventral eye regions but also the differences in the sensitivities between the phases.

Provided that the same opsin genes are expressed in solitarious and gregarious animals, the visual pigment template fits indicate that especially in blue peaking receptors, the contributions of Lo1 and Lo2 opsins are strikingly different between the two phases, resulting in a considerable shift of absorption curves to longer wavelengths in solitarious animals (Fig. 6D,D′). An alternative explanation for these differences may be circadian rather than phase-dependent changes, because gregarious locusts were tested during the day and solitarious locusts in their activity phase during the night. Diurnal and circadian changes in photoreceptor sensitivity and microvillar membrane turnover have been detected in various insect species, including locusts (e.g. Horridge et al., 1981; Fleissner, 1982). Light-induced movement of visual pigment and circadian changes in visual pigment levels have been demonstrated in mosquito photoreceptors (Hu et al., 2012). Differing secondary green sensitivity in the locust might, therefore, not be phase dependent, but daytime dependent. If so, however, circadian effects would have to be restricted to blue and green peaking receptors of the main eye, because we did not detect corresponding differences in the DRA.

MATERIALS AND METHODS

Animals

Adult male and female locusts (*Schistocerca gregaria*) were obtained from breeding colonies at the University of Marburg. Gregarious animals were kept crowded at 12 h:12 h light:dark cycle, 28°C room temperature and 50% relative humidity. Solitarious animals were reared individually in small boxes at 12 h:12 h light:dark cycle, 26.5°C and 60% relative humidity following the conditions established by Roessingh et al. (Roessingh et al., 1993). In particular, no visual, olfactory and mechanical contact occurred between individuals. Animals used for experiments had been reared in solitarious conditions for at least three generations. Typical morphological characteristics such as body colouration and size (Simpson et al., 1999; el Jundi and Homberg, 2012) served as indicators for the solitarious phase of the animals. Only locusts at least 1 week after imaginal moult were used for experiments.

Molecular cloning

Poly-A RNA was extracted from the eyes of gregarious animals using a QuickPrep micro mRNA purification kit (GE Healthcare, Uppsala, Sweden). To amplify fragments of cDNAs encoding opsins of the UV class, we carried out RT-PCR using degenerate primers designed based on consensus sequences of short wavelength (UV and blue) absorbing opsins of insects identified so far. The full-length cDNAs were obtained by the 5′- and 3′-RACE (rapid amplification of cDNA ends) methods. Both PCR and RACE products were purified, cloned using a TOPO TA cloning kit (Invitrogen, Carlsbad, CA, USA) and sequenced using ABI3130xl and BigDye terminator v1.1 (Applied Biosystems, Warrington, UK). The obtained sequences were aligned with others and processed for phylogenetic analysis by the neighbour-joining (NJ) protocols in MEGA 5.2.2 software with a bootstrap of 1000 replicates and a Poisson model for amino acid substitution.

In situ hybridization

We performed double-targeted *in situ* hybridization on paraffin sections as described previously (Awata et al., 2010). Digoxigenin and biotin labelled RNA probes were synthesized from linearized plasmids carrying the partial sequences of coding regions (Lo1: 1003 bp; Lo2: 948 bp; LoUV: 929 bp) of the mRNAs encoding the Lo1, Lo2 and LoUV opsins by *in vitro* transcription.

The compound eyes of gregarious *S. gregaria* were fixed in 4% paraformaldehyde in 0.1 mol l^{-1} sodium phosphate buffer (pH 7.2) and embedded in paraffin. The paraffin-embedded eyes were sectioned at 6 µm thickness with a rotary microtome. The sections were first de-paraffinized and treated with hybridization solution at 45°C containing 0.5 µg ml^{-1} of the mixture of two cRNA probes, one labelled with digoxigenin and another labelled with biotin, which were hybridized to different opsin mRNA. After the hybridization process, the digoxigenin-labelled probes were first detected

RESEARCH ARTICLE The Journal of Experimental Biology (2014) doi:10.1242/jeb.108514

using anti-digoxigenin antibody conjugated to alkaline phosphatase and then visualized using 4-nitroblue-tetrazolium chloride and 5-bromo-4-chloro-3-indolyl phosphate. The sections were briefly washed and treated with 100 mmol l^{-1} glycine solution (pH 2.2) to remove the unbound anti-digoxigenin antibody. The hybridized biotin-labelled probes were detected using streptavidin-alkaline phosphatase conjugate and visualized using Fast Red (Roche, Mannheim, Germany). The numbering of photoreceptor cells in ommatidia of the ordinary eye region corresponds to that used for *L. migratoria* (Wilson et al., 1978).

Electrophysiology and visual stimulation

Animals were immobilized by cutting off their legs and wings. They were mounted with wax to a metal holder and placed in the centre of an electrophysiological recording set-up. Experiments on gregarious animals were performed during the day and experiments on solitarious animals during the night. Photoreceptors were studied through ERG and intracellular recordings. For differential ERG recordings, a silver wire electrode (diameter 75 µm, Teflon coated; Science Products, Hofheim, Germany) was inserted into each eye. A third silver wire in the head capsule served as reference electrode. Responses were amplified 100× by an AC pre-amplifier (P55, Grass-Telefactor, West Warwick, RI, USA). Light stimuli were presented to one eye through the end of a light guide. To detect regional differences in spectral sensitivity, parts of the eye were covered with black paint (Decormatt Acryl, Marabu, Bietigheim-Bissingen, Germany) leaving out either the dorsal rim area (DRA), the dorsal area (DA), or the ventral area (VA) of the main retina.

For intracellular recordings, glass microelectrodes were drawn from borosilicate capillaries (inner diameter, 0.75 mm; outer diameter, 1.5 mm; Hilgenberg, Malsfeld, Germany) using a Flaming/Brown horizontal puller (P-97, Sutter Instruments, Novato, Canada). Electrode tips were filled with 4% neurobiotin (Vector Laboratories, Peterborough, UK) in 1 mol l^{-1} KCl and backed up with 3 mol l^{-1} KCl. Electrodes had resistances of 30–100 MΩ and were inserted into the region of interest through a small hole cut into the cornea. A silver wire inserted into the head of the locust served as the indifferent electrode. Signals were amplified 10× (BA-01X, NPI, Tamm, Germany), digitized at a sampling rate of 2 kHz (Digidata 1322A, Axon Instruments, Union City, CA, USA), and stored on a PC using Spike2 (Cambridge Electronic Design, Cambridge, UK) or pCLAMP10 software (Molecular Devices, Sunnyvale, CA, USA).

Monochromatic light stimuli were provided by a 75 W xenon arc lamp (L.O.T.-Oriel, Darmstadt, Germany). Light passed a monochromator (Omni-λ150, LOT-Oriel; bandwidth 10 nm), a neutral density wedge, adjusted to each wavelength to guarantee equal photon flux, and a set of filter wheels (Lambda 10-3, Sutter Instruments) containing neutral density filters (quartz glass; 2×50%, 10%, 1%, 0.1% and 0.01% transmission; L.O.T.-Oriel). Light was finally directed via a light guide (quartz glass; Schott, Mainz, Germany) positioned close to the locust's eye (angular extent at the eye 3 deg). A linear polarization filter (HNP'B, Polaroid, Cambridge, UK) could be moved in front of the light guide. The light guide and polarizer were fixed to a perimeter arm and could thus be moved around the locust with its head in the centre. The monochromator, wedge, filter wheels and polarizer were controlled via custom-programmed PC software.

Continuous flashes of white light were presented to the animal (duration 200 ms, pause 1 s), while advancing the electrode through the tissue. Penetration of a photoreceptor cell was indicated by a characteristic drop in baseline voltage followed by graded depolarizations in response to the light flashes. After penetrating a cell, the light guide was moved to the centre of the receptor's visual field, indicated by maximum response amplitude. To test for spectral response, a series of 17 monochromatic light flashes of equal quantal flux were given, starting from 310 nm to 630 nm in 20 nm steps. In some cases this procedure was repeated in the opposite direction from 630 to 310 nm. Light intensity was adjusted individually for each spectral test series to elicit response amplitudes within the estimated dynamic range of the intensity response curve. Light flash duration was 500 ms. Pauses between the flashes were 7 or 10 s in intracellular recordings and 10 or 30 s in extracellular ERG recordings.

For testing polarization response the polarizer was moved in front of the light guide and was rotated in 10 deg steps through 180 or 360 deg. While the polarizer was stationary a light flash of the most sensitive wavelength was presented (duration 500 ms, pause 10 or 15 s). As in the spectral test, light intensity was chosen to elicit response amplitudes within the dynamic range of the intensity response curve. Before starting the stimulus series, two flashes of polarized light (0 deg) were given to eliminate adaptation effects. All experiments were performed in a darkened room.

Intensity response curves (V–log I) were obtained by presenting flashes of the most effective stimulus wavelength for the penetrated cell in 14 steps of increasing intensities over 4.6 log units. Maximum light intensity in the UV range (310–350 nm) was 2.8×10^{13} photons cm^{-2} s^{-1}, in the blue range (410–450 nm) 3.9×10^{13} photons cm^{-2} s^{-1}, and in the green range (510–530 nm) 2.8×10^{13} photons cm^{-2} s^{-1}. By using the V–log I curve, we converted the spectral and polarization responses into spectral and polarization sensitivities. For the procedure, see Arikawa et al. (Arikawa et al., 2003).

In later experiments, the spectral test was shortened to reduce recording time. Instead of 17 light flashes with different wavelengths, only three light flashes were presented to the locust which fitted the mean maximum sensitivities of the receptor types found so far (350, 430 and 530 nm). The wavelength at which the highest response amplitude occurred was considered to represent the maximum sensitivity of the receptor. Further intensity response curves and tests for polarization sensitivity were performed with this wavelength. For histological evaluation neurobiotin was, finally, injected iontophoretically into the receptor cell with constant depolarized current (0.5–2 nA for 1–3 min).

Data analysis

Only recordings with a maximum response amplitude of at least 25 mV were used for data evaluation (except for a single UV cell in Fig. 6). A 20 mV limit was set for single spectral recordings with the aim to gain information on peak sensitivity. Other criteria were a stable baseline during recordings and the absence of ERG artifacts (see Fig. 4A–C). Recording files were transferred to Spike2 software for measuring voltage amplitudes. To calculate relative sensitivities of the responses, Naka–Rushton functions:

$$V/V_{max} = I^n/(I^n + K^n), \quad (1)$$

with I the stimulus intensity, V the response amplitude at a certain stimulus, V_{max} the maximum response amplitude, K the stimulus intensity causing 50% of V_{max} and n the exponential slope, were fitted to data from the V–log I curves using Origin6 software (Microcal Software, Northampton, MA, USA).

Polarization sensitivity (PS) of photoreceptors is defined as:

$$PS = S_{max}/S_{min}, \quad (2)$$

where S_{max} and S_{min} are the relative sensitivities to E-vectors exciting the receptor maximally and minimally, respectively (Labhart, 1980).

Data were tested for normal distribution using the Shapiro–Wilk test and for homogeneity of variance with the Levene test using SPSS software (version 19). Multiple comparisons of normally distributed data were performed with one-way ANOVA (combined with Scheffé *post hoc* analysis). Kruskal–Wallis tests were applied to non-normally distributed data.

Visual pigment absorption templates (Govardovskii et al., 2000) were fitted to the absorbance spectra from the intracellularly recorded photoreceptors using the curve fitting toolbox of MATLAB (MathWorks, Natick, MA, USA). In all fits, the amplitude of the β-band of visual pigment was kept at a fixed relative value of 0.26, and linear relationships between λ_{max} and both the bandwidth and amplitude of the β-band were assumed (Govardovskii et al., 2000).

Histology

Retinae and optic lobes with neurobiotin-injected cells were dissected and fixed overnight in neurobiotin fixative (4% paraformaldehyde, 0.25% glutaraldehyde, 2% saturated picric acid, in 0.1 mol l^{-1} phosphate buffer) at 4°C. Following rinses in 0.1 mol l^{-1} phosphate-buffered saline (PBS, pH 7.4) for 4×15 min the lobes were pre-incubated with 5% normal goat serum (NGS) in PBS for 3 h at room temperature, and subsequently for 2–3 days at 4°C in streptavidin-Cy3 conjugate (1:1000) and a primary antibody against *Drosophila* synapsin (1:30) (see Klagges et al., 1996) in 0.1 mol l^{-1}

The Journal of Experimental Biology (2014) doi:10.1242/jeb.108514

PBS/0.3% Triton X-100/1% NGS. After rinsing in 0.1 mol l^{-1} PBS + 0.3% Triton X-100 for 4×15 min, the preparations were incubated in secondary antibody (0.8% goat anti mouse-Cy5, 0.1% streptavidin-Cy3 and 1% NGS in 0.1 mol l^{-1} PBS + 0.3% Triton X-100) at 4°C for 2 days. Retinae/optic lobes were subsequently dehydrated through an ascending ethanol series, transferred to propylene oxide and embedded in soft Spurr's resin (Spurr, 1969). Cross-sections of the ommatidium with the stained photoreceptor cell were cut at 10 µm with a rotary microtome (Leitz, Wetzlar, Germany).

Sections were embedded in Permount (Fisher Scientific, Pittsburgh, PA, USA) and were scanned with a confocal laser scanning microscope (TCS SP5, Leica Microsystems, Wetzlar, Germany), using a 10× objective (HC PL APO 10×/0.4 Imm Corr CS; Leica, Bensheim, Germany) for overviews and a 63× objective (HCX PL APO 63×/1.32 OIL PH 3CS; Leica) for details (scanning intervals 1–2 µm). Fluorescence of stained cells was detected with a He/Ne laser (excitation wavelength 543 nm for Cy3) or an Ar/Kr laser (excitation wavelength 647 nm for Cy5). Images were processed in CLSM imaging software (LAS AF v. 2.2.1 build 4842, Leica, Mannheim, Germany) and graphic software (CorelDRAW X3, Corel). From the time of incubation with the fluorophores, the preparations were kept in the dark as much as possible.

Acknowledgements

We thank Dr Erich Buchner for supplying anti-synapsin antibodies, Dr Doekele Stavenga for advice in visual pigment template matching, Dr Frank Bremmer for providing MATLAB software, Andreas Gerber for constructing mechanical devices, Sebastian Richter for programming software for controlling the visual stimuli, and Martina Kern, Jerome Beetz and Johannes Schuh for maintaining the locust cultures.

Competing interests

The authors declare no competing financial interests.

Author contributions

F.S. performed and analysed the electrophysiological experiments and provided the first draft of the paper. T.B. performed the template fits. F.S. and J.T. performed the histological and confocal analysis for receptor identification. M.W. identified the opsin gene sequences and performed the *in situ* hybridization experiments. U.H., M.K. and K.A. designed the experiments, provided input to the interpretation of the data and contributed to the final version of the manuscript.

Funding

This research was supported by grants from Deutsche Forschungsgemeinschaft (HO 950/20-1) to U.H., Japan Society for the Promotion of Science (24570084 to M.K.), and the Ministry of Agriculture, Forestry and Fisheries of Japan (INSECT-1101 to K.A.).

References

Arikawa, K. (2003). Spectral organization of the eye of a butterfly, *Papilio*. *J. Comp. Physiol. A* **189**, 791-800.

Arikawa, K., Mizuno, S., Kinoshita, M. and Stavenga, D. G. (2003). Coexpression of two visual pigments in a photoreceptor causes an abnormally broad spectral sensitivity in the eye of the butterfly *Papilio xuthus*. *J. Neurosci.* **23**, 4527-4532.

Awata, H., Matsushita, A., Wakakuwa, M. and Arikawa, K. (2010). Eyes with basic dorsal and specific ventral regions in the glacial Apollo, *Parnassius glacialis* (Papilionidae). *J. Exp. Biol.* **213**, 4023-4029.

Barta, A. and Horváth, G. (2004). Why is it advantageous for animals to detect celestial polarization in the ultraviolet? Skylight polarization under clouds and canopies is strongest in the UV. *J. Theor. Biol.* **226**, 429-437.

Bennett, R. R., Tunstall, J. and Horridge, G. A. (1967). Spectral sensitivity of single retinula cells of the locust. *Z. Vgl. Physiol.* **55**, 195-206.

Briscoe, A. D. and Chittka, L. (2001). The evolution of color vision in insects. *Annu. Rev. Entomol.* **46**, 471-510.

Brunner, D. and Labhart, T. (1987). Behavioural evidence for polarization vision in crickets. *Physiol. Entomol.* **12**, 1-10.

Dacke, M., Nordström, P. and Scholtz, C. H. (2003). Twilight orientation to polarised light in the crepuscular dung beetle *Scarabaeus zambesianus*. *J. Exp. Biol.* **206**, 1535-1543.

Dacke, M., Byrne, M. J., Baird, E., Scholtz, C. H. and Warrant, E. J. (2011). How dim is dim? Precision of the celestial compass in moonlight and sunlight. *Philos. Trans. R. Soc. B* **366**, 697-702.

Eggers, A. and Gewecke, M. (1993). The dorsal rim area of the compound eye and polarization vision in the desert locust (*Schistocerca gregaria*). In *Sensory Systems of Arthropods* (ed. K. Wiese, F. G. Gribakin, A. V. Popov and G. Renninger), pp. 101-109. Basel: Birkhäuser.

el Jundi, B. and Homberg, U. (2012). Receptive field properties and intensity-response functions of polarization-sensitive neurons of the optic tubercle in gregarious and solitarious locusts. *J. Neurophysiol.* **108**, 1695-1710.

Fent, K. (1985). *Himmelsorientierung bei der Wüstenameise Cataglyphis bicolor: Bedeutung von Komplexaugen und Ocellen*. Dissertation, University of Zurich, Switzerland.

Fleissner, G. (1982). Isolation of an insect circadian clock. *J. Comp. Physiol. A* **149**, 311-316.

Gaten, E., Huston, S. J., Dowse, H. B. and Matheson, T. (2012). Solitary and gregarious locusts differ in circadian rhythmicity of a visual output neuron. *J. Biol. Rhythms* **27**, 196-205.

Govardovskii, V. I., Fyhrquist, N., Reuter, T., Kuzmin, D. G. and Donner, K. (2000). In search of the visual pigment template. *Vis. Neurosci.* **17**, 509-528.

Hegedüs, R., Horváth, A. and Horváth, G. (2006). Why do dusk-active cockchafers detect polarization in the green? The polarization vision in *Melolontha melolontha* is tuned to the high polarized intensity of downwelling light under canopies during sunset. *J. Theor. Biol.* **238**, 230-244.

Heinze, S. and Homberg, U. (2007). Maplike representation of celestial E-vector orientations in the brain of an insect. *Science* **315**, 995-997.

Heinze, S., Gotthardt, S. and Homberg, U. (2009). Transformation of polarized light information in the central complex of the locust. *J. Neurosci.* **29**, 11783-11793.

Henze, M. J., Dannenhauer, K., Kohler, M., Labhart, T. and Gesemann, M. (2012). Opsin evolution and expression in arthropod compound eyes and ocelli: insights from the cricket *Gryllus bimaculatus*. *BMC Evol. Biol.* **12**, 163.

Homberg, U. and el Jundi, B. (2014). Polarization vision in arthropods. In *The New Visual Neurosciences* (ed. J. S. Werner and L. M. Chalupa), pp. 1207-1217. Cambridge, MA: MIT Press.

Homberg, U., Heinze, S., Pfeiffer, K., Kinoshita, M. and el Jundi, B. (2011). Central neural coding of sky polarization in insects. *Philos. Trans. R. Soc. B* **366**, 680-687.

Homberg, U. and Paech, A. (2002). Ultrastructure and orientation of ommatidia in the dorsal rim area of the locust compound eye. *Arthropod Struct. Dev.* **30**, 271-280.

Horridge, G. A., Duniec, J. and Marčelja, L. (1981). A 24-hour cycle in single locust and mantis photoreceptors. *J. Exp. Biol.* **91**, 307-322.

Horváth, G. and Varjú, D. (2004). *Polarized Light in Animal Vision: Polarization Patterns in Nature*. Heidelberg: Springer.

Hu, X., Leming, M. T., Metoxen, A. J., Whaley, M. A. and O'Tousa, J. E. (2012). Light-mediated control of rhodopsin movement in mosquito photoreceptors. *J. Neurosci.* **32**, 13661-13667.

Hu, X., Whaley, M. A., Stein, M. M., Mitchell, B. E. and O'Tousa, J. E. (2011). Coexpression of spectrally distinct rhodopsins in *Aedes aegypti* R7 photoreceptors. *PLoS ONE* **6**, e23121.

Johnsen, S., Kelber, A., Warrant, E., Sweeney, A. M., Widder, E. A., Lee, R. L., Jr and Hernández-Andrés, J. (2006). Crepuscular and nocturnal illumination and its effects on color perception by the nocturnal hawkmoth *Deilephila elpenor*. *J. Exp. Biol.* **209**, 789-800.

Kennedy, J. S. (1951). The migration of the desert locust (*Schistocerca gregaria* Forsk). I. The behaviour of swarms. II. A theory of long-range migrations. *Phil. Trans. R. Soc. B* **235**, 163-290.

Kinoshita, M., Pfeiffer, K. and Homberg, U. (2007). Spectral properties of identified polarized-light sensitive interneurons in the brain of the desert locust *Schistocerca gregaria*. *J. Exp. Biol.* **210**, 1350-1361.

Kitamoto, J., Sakamoto, K., Ozaki, K., Mishina, Y. and Arikawa, K. (1998). Two visual pigments in a single photoreceptor cell: identification and histological localization of three mRNAs encoding visual pigment opsins in the retina of the butterfly *Papilio xuthus*. *J. Exp. Biol.* **201**, 1255-1261.

Klagges, B. R., Heimbeck, G., Godenschwege, T. A., Hofbauer, A., Pflugfelder, G. O., Reifegerste, R., Reisch, D., Schaupp, M., Buchner, S. and Buchner, E. (1996). Invertebrate synapsins: a single gene codes for several isoforms in *Drosophila*. *J. Neurosci.* **16**, 3154-3165.

Labhart, T. (1980). Specialized photoreceptors at the dorsal rim of the honeybee's compound eye: polarizational and angular sensitivity. *J. Comp. Physiol. A* **141**, 19-30.

Labhart, T. (1988). Polarization-opponent interneurons in the insect visual system. *Nature* **331**, 435-437.

Labhart, T., Hodel, B. and Valenzuela, I. (1984). The physiology of the cricket's compound eye with particular reference to the anatomically specialized dorsal rim area. *J. Comp. Physiol. A* **155**, 289-296.

Labhart, T. and Meyer, E. P. (1999). Detectors for polarized skylight in insects: a survey of ommatidial specializations in the dorsal rim area of the compound eye. *Microsc. Res. Tech.* **47**, 368-379.

Lythgoe, J. N. (1979). *The Ecology of Vision*. Oxford: Clarendon Press.

Mappes, M. and Homberg, U. (2004). Behavioral analysis of polarization vision in tethered flying locusts. *J. Comp. Physiol. A* **190**, 61-68.

Matheson, T., Rogers, S. M. and Krapp, H. G. (2004). Plasticity in the visual system is correlated with a change in lifestyle of solitarious and gregarious locusts. *J. Neurophysiol.* **91**, 1-12.

Matić, T. and Laughlin, S. B. (1981). Changes in the intensity-response function of an insect's photoreceptors due to light adaptation. *J. Comp. Physiol. A* **145**, 169-177.

Mazzoni, E. O., Celik, A., Wernet, M. F., Vasiliauskas, D., Johnston, R. J., Cook, T. A., Pichaud, F. and Desplan, C. (2008). Iroquois complex genes induce co-expression of rhodopsins in *Drosophila*. *PLoS Biol.* **6**, e97.

Ogawa, Y., Awata, H., Wakakuwa, M., Kinoshita, M., Stavenga, D. G. and Arikawa, K. (2012). Coexpression of three middle wavelength-absorbing visual pigments in sexually dimorphic photoreceptors of the butterfly *Colias erate*. *J. Comp. Physiol. A* **198**, 857-867.

Ott, S. R. and Rogers, S. M. (2010). Gregarious desert locusts have substantially larger brains with altered proportions compared with the solitarious phase. *Proc. Biol. Sci.* **277**, 3087-3096.

Pfeiffer, K. and Homberg, U. (2007). Coding of azimuthal directions via time-compensated combination of celestial compass cues. *Curr. Biol.* **17**, 960-965.

Reppert, S. M., Zhu, H. and White, R. H. (2004). Polarized light helps monarch butterflies navigate. *Curr. Biol.* **14**, 155-158.

Roessingh, P., Simpson, S. J. and James, S. (1993). Analysis of phase-related changes in behaviour of desert locust nymphs. *Proc. Biol. Sci.* **252**, 43-49.

Roffey, J. (1963). Observations on night flight in the desert locust (*Schistocerca gregaria* Forskål). *Anti-Locust Bull.* **39**, 1-32.

Roffey, J. and Magor, J. I. (2003). *Desert Locust Population Dynamics Parameters*. Desert locust technical series. Rome: Food and Agriculture organization (FAO) of the United Nations.

Rogers, S. M., Harston, G. W. J., Kilburn-Toppin, F., Matheson, T., Burrows, M., Gabbiani, F. and Krapp, H. G. (2010). Spatiotemporal receptive field properties of a looming-sensitive neuron in solitarious and gregarious phases of the desert locust. *J. Neurophysiol.* **103**, 779-792.

Sauman, I., Briscoe, A. D., Zhu, H., Shi, D., Froy, O., Stalleicken, J., Yuan, Q., Casselman, A. and Reppert, S. M. (2005). Connecting the navigational clock to sun compass input in monarch butterfly brain. *Neuron* **46**, 457-467.

Schwind, R. (1983). Zonation of the optical environment and zonation in the rhabdom structure within the eye of the backswimmer, *Notonecta glauca*. *Cell Tissue Res.* **232**, 53-63.

Simpson, S. J., McCafferey, A. R. and Hägele, B. (1999). A behavioural analysis of phase change in the desert locust. *Biol. Rev. Camb. Philos. Soc.* **74**, 461-480.

Sison-Mangus, M. P., Bernard, G. D., Lampel, J. and Briscoe, A. D. (2006). Beauty in the eye of the beholder: the two blue opsins of lycaenid butterflies and the opsin gene-driven evolution of sexually dimorphic eyes. *J. Exp. Biol.* **209**, 3079-3090.

Spurr, A. R. (1969). A low-viscosity epoxy resin embedding medium for electron microscopy. *J. Ultrastruct. Res.* **26**, 31-43.

Stange, G. (1981). The ocellar component of flight equilibrium control in dragonflies. *J. Comp. Physiol. A* **141**, 335-347.

Stavenga, D. G. and Arikawa, K. (2008). One rhodopsin per photoreceptor: Iro-C genes break the rule. *PLoS Biol.* **6**, e115.

Towner, P., Harris, P., Wolstenholme, A. J., Hill, C., Worm, K. and Gärtner, W. (1997). Primary structure of locust opsins: a speculative model which may account for ultraviolet wavelength light detection. *Vision Res.* **37**, 495-503.

Uvarov, B. (1966). *Grasshoppers and Locusts. A Handbook of General Acridology*. Cambridge: Cambridge University Press.

Vishnevskaya, T. M., Cherkasov, A. D. and Shura-Bura, T. M. (1986). Spectral sensitivity of photoreceptors in the compound eye of the locust. *Neurophysiology* **18**, 54-60.

von Frisch, K. (1949). Die Polarisation des Himmelslichtes als orientierender Faktor bei den Tänzen der Bienen. *Experientia* **5**, 142-148.

von Philipsborn, A. and Labhart, T. (1990). A behavioural study of polarization vision in the fly, *Musca domestica*. *J. Comp. Physiol. A* **167**, 737-743.

Wakakuwa, M., Kurasawa, M., Giurfa, M. and Arikawa, K. (2005). Spectral heterogeneity of honeybee ommatidia. *Naturwissenschaften* **92**, 464-467.

Waloff, Z. (1963). Field studies on solitary and transiens desert locusts in the Red Sea area. *Anti-Locust Bull.* **40**, 1-91.

Wehner, R. (1982). Himmelsnavigation bei Insekten: Neurophysiologie und Verhalten. *Neujahrsblatt Naturforsch. Ges. Zürich* **184**, 1-132.

Wehner, R. and Labhart, T. (2006). Polarisation vision. In *Invertebrate Vision* (ed. E. Warrant and D. E. Nilsson), pp. 291-348. Cambridge: Cambridge University Press.

Wehner, R. and Müller, M. (2006). The significance of direct sunlight and polarized skylight in the ant's celestial system of navigation. *Proc. Natl. Acad. Sci. USA* **103**, 12575-12579.

Weir, P. T. and Dickinson, M. H. (2012). Flying *Drosophila* orient to sky polarization. *Curr. Biol.* **22**, 21-27.

Wilson, M., Garrard, P. and McGinness, S. (1978). The unit structure of the locust compound eye. *Cell Tissue Res.* **195**, 205-226.

Zufall, F., Schmitt, M. and Menzel, R. (1989). Spectral and polarized light sensitivity of photoreceptors in the compound eye of the cricket (*Gryllus bimaculatus*). *J. Comp. Physiol. A* **164**, 597-608.

CHAPTER 2

Photoreceptor projections and receptive fields in the dorsal rim area and main retina of the locust eye

J Comp Physiol A
DOI 10.1007/s00359-015-0990-y

ORIGINAL PAPER

Photoreceptor projections and receptive fields in the dorsal rim area and main retina of the locust eye

Fabian Schmeling · Jennifer Tegtmeier · Michiyo Kinoshita · Uwe Homberg

Received: 1 December 2014 / Revised: 10 February 2015 / Accepted: 12 February 2015

Abstract In many insect species, photoreceptors of a small dorsal rim area of the eye are specialized for sensitivity to the oscillation plane of polarized skylight and, thus, serve a role in sky compass orientation. To further understand peripheral mechanisms of polarized-light processing in the optic lobe, we have studied the projections of photoreceptors and their receptive fields in the main eye and dorsal rim area of the desert locust, a model system for polarization vision analysis. In both eye regions, one photoreceptor per ommatidium, R7, has a long visual fiber projecting through the lamina to the medulla. Axonal fibers from R7 receptors of the dorsal rim area have short side branches throughout the depth of the dorsal lamina and maintain retinotopic projections to the dorsal medulla following the first optic chiasma. Receptive fields of dorsal rim photoreceptors are considerably larger (average acceptance angle 33°) than those of the main eye (average acceptance angle 2.04°) and, taken together, cover almost the entire sky. The data challenge previous reports of two long visual fibers per ommatidium in the main eye of the locust and provide data for future analysis of peripheral networks underlying polarization opponency in the locust brain.

Keywords Compound eye · Dorsal rim area · Receptive fields · Photoreceptor projections · Desert locust

F. Schmeling · J. Tegtmeier · U. Homberg (✉)
Faculty of Biology, Animal Physiology, Philipps University of Marburg, 35032 Marburg, Germany
e-mail: homberg@biologie.uni-marburg.de

M. Kinoshita
Laboratory of Neuroethology, Sokendai (The Graduate University for Advanced Studies), Shonan Village, Hayama, Kanagawa 240-0193, Japan

Introduction

The polarization pattern of the blue sky is one of several celestial cues that are used by insects as directional reference in sky compass orientation (reviewed in Horváth and Varjú 2004; Wehner and Labhart 2006; Homberg and el Jundi 2013). Navigational responses to polarized light have been documented in several insect species under field and laboratory conditions (honeybee: von Frisch 1949; field cricket: Brunner and Labhart 1987; flies: von Philipsborn and Labhart 1990; Weir and Dickinson 2012; dung beetle: Dacke et al. 2003; desert locust: Mappes and Homberg 2004; monarch butterfly: Reppert et al. 2004; desert ant: Wehner and Müller 2006), and in all species studied, orientation responses to dorsally presented polarized light are mediated by specialized photoreceptors in a dorsal rim area (DRA) of the compound eye.

Photoreceptors of the DRA involved in polarization plane signaling share a number of specializations across insect species (Labhart and Meyer 1999). High polarization sensitivity is achieved by highly aligned microvilli, organized in two orthogonally arranged blocks in each DRA ommatidium. Further specializations include homochromacy, i.e., identical spectral sensitivity of DRA photoreceptors that contribute to polarization vision in the UV (honeybee, desert ant), blue (field cricket, desert locust), or green (cockchafer) range of the spectrum. As demonstrated in crickets, high absolute sensitivity of DRA photoreceptors to polarized light is, finally, accomplished by the lack of screening pigment, resulting in considerably wider receptive fields than in photoreceptors of the main retina (Labhart et al. 1984).

In the desert locust, DRA ommatidia contain 8 photoreceptor cells with the microvilli of R7 orthogonally opposing those of the remaining cells R1-6 and R8 (Homberg

Published online: 26 February 2015

and Paech 2002). Opponent processing of signals from these two sets of photoreceptors is believed to underlie the phenomenon of polarization opponency (Labhart and Petzold 1993; Wehner and Labhart 2006), found widely in polarization-sensitive interneurons in the brains of crickets, locusts, and monarch butterflies (Homberg et al. 2011).

Following our analysis of opsin expression patterns and spectral sensitivities of photoreceptors of the DRA and main eye of the desert locust (Schmeling et al. 2014), we report here on the patterns of central axonal projections of photoreceptors and their receptive fields. The data complement our earlier investigation and provide an important basis for future analysis of peripheral mechanisms in polarized light processing in the desert locust and other insects.

Materials and methods

Animal rearing

Experiments were performed on gregarious and solitarious desert locusts (*Schistocerca gregaria*). Gregarious adult male and female locusts were obtained from breeding colonies at the University of Marburg. Animals were kept in crowded cultures at 12:12 h light:dark cycle, 28 °C room temperature, and 50 % relative humidity. Following the conditions established by Roessingh et al. (1993), solitarious male and female animals were reared individually in small boxes at 12:12 h light:dark cycle, at 26.5 °C and 60 % relative humidity. Care was taken to ensure that no visual, olfactory and mechanical contact occurred between individuals. Animals were reared in solitarious conditions for at least three generations before being used for experiments. For identifying the solitarious phase, typical morphological characteristics such as body coloration and size (Simpson et al. 1999; el Jundi and Homberg 2012) were observed. Only locusts at least one week after imaginal moult were used for experiments.

Electrophysiology and visual stimulation

Animal preparation, experimental setup, and procedures for intracellular recording were identical with those in Schmeling et al. (2014). To compare angular sensitivity data from different animals, great care was taken to position and orient locusts in the experimental setup in identical ways by microscopic inspection of the locust`s head in relation to visual landmarks of the perimeter apparatus. Intracellular recordings were obtained from DRA and non-DRA photoreceptor cells in the locust eye using glass microelectrodes. The electrode tips were filled with 4 % Neurobiotin (Vector Laboratories, Burlingame, UK) in 1 mol l^{-1} KCl backed up with 3 mol l^{-1} KCl. The resistance of the electrodes in the tissue was 30–100 MΩ. Recording electrodes were inserted into the retina through a small hole cut into the cornea, while a silver wire serving as the indifferent electrode was inserted into the head capsule of the locust. Signals were amplified 10x. Digitized data were stored on a PC using Spike 2 or pClamp10 software with a sampling rate of 2 kHz.

For visual stimulation, a xenon arc lamp served as the light source. Wavelength and intensity of light produced by the xenon lamp could be modulated by a monochromator and a set of neutral density filters. The resulting light beam was focused to the end of a light guide. The other end of the light guide was pointed at the locust's eye. It was fixed to the arm of a perimeter and could be moved along a virtual sphere with the locust's head in its center (angular size at the eye 3°). Monochromator and neutral density filters were controlled by custom-made software.

After penetrating a photoreceptor cell, the light guide was positioned in the center of the receptor's receptive field determined as the position eliciting maximum responses to a series of light flashes. The spectral type of the photoreceptor was determined by testing a series of monochromatic light flashes of equal quantal flux (310–630 nm in 20 nm steps; stimulus duration 500 ms). Quantum flux was adjusted in each recording to elicit responses within the range of the intensity response curve. In some cases only 350, 450 or 530 nm were tested to roughly determine the spectral type.

Response–stimulus intensity (*V*-log *I*) functions were obtained by recording the responses to light flashes of the peak wavelength of the receptor, starting at low light levels, up to the maximum intensity (310–350 nm: 2.8×10^{13} photons cm^{-2} s^{-1}, 410–450 nm: 3.9×10^{13}, 510–530 nm: 2.8×10^{13}) of the setup. Light intensities were calibrated with a radiometer (P-9201, Gigahertz-Optic, Puchheim, Germany).

Angular sensitivity was measured using the wavelength eliciting the largest response by moving the light guide along the horizontal and vertical axis around the animal's head. When recording from the DRA, 5° or 10° steps were made between two light flashes. Step size was 1° when recording from the main retina, starting from the visual center. Subsequently, Neurobiotin was injected iontophoretically into the cell by constant depolarized current (0.5–2 nA for 1–3 min).

Data evaluation: electrophysiology

For angular sensitivity measurements, relative sensitivities at the tested positions were calculated by converting voltage amplitudes to equivalent photon numbers from the *V*-log *I* function of the receptor (see Schmeling et al. 2014). The normalized reciprocal of the relative photon number

was then calculated as the relative sensitivity. Sensitivity values were plotted as a function of angular stimulus position. Because the positions for sensitivity measurements along horizontal directions were not on a great circle around the locust`s head, their perimeter readings were corrected accordingly (Burkhardt and Streck 1965). Acceptance angles were determined as the half widths of the plotted functions at 50 % relative sensitivity. *V*-log *I* curve processing and graph plotting were performed with Origin6 software (Microcal Software, Northhampton, USA). SPSS software (version 19) was used for statistical evaluations. The Shapiro–Wilk test was used to test for normality of data distribution. Group testing of not normally distributed data was performed with the Kruskal–Wallis test.

Histological procedure for single cell staining

Tissue preparation and histological procedures were similar to those in Schmeling et al. (2014). Optic lobes were removed from the head capsule and immersed in Neurobiotin fixative (4 % paraformaldehyde, 0.25 % glutaraldehyde, 2 % saturated picric acid, in 0.1 mol l^{-1} phosphate buffer) at 4 °C. After rinsing in phosphate-buffered saline (PBS, 0.1 mol l^{-1}, pH 7.4) for 4 × 15 min and preincubation in normal goat serum (NGS, 5 % in PBS) for 3 h at room temperature, incubation with streptavidin-Cy3 conjugate (1:1000) for 2–3 days and primary antibody against *Drosophila* synapsin (1:30) in 0.1 mol l^{-1} PBS/0.3 % Triton X-100/1 % NGS followed. The monoclonal anti-synapsin antibody (SYNORF1, kindly provided by Dr. E. Buchner, Würzburg, Germany) was raised in mouse against fusion proteins consisting of glutathione-S-transferase and the *Drosophila* SYN1 protein (Klagges et al. 1996). It labels synaptic neuropil as demonstrated in several insect species (e.g., *Drosophila*: Klagges et al. 1996; *Schistocerca*: Heinze and Homberg 2008). After rinsing in 0.1 mol l^{-1} PBS + 0.3 % Triton X-100 for 4 × 15 min, incubation proceeded with a secondary antibody (0.8 % goat anti mouse-Cy5, 0.1 % streptavidin-Cy3 and 1 % NGS in 0.1 mol l^{-1} PBS + 0.3 % Triton X-100) at 4 °C for 2 days. The preparations were dehydrated in an ethanol series and embedded in soft Spurr's embedding medium (Spurr 1969). Sections were cut with a rotary microtome (Leitz, Wetzlar, Germany) in orientations with respect to the observed structure and were, finally, embedded in Permount (Fisher Scientific, Pittsburgh, PA, USA) under glass coverslips.

Mass staining of photoreceptors

Animals were immobilized by cutting off their legs and wings. Movable body parts were fixed with wax. For tracer injection into the optic lobe, the head capsule was opened frontally. Ocelli and antennae were removed, leaving the compound eyes and the central brain intact. A cut was made in the neurilemma in the region of either the dorsal rim of the medulla or the medulla. A single crystal of dextran conjugated to the fluorescent dye Texas Red (3,000 MW, Molecular Probes, Eugene, OR, USA) was inserted into the opening and was taken up by the damaged fibers.

For dye application to the DRA of the retina, small cuts were made into the cornea anteriorly and posteriorly in the DRA. Crystals of dextran–Texas Red were applied to the anterior and crystalline Neurobiotin to the posterior hole. For staining photoreceptors of the main retina, large parts of the retinal cornea were removed, and dextran–Texas Red was applied to the bare retina.

If dextran–Texas Red was solely applied, animals were left for about two hours at 4 °C in humid conditions to allow for diffusion of the tracer. Afterwards, brains were dissected from the head capsule and kept in fixative solution composed of 1 part 0.2 mol l^{-1} cacodylate and 1 part 4 % paraformaldehyde for another two hours. The optic lobes were then washed in 0.2 mol l^{-1} cacodylate for 10 min. When Neurobiotin and dextran–Texas Red were coapplied as tracers followed by synapsin immunostaining, brains were fixed in Neurobiotin fixative over night. Optic lobes were rinsed in 0.1 mol l^{-1} PBS containing 1 % Triton X-100. After preincubation in 5 % normal goat serum, primary antibody against *Drosophila* synapsin (1:30) (see Klagges et al. 1996) was applied in 0.1 mol l^{-1} PBS/0.3 % Triton X-100/1 % NGS. Incubation with secondary antibody (0.8 % goat anti mouse-Cy5) and 0.1 % streptavidin-Cy3 diluted with 1 % NGS in 0.1 mol l^{-1} PBS + 0.3 % Triton X-100 followed at 4 °C for 2 days. In all cases, optic lobes were dehydrated in an ascending ethanol series, transferred to propylene oxide and finally embedded in soft Spurr`s resin. Sections of 8–10 µm for retina tissue and 60 µm for optic lobe tissue were made with a rotary microtome in individual orientations. Starting from the incubation with fluorophores, the preparations were kept in the dark as much as possible.

Confocal microscopy

Stained sections were scanned with a confocal laser scanning microsope (TCS SP5, Leica Microsystems, Wetzlar, Germany), using a 10× objective (HC PL APO 10×/0.4 Imm Corr CS; Leica, Bensheim, Germany) for overviews and a 63× objective (HCX PL APO 63×/1.32 OIL PH 3CS; Leica) for details (scanning intervals 1–2 µm). A He/Ne laser (excitation wavelength 543 nm for Cy3 and 595 nm for Texas Red) and an Ar/Kr laser (excitation wavelength 647 nm for Cy5) were used to detect fluorescence. Image processing was performed with CLSM imaging software (LAS AF v. 2.2.1 build 4842, Leica, Mannheim, Germany) and graphic software (CorelDRAW X3, Corel).

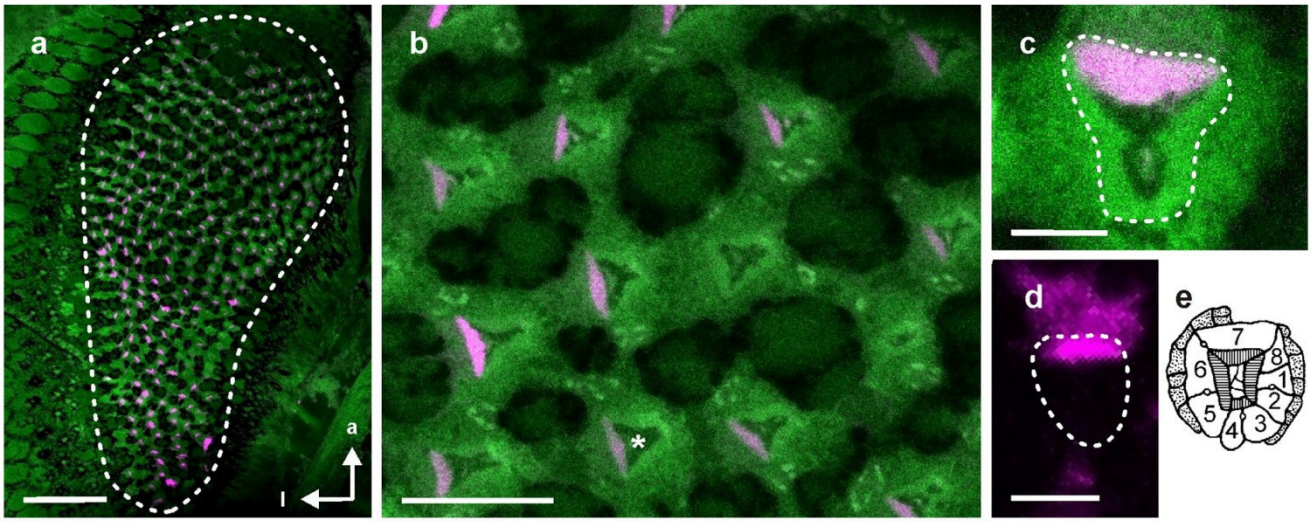

Fig. 1 Retrograde mass staining of DRA photoreceptors. Long visual fibers of the DRA were labeled by injecting dextran-conjugated Texas Red into the dorsal rim of the medulla. Stained photoreceptors are shown in *magenta* against a *green* fluorescent background. Only R7 photoreceptor cells were labeled, indicating that they are the only DRA cells projecting to the dorsal rim of the medulla. **a** Cross section showing the pattern of stained cells in the DRA of the eye. **b** *Detail* from **a.** An *asterisk* marks the position of the crystalline cone in the center of an ommatidium. **c** Cross section of a stained ommatidium. **d** Staining of a single DRA ommatidium. Detection sensitivity of the confocal microscope was adjusted to visualize the weakly stained cell bodies. *Green* background fluorescence was removed for clarity. **e** Schematic drawing of a DRA ommatidium at the height of the sections in **a–d** (from Homberg and Paech 2002). *White dashed lines* indicate the margin of the DRA in **a** and of the rhabdoms in **c** and **d.** *Scale bars* **a**: 100 µm; **b, d** 10 µm; **c** 5 µm. Orientations are indicated by *arrows* (*l* lateral, *a* anterior)

To identify cellular structures and neuropil boundaries or weakly labeled processes, several preparations were scanned multiple times with varying detection sensitivity of the confocal laser scanning microscope. Tissue slices were observed once with low and once with high scanning sensitivity. Thereby, strong and weak fluorescent structures could be distinguished in detail. Information from scans with high and low sensitivity was combined for figure illustration.

Results

Identification of long and short visual fibers of the DRA

Neuronal tracer, injected into the dorsal rim of the medulla, was taken up by photoreceptor axons and was distributed throughout the whole cells. Therefore, all photoreceptors stained at the level of the retina are considered to be long visual fibers terminating in the dorsal rim of the medulla. In contrast, all unlabelled photoreceptor cells are considered short visual fibers. Retinal cross sections demonstrate that it was possible to trace stained photoreceptor profiles across the whole DRA (Fig. 1a). Boundaries of ommatidia were identified by their higher fluorescence compared with the surrounding tissue (Fig. 1b). In contrast, individual unlabelled retinula cells could not be distinguished clearly from each other. The extension of the crystalline cone appeared as a non-fluorescent area in the center of the rhabdoms (Fig. 1b, c).

In stained photoreceptors, microvillar regions showed considerably stronger fluorescence than the rest of the cell body, which was only visible by raising the detection sensitivity of the confocal scanning process (Fig. 1c, d). In contrast to the highly structured rhabdom, photoreceptor cell margins had highly irregular shapes. Usually one cell per ommatidium was stained, with only few exceptions in which no cell had taken up the tracer (Fig. 1b). Stained cells could be identified as receptor cell R7, using rhabdom shape and microvilli orientation as criteria (Fig. 1c, e; compare Homberg and Paech 2002; Schmeling et al. 2014). The data show that R7 photoreceptors in the DRA are long visual fibers while R1–R6 and R8 are short visual fibers terminating in the lamina.

Optic chiasma and retinotopy within the dorsal rim areas of the lamina and medulla

Anterograde mass staining revealed an optic chiasma of long visual fibers in the horizontal plane between the dorsal rim area of the lamina (DRLA) and medulla (DRME). Axonal projections from the DRA of the eye extended to corresponding positions of the DRLA (Fig. 2a, inset), but long visual fibers terminated in positions of the DRME corresponding to the inversion of the anterior-posterior axis (Fig. 2a, b). Thus, a long visual fiber originating from the

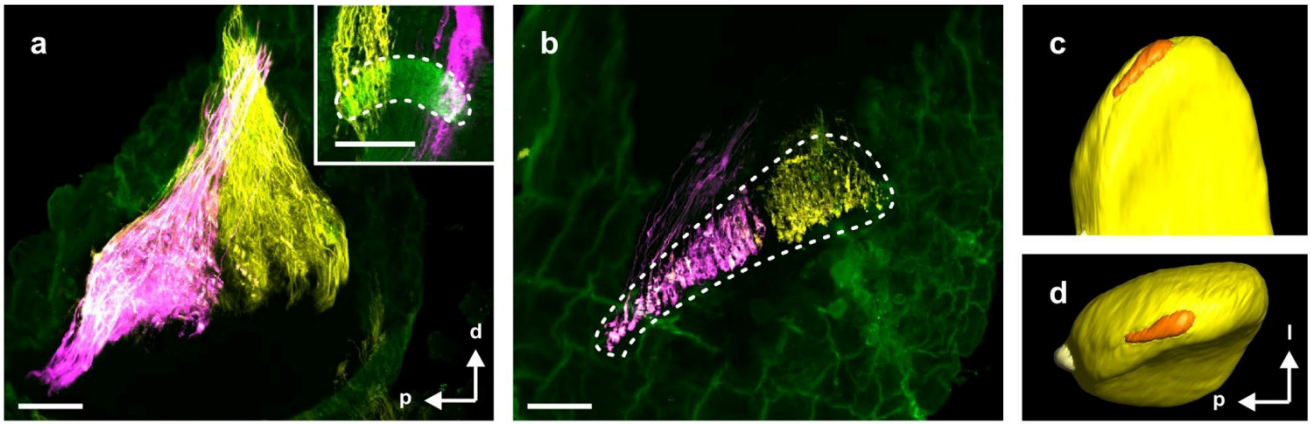

Fig. 2 Anterograde mass staining of long visual fibers projecting from the DRA of the eye to the dorsal rim of the medulla. Two different tracers were injected into the anterior (dextran–Texas *Red*, *magenta*) and posterior (Neurobiotin, *yellow*) part of the DRA. **a** Sagittal section with a slight horizontal angle through the dorsal rim of the medulla. *Inset* shows projections through the DRLA. **b** Sagittal section with a slight horizontal angle from the same optic lobe showing a more ventral region of the dorsal rim of the medulla. **c**, **d** 3D reconstruction of the medulla (*yellow*), including the DRME (*orange*) and the accessory medulla (*light yellow*). Neuropil margins in **a** and **b** are indicated by *dashed lines*. *Scale bars* 50 µm. Orientations (identical **a**, **b** and **c)** are indicated by *arrows* (*d* dorsal, *p* posterior, *l* lateral)

anterior edge of the DRA extended to the anterior DRLA but the continuing neurite changed direction and terminated near the posterior edge of the DRME. The shape of the DRME resembles that of the DRA of the eye with a wide anterior and a more slender posterior part. A 3D reconstruction of the neuropils demonstrates how the DRME is embedded in the medulla (Fig. 2c, d; data from Kurylas et al. 2008). Retinula cell projections end relatively irregularly within the DRME but are largely confined to the upper two-thirds of the DRME (Figs. 2b, 3e, 5c, f).

Single cell stainings following electrophysiological recordings were used to reveal axonal projection patterns along the lateral–medial axis. Figure 3 shows a full histological dataset of a stained R7 retinula cell. It includes information on the cell's position within the DRA, receptor identity, an overview of axonal projections, and details of arborizations within the DRLA (Fig. 3d) and DRME (Fig. 3e).

Retinotopic projections of visual fibers from the DRA to the DRLA and DRME were also obvious in frontal plane, lacking an optic chiasma (Figs. 4, 5). Receptor position within the DRA of the retina strongly correlates with its axonal projection sites in the DRLA and DRME. Receptors in lateral positions of the DRA send their projections to lateral sides of the DRLA and DRME and the more a receptor's position is shifted medially, the more medial are its terminations.

Structure and shape of axonal projections

In general, fine axonal arborizations were spatially confined to a narrow area close to the main axon. Short visual fibers penetrated deeply into the DRLA and gave rise to bulbous, club-like terminals, in some cases with short spiny extensions in close proximity to the main fiber. No indications of synaptic contacts were found throughout the distal half of the DRLA (Fig. 4).

In contrast, long visual fibers had short and usually fine lateral extensions throughout the depth of the DRLA, again in close proximity to the main fiber (Figs. 5b, e, 6a). In the DRME, projection depth varied but the most ventral part of the DRME was usually not invaded (Figs. 3e, 5c, f, 6b). This is consistent with the findings of anterograde mass stainings (Fig. 2). Terminations appeared again prominently varicose. Cases were found in which a bulb of small arborizations originated from the main axon (Figs. 5f; 6b). In other cases, only few short thin fibers seemed to extend from the main axon (Fig. 5c). The uppermost, distal quarter of the DRME was conspicuously free of side branches or termination sites (Fig. 3e, 5c, f, 6b). Between the retina and lamina and within the DRLA, axons of long visual fibers had larger diameters (about 3 µm) than short visual fibers (about 1 µm). After leaving the DRLA, however, axons of long visual fibers abruptly decreased in thickness to about 1 µm (Fig. 6a). The site of change in fiber diameter correlated with a bend in axonal trajectory.

Visual fiber projections in the main eye

Retrograde mass staining from the main medulla, as from the DRME, labeled a single photoreceptor per ommatidium in the main retina (Fig. 7). Cross sections at a deeper level through the axonal bundles leaving the retina, likewise, showed only one stained retinula cell axon per ommatidium

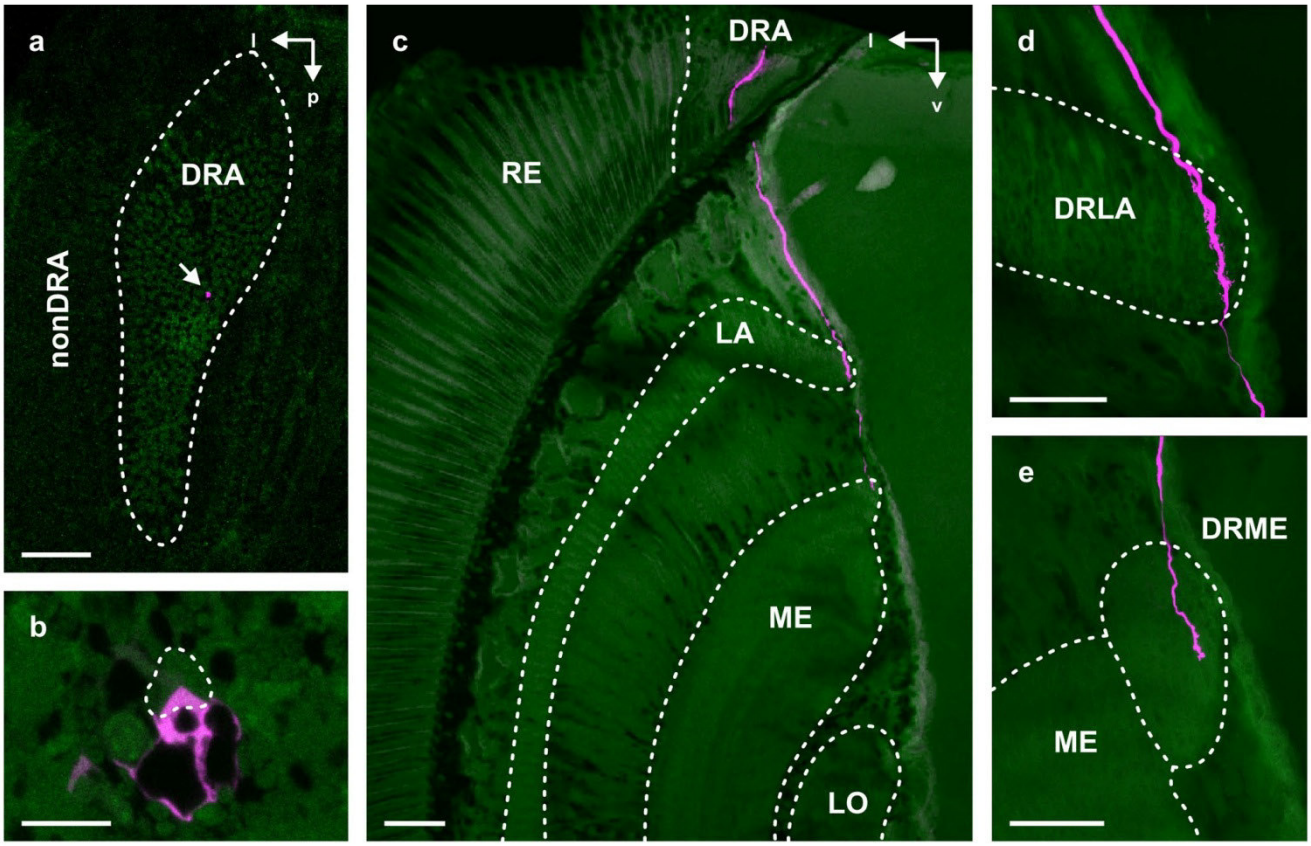

Fig. 3 Staining of a single DRA photoreceptor. Neurobiotin was injected iontophoretically into the receptor cell after electrophysiological recording. The stained R7 photoreceptor (*magenta*) is a long visual fiber with projections through the DRLA and terminal projections in the DRME. **a** Cross section of the DRA. The stained cell is indicated by a *white arrow*. **b** Magnification from (**a**). The size of the cell's rhabdomere, its triangular shape and orientation within the DRA identifies it as an R7 photoreceptor. **c** Frontal section through the optic lobe, showing an overview of the axonal projection of the photoreceptor. *LA* lamina, *LO* lobula, *ME* medulla, *RE* retina. **d, e** Frontal sections through the dorsal rim of the lamina (*DRLA*, **d**) and medulla (*DRME*, **e**). *Scale bars* **a, c** 100 µm; **d, e** 50 µm; **b**: 10 µm. *Dashed lines* show margins of DRA and neuropils. Orientations, identical in **a, b**, and in **c–e**, are indicated by *arrows* (*l* lateral, *p* posterior, *v* ventral)

(data not shown). Two types of ommatidia could be distinguished with the stained photoreceptor pointing either anterior-dorsally or anterior-ventrally within an ommatidium (Fig. 7b, c). Both types were randomly distributed throughout the main eye. A highly similar arrangement of photoreceptors expressing UV and blue opsins in locust ommatidia was recently established by Schmeling et al. (2014). Based on that study, we conclude that the stained cell is R7. Anterograde mass staining further revealed that all long visual fibers terminate in distal layer 3 of the medulla (Fig. 7d). This layer was identified by comparison with observations of Wendt and Homberg (1992) and Gebhardt and Homberg (2004). A horizontally projecting fiber bundle which lies medially from layer 4 (el Jundi et al. 2011) also served as an anatomical landmark for layer identification (asterisk in Fig. 7d). While running through the outer layers of the medulla, receptor axons showed no apparent arborizations until they reached a narrow band of terminations characterized by relatively short and spatially highly aligned bulbous endings (Fig. 7e).

Dye application following intracellular recording from blue/green sensitive photoreceptors consistently ($n = 4$) resulted in co-labeling of 5 stained receptor cells terminating in the lamina but at different depths (Fig. 8). In accordance with Schmeling et al. (2014), those cells were identified as R2, R3, R5, R6, and R8 photoreceptors. These receptors contribute microvilli through the whole length of the rhabdom. In contrast, receptors R1, R4, and R7 remained unstained. R7 is a distal photoreceptor, while R1 and R4 are proximal photoreceptors (Wilson et al. 1978; Schmeling et al. 2014).

Receptive fields

Recording data were collected from gregarious and solitarious locusts. From the center of the receptive fields, the relative sensitivity decreased with increasing distance in an

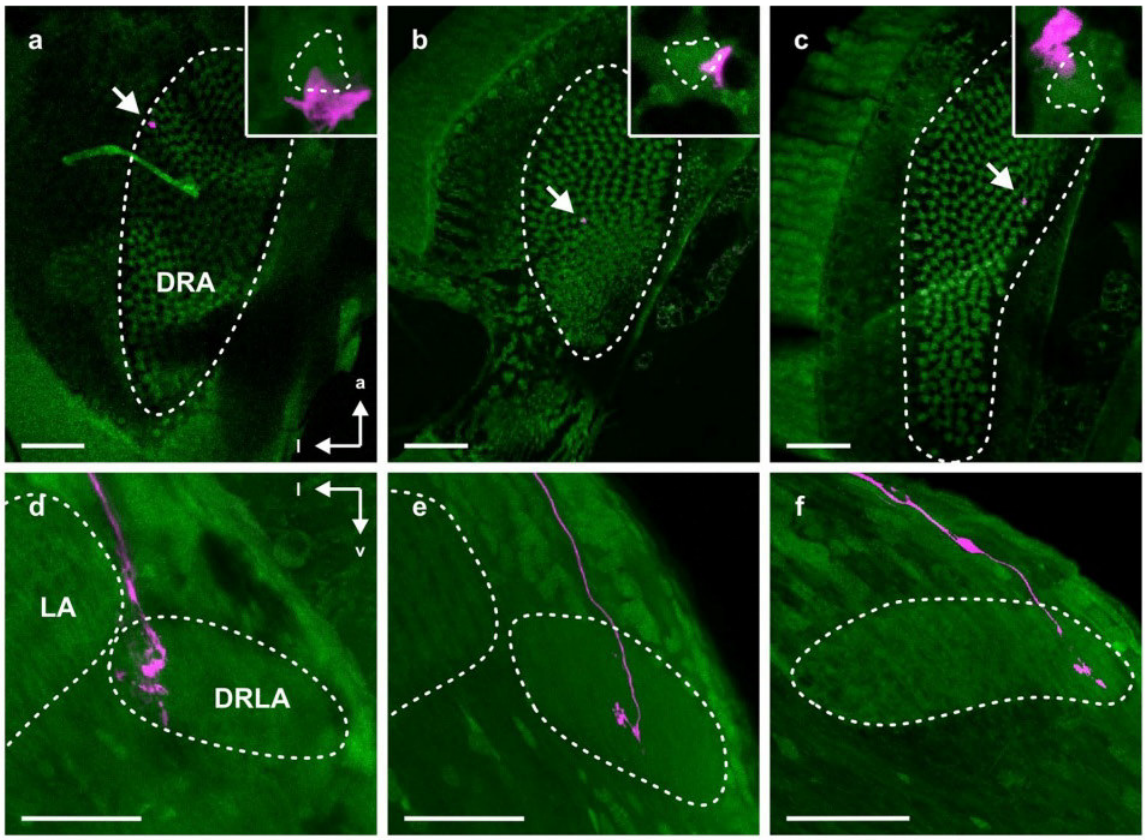

Fig. 4 Axonal projections of short visual fibers from the DRA to the DRLA. Single cell stainings demonstrate retinotopy across the medio-lateral axis. **a–c** Cross sections of the DRA with single cells stained (*white arrows*). *Insets* show magnifications of the corresponding images, revealing the identity of photoreceptors as R1 (**a**) and R1 or R2 (**b, c**). **d–f** Frontal sections through the DRLA showing axonal projections (*magenta*) of the receptors in **a–c**. For neuropil background staining, a synapsin antibody with Cy5 as fluorophore was used. *White dashed lines* show outlines of the DRA (**a–c**) and the LA and DRLA (**d–f**). *Scale bars* 50 µm. Orientation of figures is identical in **a–c** and **d–f** (*l* lateral, *a* anterior, *v* ventral)

exponential manner (Fig. 9), as has been observed in other insects (Labhart 1980; Labhart et al. 1984; Stalleicken et al. 2006). The two main parameters of a receptive field are its acceptance angle and its total extent. The acceptance angle (half-width of angular sensitivity) was further used for statistical tests. The visual fields within the acceptance angle appear symmetrically shaped in the DRA and main eye, and no significant difference in acceptance angle width was found along the lateral–medial and anterior–posterior axis as well as between gregarious and solitarious locusts (gregarious: $n = 10$ DRA, $n = 22$ main eye; solitarious: $n = 7$ DRA, $n = 10$ main eye). Data were, therefore, pooled. The average acceptance angle of DRA receptors was 33° (±18.6°), and of receptors of the main eye, 2.04° (±1.3°). The widest visual field extent of a single receptor in the DRA was 149° and 43° in the main retina. Especially in the main retina, a relatively small center of high sensitivity could be distinguished from a wide surrounding region of extremely low sensitivity (falling below 10 % when exceeding 8°, Fig. 9b), which matches observations in the bee (Labhart 1980).

While the receptive fields beyond the acceptance angle were circularly shaped in the main retina, there was often a remarkable asymmetry in the DRA, especially along the lateral–medial axis. Often receptor sensitivity decreased more strongly in medial than in lateral direction. This effect can be seen even in the averaged curves in Fig. 9a. All receptive field centers of DRA photoreceptors point contralaterally. An estimate of the DRA's total visual field was obtained by overlaying measurements of all recorded receptors (Fig. 10). The visual field of the DRA (at 50 % sensitivity) is 80° along the lateral–medial axis and 100° across the anterior–posterior axis. Its total width is 160° dorso-ventrally and posterior–anteriorly and thereby covers almost the whole dorsal hemisphere.

Discussion

Photoreceptor projections and their receptive fields differ in several aspects between the DRA and main retina of

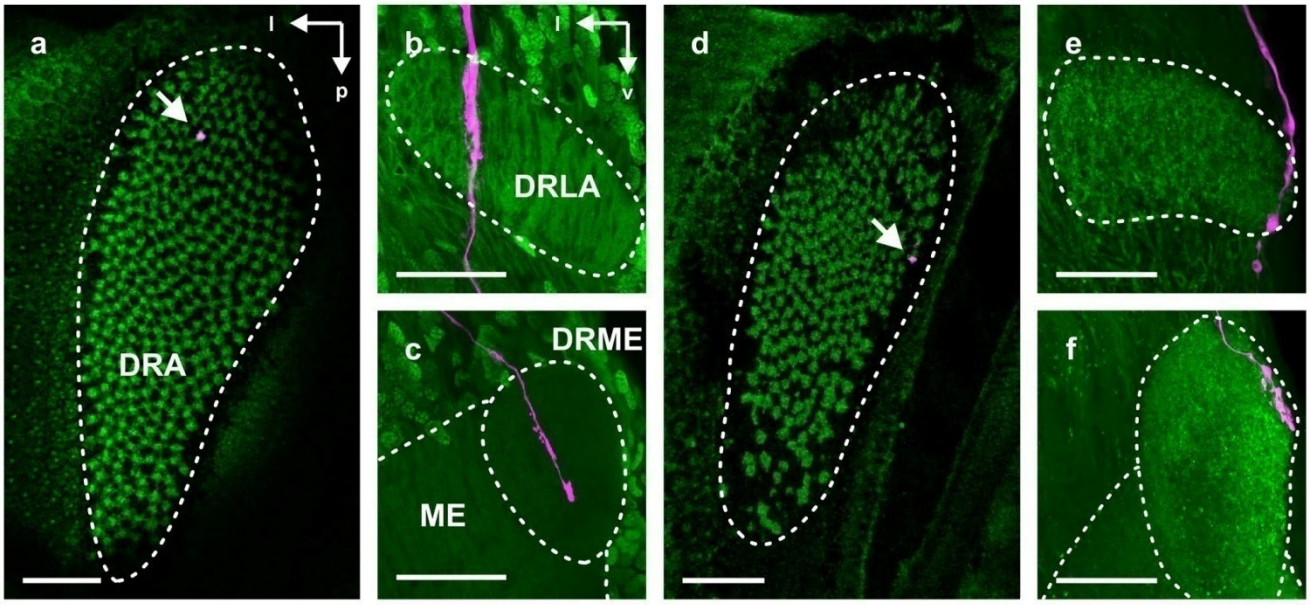

Fig. 5 Axonal projections of long visual fibers to the DRLA and DRME. As for short visual fibers, stainings demonstrate retinotopic projections. **a, d** Cross sections of the DRA with single cells stained (*white arrow*). **b, c** and **e, f** Frontal sections through the DRLA and DRME showing axonal projections (*magenta*) of the receptors in **a** and **d**. *Scale bars* **a, d** 100 µm; **b, c, e, f** 50 µm. Orientation is identical in **a, d** and **b, c, e, f** (*l* lateral, *p* posterior, *v* ventral)

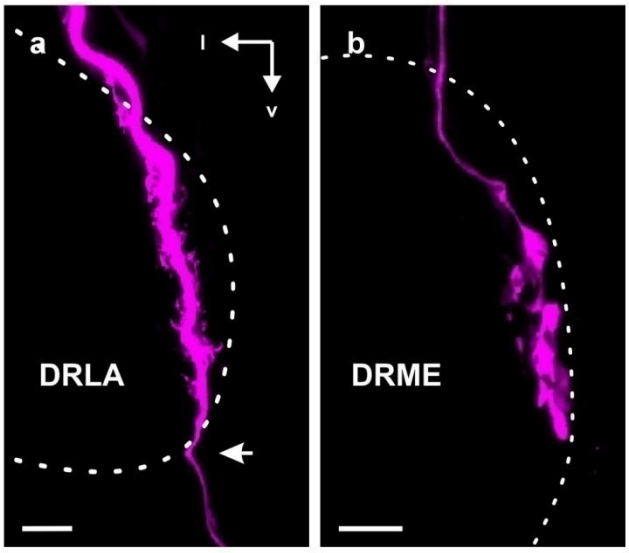

Fig. 6 Details of R7 photoreceptor projections from the DRA. **a** Fine short arborizations cover the whole length of the axon in the DRLA. The axon diameter decreases greatly after a strong bend (indicated by *arrow*), when leaving the neuropil. **b** Axonal projections (from a different preparation) terminate in the form of small knots within the DRME. Orientations, identical in **a** and **b**, are indicated by *arrows* (*l* lateral, *v* ventral). *Scale bars* 10 µm

the desert locust, while other features show similarities. In both eye regions, a single retinula cell per ommatidium, identified as R7, projects a long visual fiber to the medulla, whereas R1–R6 and R8 are short visual fibers terminating in the lamina. As in the main visual system, retinotopy of photoreceptor projections is maintained in the DRLA and DRME. The receptive fields of DRA receptors are about 180 times larger in area than those of receptors from the main eye. In contrast to the ipsilateral visual field of the main eye, the DRA as a whole covers an ellipsoid visual field of roughly 80° × 100° in the contralateral visual field near the zenith.

Central projections of DRA photoreceptors

As in the cricket (Blum and Labhart 2000), each ommatidium of the DRA of the locust *S. gregaria* contains only one long visual fiber, R7 (Fig. 1), while the remaining cells have short fibers terminating in the lamina. Projections of photoreceptors to the DRLA and DRME are retinotopically organized and, in case of R7 photoreceptors, follow the fiber crossings of the first optic chiasma, despite the fact that both neuropils appear relatively unstructured and show no layer arrangement as seen in the main medulla (Fig. 7d). Retinotopic organization of the DRME would allow for spatially distinct input to postsynaptic transmedulla neurons projecting to the lower division of the anterior optic tubercle (Homberg et al. 2003), but the ramification patterns of those interneurons in the DRME have not yet been determined.

At the level of the DRLA, long and short visual fibers strongly differ in their morphology. The axons of long visual fibers have considerably larger diameters than

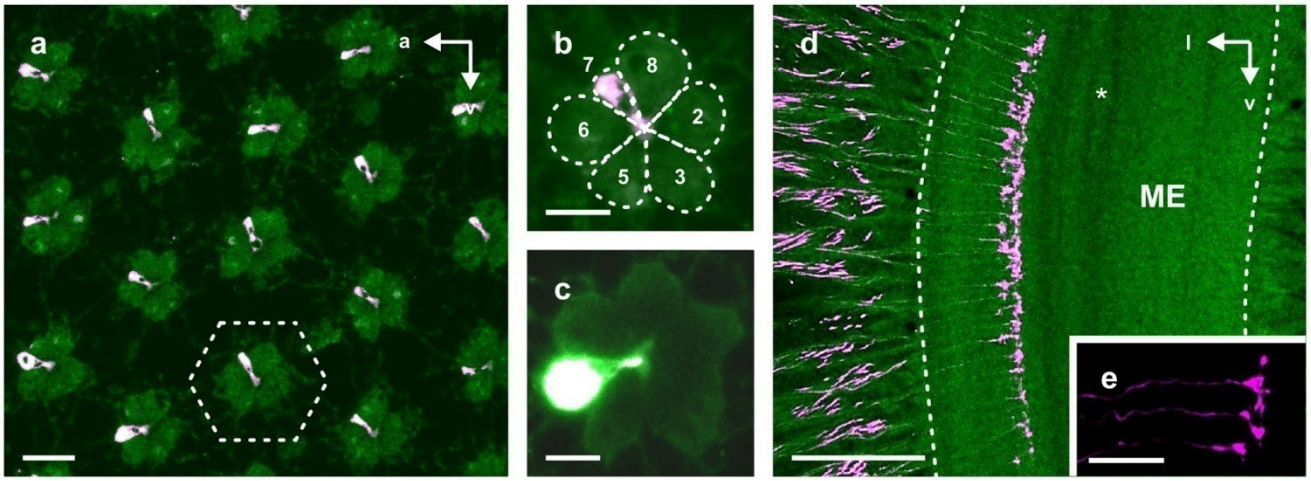

Fig. 7 Retrograde and anterograde mass staining of photoreceptors of the main retina. Long visual fibers were labelled by injecting dextran–Texas Red into the medulla or the retina. Stained photoreceptors are shown in *magenta*; background staining originates from synapsin labelling (*green*). Exclusively R7 receptor cells are stained, indicating that they are the only cells with long visual fibers projecting to the medulla, terminating in layer 3. **a** Cross section of the main retina showing stained photoreceptors in two different orientations within the ommatidia, either pointing anterior-dorsally or anterior-ventrally. *Dashed line* outlines a corresponding facet. **b** Details of a single ommatidium with the stained cell pointing anterior-dorsally. *Dashed lines* outline the retinula cells of the ommatidium. **c** Details of the second type of ommatidium with the stained cell pointing anterior-ventrally (cross section 8 µm). **d** Frontal section through the *ME* showing an overview of axonal projections. **e** Details of axonal terminals. *Dashed lines* indicate the *ME* boundaries. An *asterisk* marks a horizontally projecting fiber bundle which lies medially from layer 4 and was used as an anatomical landmark for layer definition. *Scale bars* **a** 10 µm; **b, c**: 5 µm; **d** 100 µm; **e** 25 µm. Orientations are indicated by *arrows* and are identical in **a–c** (*a* anterior, *l* lateral, *v* ventral)

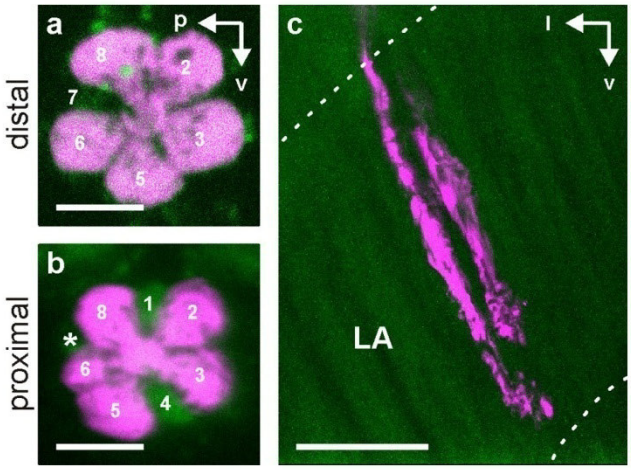

Fig. 8 Axonal projections of short visual fibers from the main retina to the lamina. Five receptor cells (R2, R3, R5, R6, and R8) were co-labelled following Neurobiotin injection after single-cell intracellular recording. The long photoreceptor R7 and the two proximal receptors R1 and R4 remained unlabelled. At least two axon bundles with different lengths can be recognized. **a–b** Cross sections of the retina at a distal (**a**) and proximal level (**b**) of the rhabdom. **c** Frontal section through the lamina (*LA*). The *asterisk* in **b** indicates the position of R7. *Scale bars* **a, b** 5 µm; **c** 25 µm

short visual fibers and, thus, should show a smaller decrement of light-induced depolarizations along their axons. As a consequence, they should reach critical levels of depolarizations at synaptic release sites faster than the short fibers. This may be of functional relevance considering the mechanisms proposed to underlie polarization opponency (Labhart and Petzold 1993; Wehner and Labhart 2006). Many polarization-sensitive interneurons in the brain of locusts, crickets and other insects receive excitatory input at a particular *E*-vector orientation, termed Φ_{max}, and inhibitory input at orthogonal *E*-vector orientation, Φ_{min} (Labhart and Meyer 2002; Homberg et al. 2011). This property, termed polarization opponency, may arise from antagonistic processing and convergence of inputs from the two sets of photoreceptors with orthogonal microvilli orientations in each DRA ommatidium (Wehner 1982; Labhart 1988). Insect photoreceptors, including those of the locust DRA, use histamine as a neurotransmitter (Hardie 1987, 1989; Nässel 1999; Gebhardt and Homberg 2004). Light-induced histamine release leads to opening of chloride channels resulting in neuronal inhibition. Polarization opponency, however, requires one of the two input channels to be excitatory. This could be achieved by an intercalated interneuron switching the photoreceptor's effect on a DRLA polarization opponent interneuron to excitation. Because an intercalated interneuron would lead to a delay in information processing, compensation by a larger axon diameter and, thus, faster depolarization at synapses in the indirect input channel to the polarization opponent interneuron may be a way to assure that the opponent inputs arrive at the same

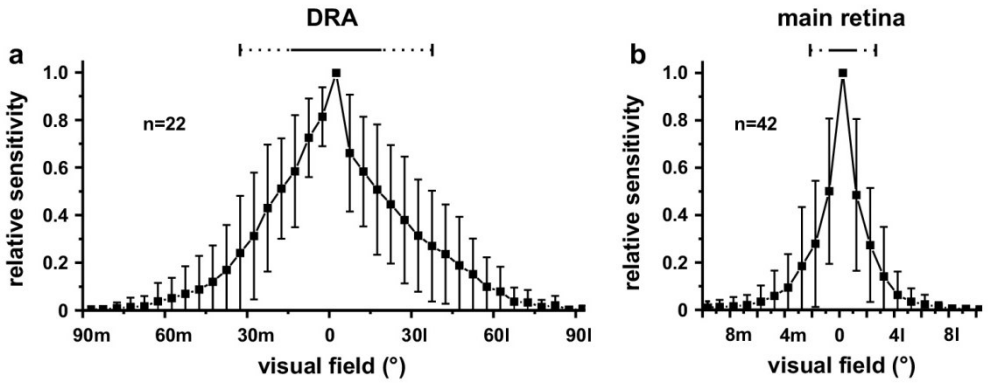

Fig. 9 Receptive fields (means, SD) of photoreceptors from the DRA (**a**) and main retina (**b**). Relative sensitivities are plotted as a function of binned positions (5° bins in **a**; 1° bins in **b**) of the stimulus. Visual fields in the DRA are considerably larger than in the main retina, while the shapes are similar. With increasing distance medially (*m*) and laterally (*l*) from the visual center, relative sensitivity decreases in an exponential manner. The averaged acceptance angles (*solid lines*) and their standard deviations (*dotted lines*) are indicated by the bars above the graphs

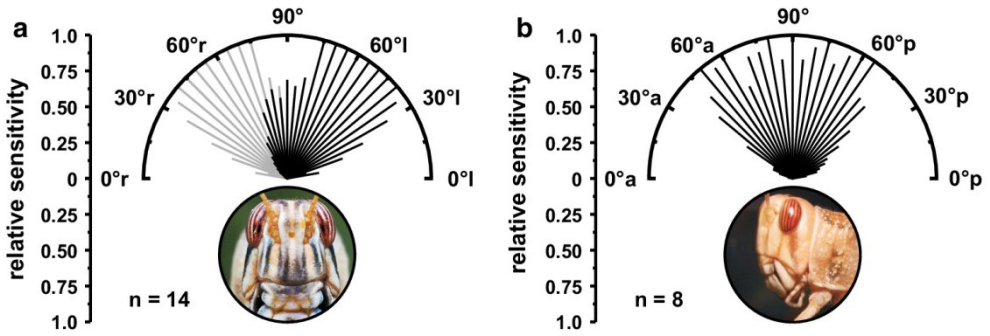

Fig. 10 Overlays of all single visual fields measured in the DRA. Relative sensitivities are plotted as a function of binned positions (5° bins) of the stimulus. **a** Visual field extensions along the medial–lateral axis. The *black bars* indicate relative sensitivity distributions of pooled right eye photoreceptors. Measurements from the left eye were mirrored and added. Pooled data were mirrored to indicate the visual field of the left DRA (*gray bars*). **b** Visual field extensions along the anterior–posterior axis. Data from gregarious and solitarious locusts were pooled with *n* indicating the number of recorded cells. (*r* right, *l* left, *a* anterior, *p* posterior)

time. R7 would, therefore, be an attractive candidate photoreceptor in the indirect longer pathway mediating excitatory input to polarization opponent interneurons at the level of the DRLA.

Another main difference between short and long visual fibers concerns the distribution of arborizations in the DRLA. Axonal side branches were found over the whole length of the long visual fibers but were basically absent in short visual fibers in the distal half of the DRLA. What are the postsynaptic partners of long visual fibers in the more distal region of the DRLA? An additional neuron type could be the answer to that question. The neuronal elements of the lamina subserving the main eye of *S. gregaria* have been studied by Nowel and Shelton (1981). They reported similar differences between long and short visual fibers, as shown here, concerning details of finer arborizations. Differences in length between short visual fibers and in the position of their finer arborizations, as reported by Nowel and Shelton (1981) for the main eye, have not been found by us in the DRLA.

When leaving the DRLA, long visual fibers show an abrupt reduction in fiber diameter, which might again be relevant for coincident integration of polarization opponent input in the DRME. The single cell stainings confirmed the findings of mass stainings (Fig. 2b) that long visual fibers usually do not extend fully through the DRME. Final terminations are located at about the last two-thirds of the fiber, which differs strongly from the locally more narrow terminations of long visual fibers in the main medulla. This might be due to the fact that no obvious layering occurs in the DRME, while the main medulla appears heavily structured (Gebhardt and Homberg 2004).

Photoreceptors of the main retina

In the main retina as in the DRA, only R7 was identified as a long visual fiber (Fig. 7). This contrasts with earlier findings by Horridge and Meinertzhagen (1970) and Nowel and Shelton (1981) who reported two long visual fibers in *S. gregaria*. In the first publication, photoreceptor projections were traced through the first optic chiasma on transverse sections of axonal tissue but the authors did not provide original data for the locust. Nowel and Shelton (1981) distinguished two morphological types of long visual fibers based on Golgi impregnations but whether these two types are present in the same ommatidium was not addressed. Using the same technique and premise as Nowel and Shelton (1981), Ribi (1975a) reported three long visual fibers in the desert ant, but that was later corrected to two long fibers by Meyer (1984), who used a retrograde staining technique similar to ours. The question arises whether retinula cell axon morphology is sufficient to conclude on the contributing ommatidium. In view of our current data, together with evidence from Schmeling et al. (2014) indicating that two types of ommatidia exist with an R7 photoreceptor expressing either a blue or a UV opsin gene, it may be more likely that the two types of long visual fibers reported by Nowel and Shelton (1981) are in fact the two spectral types of R7 photoreceptors occurring in different ommatidia throughout the main eye. Two different types of R7 (and R8) distributed over the retina are also present in the fruit fly (Wernet and Desplan 2004).

Two long visual fibers have been reported most often in pterygote insects (Strausfeld 1971; Pollack and Hofbauer 1991; Ribi 1975b; Wolburg-Buchholz 1979; Armett-Kibel and Meinertzhagen 1985; Fischbach and Dittrich 1989; Zufall et al. 1989), but cases of three long visual fibers per ommatidium are also known (Shimohigashi and Tominaga 1991; Greiner et al. 2004; Takemura et al. 2005; Paulk et al. 2009), as well as the total absence of long fibers (Buschbeck et al. 2003). Interestingly in the insect species studied so far, R7 is usually among the long visual fibers (together with R8), while R1–R6 are short visual fibers, but again, several exceptions occur, including eye region-specific and sex-specific differences (e.g., Hardie et al. 1981).

Long visual fibers usually terminate in distal layers of the medulla. In the few cases in which termination sites were identified, they occurred in medulla layer 2 (honeybee: Ribi and Scheel 1981; bumblebee: Paulk et al. 2009), layer 2 and 3 (a nocturnal bee: Greiner et al. 2004), layer 4 (butterfly: Hamanaka et al. 2013) or 3 and 6 (fruit fly: Takemura et al. 2008). Terminations of all long visual fibers in the locust medulla occur in a single layer, as illustrated in Fig. 7d. This has also been observed in histamine immunostaining (Gebhardt and Homberg 2004). Gebhardt and Homberg (2004) reported that histamine-immunostained terminals of long visual fibers were confined to layer 4 of the medulla, but careful comparison with the layering of the locust medulla established by Wendt and Homberg (1992) reveals a slightly more distal position in layer 3.

In *S. gregaria*, R2-3 and R5-6 are short visual fibers as in other insect species (Fig. 8) but, in contrast to many other insects, R8 also terminates in the lamina. The axons of these five short visual receptors form two bundles which terminate at different depths of the lamina. This fits to the findings by Nowel and Shelton (1981), based on Golgi impregnations, that short visual fibers differ in their depth of penetration of the lamina. This may imply synaptic connection patterns to different lamina monopolar and horizontal cells (Nowel and Shelton 1981) or even to different transmedulla neurons which in some cases arborize in certain depths of the lamina (Homberg and Würden 1997). Dye injection following intracellular recording of one of these receptors consistently stained the complete set of five photoreceptor cells. A likely explanation is electrical coupling of photoreceptors, which has already been suggested for locust photoreceptors through physiological recordings (Shaw 1967, 1969; Lillywhite 1978). All co-labeled receptors directly contact each other at the distal region of the ommatidium (Fig. 8a), but gap junctions may of course also occur in the region of the rhabdom. All five dye-coupled receptors (R2, R3, R5, R6, R8) contain blue as well as green opsin (Schmeling et al. 2014) supporting a common functional role. The receptors R1 and R4 could not be stained in any of the recordings. Both receptors are green sensitive (Schmeling et al. 2014) and, judged from the mass backfill experiments (Fig. 7), are short visual fibers.

The color vision system of many insects consists of two long visual fibers, UV or blue sensitive, and green sensitive short visual fibers (Zufall et al. 1989; Briscoe et al. 2003; White et al. 2003; Spaethe and Briscoe 2005; Wakakuwa et al. 2005). A similar trichromatic color vision system may be present in the desert locust consisting of UV and blue sensitive long visual fibers (in different ommatidia) and green sensitive short visual fibers (in each ommatidium; Schmeling et al. 2014). The observation that the UV or blue photoreceptor R7 in *S. gregaria* has a rhabdomere confined to distal parts of the ommatidium, whereas the two green receptors only contribute to the rhabdom proximally (Schmeling et al. 2014), may support their adaptation to vision at daylight intensities, and is similar to the situation in the migratory locust (Wilson et al. 1978).

Receptive fields

With a mean acceptance angle of 33° in the DRA and 2.04° in the main retina, the photoreceptors in *S. gregaria* have similar angular sensitivities as those of the field cricket *Gryllus campestris* (DRA: 10°–35°, main retina: 6°; Labhart

et al. 1984) and the migratory locust in dark adapted state (main retina: 2.8°; Williams 1983). Certain other insect species show considerably smaller acceptance angles in their DRA, down to about 4° (bee: Labhart 1980; ant: Labhart 1986; butterfly: Stalleicken et al. 2006). The large angular sensitivity in the locust DRA correlates with anatomical specializations of the optic apparatus, like absence of screening pigment and the presence of light scattering structures (Homberg and Paech 2002). This way more photons can be collected from DRA receptors, compared with receptors from the main eye, resulting in enhanced overall light sensitivity. The receptive fields of locust DRA receptors are about 180 times larger than those of receptors in the main eye, suggesting a similar increase in sensitivity (compare Schmeling et al. 2014, Fig. 8). Considering receptive field size, a factor of 600 was found in a cricket by Zufall (1984). When stimulating with small light spots, cricket DRA receptors were less sensitive than receptors in the main retina, but considering their wider receptive field, Zufall et al. (1989) concluded that cricket DRA receptors are actually 60 times more sensitive to an extended source of light.

Summing up the receptive fields of all receptors in both DRAs, three facts become apparent: (1) the combined visual fields cover most parts of the sky, (2) the visual field is limited to areas above the horizon, and (3) the relative sensitivity of each DRA at the zenith is only about 50 % but here, both DRAs overlap in their visual fields. The main effect of the large size of the visual field is that the celestial polarization pattern is detected as completely as possible. Especially during inhomogeneous sky conditions, this might be an advantage. Even if the celestial *E*-vector pattern is partly occluded by clouds, as many free spots as possible in the sky would lie within the DRAs' visual field and can contribute to solar azimuth signaling, thereby enhancing accuracy (Labhart 1999). The large visual fields are, moreover, a prerequisite for matched filter properties of polarization-sensitive neurons in the central brain and may allow the solar and anti-solar hemispheres of the sky to be distinguished, particularly at higher solar elevations (Bech et al. 2014). Interestingly, a complete view of the sky is not always present in insect species sensitive to the sky polarization pattern. The DRAs of the monarch butterfly and desert ant have rather narrow visual fields (Stalleicken et al. 2006; Labhart 1986). However, the intuitive conclusion that monarch butterflies possess an inferior polarization detecting system compared to locusts has still to be proven. It has to be kept in mind that insects use several celestial cues for orientation, complementing each other, but with different weight. Perhaps polarized light plays a dominant role in locusts, as in ants (Wehner and Müller 2006), while in monarch butterflies the position of the sun may be the most important cue (Mouritsen et al. 2013; Oberhauser et al. 2013).

S. gregaria do not only detect polarized light from above but also show a behavioral response, when polarized light is presented from below (Shashar et al. 2005; el Jundi and Homberg 2010). With receptors basically looking upwards, the DRA is unlikely to provide the explanation for this polarization sensitivity. In this case, polarized light is more likely to be detected by photoreceptors of the main eye. The visual field of the main eye covers regions below the horizon and might show sufficient polarization sensitivity even with low PS values (Schmeling et al. 2014) as discussed by Wernet et al. (2012).

Whether the relatively low sensitivity of the DRA in the zenith (Fig. 10a) serves a particular function remains unclear. However, despite the relatively weak sensitivities of each single DRA in this region, their combined overlapping visual fields still may provide sufficient signal amplitude to accurately detect zenithal *E*-vector orientations, leaving no blind spot. In fact relative sensitivity in the zenith is about 50 % for each DRA, which would sum up to 100 %, when signals from both eyes are combined. The asymmetrically shaped visual field of the locust DRA might result from the fact that the head capsule limits receptor sight in the contralateral direction that results in a rapid decrease of sensitivity contralaterally to the receptors' visual field center. No obstacles occur ipsilaterally, and visual sensitivity decreases gradually. This effect is still recognizable in the averaged measurements (Fig. 9) and adds up when observing the DRA's whole visual field (Fig. 10a).

Acknowledgments We are grateful to Dr. Erich Buchner (University of Würzburg) for donation of the anti-synapsin antibody. We thank Matthias Schön for technical assistance and Martina Kern, Jerome Beetz, and Johannes Schuh for maintaining the locust cultures. This work was supported by grants from Deutsche Forschungsgemeinschaft (HO 950/20-1) to UH and the Japan Society for the Promotion of Science (#24570084) to MK.

References

Armett-Kibel C, Meinertzhagen IA (1985) The long visual fibers of the dragonfly optic lobe: their cells of origin and lamina connections. J Comp Neurol 242:459–474

Bech M, Homberg U, Pfeiffer K (2014) Receptive fields of locust brain neurons are matched to polarization patterns of the sky. Curr Biol 24:2124–2129

Blum M, Labhart T (2000) Photoreceptor visual fields, ommatidial array, and receptor axon projections in the polarisation-sensitive dorsal rim area of the cricket compound eye. J Comp Physiol A 186:119–128

Briscoe AD, Bernard GD, Szeto AS, Nagy LM, White RH (2003) Not all butterfly eyes are created equal: rhodopsin absorption spectra, molecular identification, and localization of ultraviolet-, blue-, and green-sensitive rhodopsin-encoding mRNAs in the retina of *Vanessa cardui*. J Comp Neurol 458:334–349

Brunner D, Labhart T (1987) Behavioural evidence for polarization vision in crickets. Physiol Entomol 12:1–10

Burkhardt D, Streck P (1965) Das Sehfeld einzelner Sehzellen: Eine Richtigstellung. Z Vgl Physiol 51:151–152

Buschbeck EK, Ehmer B, Hoy RR (2003) The unusual visual system of the Strepsiptera: external eye and neuropils. J Comp Physiol A 189:617–630

Dacke M, Nordström P, Scholtz C (2003) Twilight orientation to polarized light in the crepuscular dung beetle *Scarabaeus zambesianus*. J Exp Biol 206:1535–1543

el Jundi B, Homberg U (2010) Evidence for the possible existence of a second polarization-vision pathway in the locust brain. J Insect Physiol 56:971–979

el Jundi B, Homberg U (2012) Receptive field properties and intensity-response functions of polarization-sensitive neurons of the optic tubercle in gregarious and solitarious locusts. J Neurophysiol 108:1695–1710

el Jundi B, Pfeiffer K, Homberg U (2011) A distinct layer of the medulla integrates sky compass signals in the brain of an insect. PLoS One 6:e27855

Fischbach KF, Dittrich APM (1989) The optic lobe of *Drosophila melanogaster*. I. A Golgi analysis of wild-type structure. Cell Tissue Res 258:441–475

Gebhardt S, Homberg U (2004) Immunocytochemistry of histamine in the brain of the locust *Schistocerca gregaria*. Cell Tissue Res 317:195–205

Greiner B, Ribi WA, Wcislo WT, Warrant EJ (2004) Neural organization in the first optic ganglion of the nocturnal bee *Megalopta genalis*. Cell Tissue Res 318:429–437

Hamanaka Y, Shibasaki H, Kinoshita M, Arikawa K (2013) Neurons innervating the lamina in the butterfly, *Papilio xuthus*. J Comp Physiol A 199:341–351

Hardie RC (1987) Is histamine a neurotransmitter in insect photoreceptors? J Comp Physiol A 161:201–213

Hardie RC (1989) A histamine-activated chloride channel involved in neurotransmission at a photoreceptor synapse. Nature 339:704–706

Hardie RC, Franceschini N, Ribi W, Kirschfeld K (1981) Distribution and properties of sex-specific photoreceptors in the fly *Musca domestica*. J Comp Physiol A 145:139–152

Heinze S, Homberg U (2008) Neuroarchitecture of the central complex of the desert locust: intrinsic and columnar neurons. J Comp Neurol 511:454–478

Homberg U, el Jundi B (2013) Polarization vision in arthropods. In: Werner JS, Chalupa LM (eds) The new visual neurosciences. MIT Press, Cambridge, pp 1207–1217

Homberg U, Paech A (2002) Ultrastructure and orientation of ommatidia in the dorsal rim of the locust compound eye. Arthropod Struct Dev 30:271–280

Homberg U, Würden S (1997) Movement-sensitive, polarization-sensitive, and light-sensitive neurons of the medulla and accessory medulla of the locust, *Schistocerca gregaria*. J Comp Neurol 386:329–346

Homberg U, Hofer S, Pfeiffer K, Gebhardt S (2003) Organization and neural connections of the anterior optic tubercle in the brain of the desert locust, *Schistocerca gregaria*. J Comp Neurol 462:415–430

Homberg U, Heinze S, Pfeiffer K, Kinoshita M, el Jundi B (2011) Central neural coding of sky polarization in insects. Philos Trans R Soc B 366:680–687

Horridge GA, Meinertzhagen IA (1970) The exact neural projection of the visual fields upon first and second ganglia of the insect eye. Z Vgl Physiol 66:369–378

Horváth G, Varjú D (2004) Polarized light in animal vision: Polarization patterns in nature. Springer, Heidelberg

Klagges BR, Heimbeck G, Godenschwege TA, Hofbauer A, Pflugfelder GO, Reifegerste R, Reisch D, Schaupp M, Buchner S, Buchner E (1996) Invertebrate synapsins: a single gene codes for several isoforms in *Drosophila*. J Neurosci 16:3154–3165

Kurylas AE, Rohlfing T, Krofczik S, Jenett A, Homberg U (2008) Standardized atlas of the brain of the desert locust, *Schistocerca gregaria*. Cell Tissue Res 333:125–145

Labhart T (1980) Specialized photoreceptors at the dorsal rim of the honeybee's compound eye: polarizational and angular sensitivity. J Comp Physiol A 141:19–30

Labhart T (1986) The electrophysiology of photoreceptors in different eye regions of the desert ant *Cataglyphis bicolor*. J Comp Physiol A 158:1–7

Labhart T (1988) Polarization-opponent interneurons in the insect visual system. Nature 331:435–437

Labhart T (1999) How polarization-sensitive interneurons of crickets see the polarization pattern of the sky: a field study with an opto-electronic model neuron. J Exp Biol 202:757–770

Labhart T, Meyer E (1999) Detectors for polarized skylight in insects: a survey of ommatidial specializations in the dorsal rim area of the compound eye. Microsc Res Tech 47:368–379

Labhart T, Meyer E (2002) Neural mechanism in insect navigation: polarization compass and odometer. Curr Opin Neurobiol 12:707–714

Labhart T, Petzold J (1993) Processing of polarized light information in the visual system of crickets. In: Wiese K, Gribakin FG, Popov AV, Renninger G (eds) Sensory systems of arthropods. Birkhäuser, Basel, pp 158–169

Labhart T, Hodel B, Valenzuela I (1984) The physiology of the cricket's compound eye with particular references to the anatomically specialized dorsal rim area. J Comp Physiol A 155:289–296

Lillywhite PG (1978) Coupling between locust photoreceptors revealed by study of quantum bumps. J Comp Physiol A 125:13–27

Mappes M, Homberg U (2004) Behavioral analysis of polarization vision in tethered flying locusts. J Comp Physiol A 190:61–68

Meyer EP (1984) Retrograde labeling of photoreceptors in different eye regions of the compound eye of bees and ants. J Neurocytol 13:825–836

Mouritsen H, Derbyshire R, Stalleicken J, Mouritsen OØ, Frost BJ, Norris DR (2013) An experimental displacement and over 50 years of tag-recoveries show that monarch butterflies are not true navigators. Proc Natl Acad Sci 110:7348–7353

Nässel DR (1999) Histamine in the brain of insects: a review. Microsc Res Tech 44:121–136

Nowel MS, Shelton PMJ (1981) A Golgi-electron-microscopical study of the structure and developement of the lamina ganglionaris of the locust optic lobe. Cell Tissue Res 216:377–401

Oberhauser KS, Taylor OR, Reppert SM, Dingle H, Nail KR, Pyle RM, Stenoien C (2013) Are monarch butterflies true navigators? The jury is still out. Proc Natl Acad Sci 110:E3680

Paulk AC, Dacks AM, Gronenberg W (2009) Color processing in the medulla of the bumblebee (Apidae: *Bombus impatiens*). J Comp Neurol 513:441–456

Pollack I, Hofbauer A (1991) Histamine-like immunoreactivity in the visual system and brain of *Drosophila melanogaster*. Cell Tissue Res 226:391–398

Reppert SM, Zhu H, White RH (2004) Polarized light helps monarch butterflies navigate. Curr Biol 14:155–158

Ribi WA (1975a) Golgi studies of the first optic ganglion of the ant, *Cataglyphis bicolor*. Cell Tissue Res 160:207–217

Ribi WA (1975b) The first optic ganglion of the bee. Cell Tissue Res 165:103–111

Ribi WA, Scheel M (1981) The second and third optic ganglia of the worker bee. Cell Tissue Res 221:17–43

Schmeling F, Wakakuwa M, Tegtmeier J, Kinoshita M, Bockhorst T, Arikawa K, Homberg U (2014) Opsin expression, physiological characterization and identification of photoreceptor cells in the dorsal rim area and main retina of the desert locust, *Schistocerca gregaria*. J Exp Biol 217:3557–3568

Shashar N, Sabbah S, Aharoni N (2005) Migratory locusts can detect polarized reflections to avoid flying over the sea. Biol Lett 1:472–475

Shaw SR (1967) Simultaneous recording from two cells in the locust retina. Z Vgl Physiol 55:183–194

Shaw SR (1969) Interreceptor coupling in ommatidia of drone honeybee and locust compound eyes. Vis Res 9:999–1029

Shimohigashi M, Tominaga Y (1991) Identification of UV, green and red receptors, and their projection to lamina in the cabbage butterfly, *Pieris rapae*. Cell Tissue Res 263:49–59

Simpson S, McCaffery A, Hägele BF (1999) A behavioural analysis of phase change in the desert locust. Biol Rev 74:461–480

Spaethe J, Briscoe AD (2005) Molecular characterization and expression of the UV opsin in bumblebees: three ommatidial subtypes in the retina and a new photoreceptor organ in the lamina. J Exp Biol 208:2347–2361

Spurr AR (1969) A low-viscosity epoxy resin embedding medium for electron microscopy. J Ultrastruct Res 26:31–43

Stalleicken J, Labhart T, Mouritsen H (2006) Physiological characterization of the compound eye in monarch butterflies with focus on the dorsal rim area. J Comp Physiol A 192:321–331

Strausfeld NJ (1971) The organization of the insect visual system (light microscopy) - I. Projections and arrangements of neurons in the lamina ganglionaris of Diptera. Z Zellforsch 121:377–441

Takemura S-Y, Kinoshita M, Arikawa K (2005) Photoreceptor projection reveals heterogeneity of lamina cartridges in the visual system of the Japanese yellow swallowtail butterfly, *Papilio xuthus*. J Comp Neurol 483:341–350

Takemura S-Y, Lu Z, Meinertzhagen IA (2008) Synaptic circuits of the *Drosophila* optic lobe: the input terminals to the medulla. J Comp Neurol 509:493–513

von Frisch K (1949) Die Polarisation des Himmelslichts als orientierender Faktor bei den Tänzen der Biene. Experientia 5:142–148

von Philipsborn A, Labhart T (1990) A behavioural study of polarization vision in the fly, *Musca domestica*. J Comp Physiol A 167:737–743

Wakakuwa M, Kurasawa M, Giurfa M, Arikawa K (2005) Spectral heterogeneity of honeybee ommatidia. Naturwissenschaften 92:464–467

Wehner R (1982) Himmelsnavigation bei Insekten: Neurophysiologie und Verhalten. Neujahrsblatt Naturforsch Ges Zürich 184:1–132

Wehner R, Labhart T (2006) Polarization vision. In: Warrant E, Nilsson D-E (eds) Invertebrate Vision. Cambridge University Press, Cambridge, pp 291–348

Wehner R, Müller M (2006) The significance of direct sunlight and polarized skylight in the ant's celestial system of navigation. Proc Natl Acad Sci 103:12575–12579

Weir PT, Dickinson MH (2012) Flying *Drosophila* orient to sky polarization. Curr Biol 22:21–27

Wendt B, Homberg U (1992) Immunocytochemistry of dopamine in the brain of the locust *Schistocerca gregaria*. J Comp Neurol 321:387–403

Wernet MF, Desplan C (2004) Building a retinal mosaic: cell-fate decision in the fly eye. Trends Cell Biol 14:576–584

Wernet MF, Velez MM, Clark DA, Baumann-Klausener F, Brown JR, Klovstad M, Labhart T, Clandinin TR (2012) Genetic dissection reveals two separate retinal substrates for polarization vision in *Drosophila*. Curr Biol 22:12–20

White RH, Xu H, Münch TA, Bennett RR, Grable EA (2003) The retina of *Manduca sexta*: rhodopsin expression, the mosaic of green-, blue- and UV-sensitive photoreceptors, and regional specialization. J Exp Biol 206:3337–3348

Williams DS (1983) Changes of photoreceptor performance associated with the daily turnover of photoreceptor membrane in locusts. J Comp Physiol 150:509–519

Wilson M, Garrard P, McGinness S (1978) The unit structure of the locust compound eye. Cell Tissue Res 195:205–226

Wolburg-Buchholz K (1979) The organization of the lamina ganglionaris of the hemipteran insects, *Notonecta glauca*, *Corixa punctata* and *Gerris lacustris*. Cell Tissue Res 197:39–59

Zufall F (1984) Physiologische und morphologische Charakterisierung der Retinulazellen im Komplexauge der Grillen (*Gryllus bimaculatus*). Diploma thesis, Freie Universität Berlin

Zufall F, Schmitt M, Menzel R (1989) Spectral and polarized light sensitivity of photoreceptors in the compound eye of the cricket (*Gryllus bimaculatus*). J Comp Physiol A 164:597–608

GENERAL DISCUSSION

EXAMINATION OF THE DRA

ADAPTATION OF THE DRA TO NOCTURNAL LIGHT CONDITIONS

Depending on its phase, *Schistocerca gregaria* can be considered as diurnal, or as nocturnal. Its dorsal rim area exclusively contains blue receptors and all of them seem to contribute to the polarization pathway (Schmeling et al. 2014). Detecting polarized light in the blue spectrum of the sky is widely considered to be an adaptation for nocturnal light conditions (Herzmann and Labhart 1989). Because low light levels might become a limiting factor at night, it also seems reasonable that as many photoreceptors as possible contribute to collect photons. In contrast, the DRAs of some diurnal insects, like honey bees and ants, also contain additional green receptors, which seem not to contribute to polarization vision (Labhart 1980, 1986).

In the desert locust, DRA photoreceptors started to respond at a threshold of about 4.9 x 10^9 photons $cm^{-2}s^{-1}$ in the blue spectrum (Schmeling et al. 2014), but actual light intensities at sunrise or at night do not reach this level (Johnsen et al. 2006, see also Fig.12). However, as discussed in Schmeling et al. (2014, 2015), locust DRA photoreceptors are probably more sensitive than implied by the laboratory experiments. Considering the large angular sensitivity of DRA receptors, a factor calculated in Schmeling et al. (2015) was applied to the receptor response curves in Fig.10. In this case the receptors response threshold is at about 10^7 photons $cm^{-2}s^{-1}$.

When the sun is closely below the horizon or during full moon, light levels in the blue spectrum are still above the light level of 10^7 photons $cm^{-2}s^{-1}$ (Johnsen et al. 2006, see also Fig.12) and thereby above the calculated threshold of desert locust photoreceptors. In conclusion, spectral and absolute sensitivity of the locust DRA appear to be adequately adapted to light conditions at night, perhaps to detect the polarized light of the moon. This is the case in both locust phases, even though only one phase is nocturnal (for further discussion see later paragraph).

NEURONAL CODING WITHIN THE DORSAL RIM OF LAMINA AND MEDULLA

There are two ways *E*-vectors can be coded at interneuron level. Either by simply modulating the response strength depending on the perceived *E*-vector orientation, like in DRA photoreceptors, or the neuron can respond with polarization opponency (see Fig.7). Whether the later already exists at level of the DRLA or whether it is established in the DRME is not clear.

The prerequisite of polarization opponency is an antagonistic interaction of signals from photoreceptors with orthogonal microvilli orientations coding for perpendicular *E*-vectors. In the desert locust this *E*-vector information is proceeded either by short or long visual fibers. A direct interaction of these fibers to cause polarization opponency is unlikely, since insect photoreceptors, in general, seem to use histamin as neurotransmitter, which

has an inhibitory effect (Hardie 1987, 1989, Nässel 1999, Gebhardt and Homberg 2004). To provide the excitatory signals, which are essential for polarization opponency, additional interneurons would be required to invert the otherwise exclusively inhibitory signals from either the short or long visual fibers.

The first stage at which such interneurons could occur is the DRLA. Both, long and short visual fibers have arborizations in the DRLA, but it is noteworthy that they are not completely overlapping. The main axons of the long visual fibers pass through the DRLA and posses fine arborizations over the whole depth of the neuropil, while the arborizations of the R1-6 and R8 short visual fiber terminations in this neuropil are mainly restricted to the proximal region of the DRLA (Schmeling et al. 2015). These incongruent arborization patterns could indicate that the two fiber types are not exchanging information in this neuropil. In the locust main eye there are types of monopolar cells with arborizations basically congruent to either short or long visual fibers of the DRLA (Nowel and Shelton 1981, see also Fig.13). It is possible that similar monopolar cell types are present in the DRLA as well. A likely hypothesis is that inhibitory signals of the short visual fibers are inverted by such monopolar cells connecting the DRLA and DRME. In the DRME, this information could be combined with the still inhibitory signals of long visual fibers and could cause polarization opponency is another subsequent interneurons of the DRME. One reason why the DRME is highly suspected to be the first neuronal stage with polarization opponency is the fact that in crickets the first interneurons showing polarization opponency are the so called POL-1 neurons which receive direct input in the DMRE (review: Labhart et al. 2001). A similar situation compared to the cricket might be assumed in the desert locust.

DEVELOPMENT AND POSSIBLE PURPOSE OF RETINOTOPY

In insect main eyes, photoreceptors generally project in a retinotopic pattern into the optic lobe. Receptor terminations of long and short visual fibers are arranged retinotopic as well in the DRLE and DRME (Schmeling et al. 2015). This is surprising because these neuropils appear unstructured (Homberg and Paech 2002), unlike the clearly structured lamina and medulla of the main eye (Nowel and Shelton 1981, Wendt and Homberg 1992, Gebhardt and Homberg 2004, Homberg et al. 2004). Several mechanisms are known to develop such topographic patterns as found in the main retina, lamina and medulla. They involve molecule gradients and cell surface molecules (Dearborn et al. 2002, Luo and Flanagan 2007). In particular in the case of photoreceptors, new growing axons simply follow the projection of their already existing neighbors (Luo and Flanagan 2007). During the postembryonic development of the hemimetabolous desert locust, this topography is maintained by the fact that new ommatidia are proliferated at the anterior margin of the eye, and the lamina seems to grow in a similar way (Anderson 1978a, 1978b). It can be assumed that the same mechanisms are present in the development of the DRA, DRLA and DRME.

Topographic arrangement of neurons has the general advantage that subsequent neurons, on which information converges, can be held simple in their arborizations. However, topographic organization also seems to play a role in processing of information

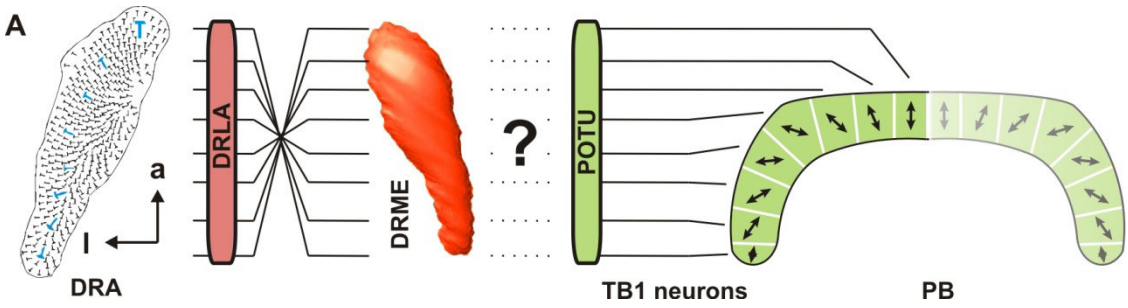

Fig.9: Similarities between microvilli orientations in the dorsal rim area and *E*-vector tuning in interneurons of the central complex. The fan-shaped distribution of microvilli orientations in the dorsal rim area shows general similarity to preferred *E*-vector orientations of TB1 neurons which connect the posterior optic tubercle and the protocerebral bridge. However, it has to be pointed out that the microvilli distribution is not exactly as precise as the *E*-vector tuning in the protocerebral bridge. A: Possible retinotopic pathway from dorsal rim area throughout dorsal rim lamina and dorsal rim medulla via proposed connections toward posterior optic tubercle and protocerebral bridge. A schematic drawing of the dorsal rim area of the left eye is shown, with the orthogonal microvillar orientations of the single ommatidia indicated by the T-shaped symbols. Microvilli orientations which illustrate the fan-shaped distribution are highlighted blue. Black arrowheads indicate the preferred *E*-vector orientations of TB1 neurons which innervate the eight columns in a half of the protocerebral bridge. Dorsal rim area (histological drawing), dorsal rim medulla (3D reconstruction) and protocerebral bridge (schematic drawing) are not in scale but in correct orientation to each other. Dorsal view in all cases. B: Microvilli orientations, demonstrating the fan shaped distribution in the dorsal rim area, show strong similarity with the preferred *E*-vector tuning in TB1 neurons. Orientations are indicated by arrows (a: anterior, l: lateral). DRA: dorsal rim area, DRLA: dorsal rim lamina, DRME: dorsal rim medulla, POTU: posterior optic tubercle, PB: protocerebral bridge. Adapted from Homberg (2004) and modified from the data set of Kurylas et al. (2008).

in higher brain regions. Neuropils of the posterior polarization pathway, namely the posterior optic tubercle and the protocerebral bridge, are structured topographically in a way comparable to the DRA, DRLA and DRME (Beetz et al. 2015, Heinze and Homberg 2007).

The similarities are the following: Photoreceptor microvilli orientations are distributed in a fan-shaped manner over the DRA (Fig.9). Therefore, orientations of the detected *E*-vectors rotate accordingly over the length of the DRA. Due to retinotopic projections, this spatial pattern of *E*-vector tuning is maintained in the DRLA and DRME. A similar gradual rotation of *E*-vector tuning occurs in neurons which connect the posterior optic tubercle and the protocerebral bridge (Heinze and Homberg 2007; Fig.9). The latter is considered to be an important internal *E*-vector compass. This pattern of *E*-vector tuning is completed by information from further interneurons and the polarotopic map of *E*-vectors is projected on the central body's upper division in the central complex.

Nevertheless, even though there are similarities in *E*-vector tuning between neurons in peripheral and central neuropils of the polarization pathway, it has to be considered that

the retinotopic pattern appears to be lost in the anterior polarization pathway which is connecting these neuropils. In particular in tangential neurons of the central bodies lower division information is no longer proceeded by numerous interneurons which are all arranged topographically but by few neurons, of which only the diverging arborizations are arranged topographically (Vitzthum et al. 2002). In this context it might be concluded that the topographic organization of the posterior optic tubercle and the protocerebral bridge has evolved secondarily. Little is known about the precise projections of the posterior polarization pathway and to what extend retinotopy is present in it.

PROCESSING OF *E*-VECTOR INFORMATION IN INTERNEURONS - AN EXAMPLE

An opportunity to compare the properties of *E*-vector responses in photoreceptors and subsequent interneurons is provided by Pfeiffer et al. (2005) and Kinoshita et al. (2007). Like in the present work they studied intensity response curves and polarization sensitivity in the desert locust. The focus of both investigations were several types of interneurons in the anterior optic tubercle, which is part of the anterior polarization pathway and is considered to be an early relay station for polarized light information toward the central complex (Homberg et al. 2003). Two of these cell types, lobula tubercle neurons (LoTu1) and tubercle-tubercle neurons (TuTu1), respond to polarized light and will be discussed here.

In Fig.10, intensity response curves of LoTu1, TuTu1 and DRA photoreceptors are compared. Considering the large visual fields of DRA receptors they might be actually more sensitive under the free sky than measured in laboratory experiments and the same might be true for the discussed interneurons (Schmeling et al. 2015). Therefore the curves in Fig.10 are shifted accordingly by a factor calculated in Schmeling et al. (2015). However, it has to be pointed out that information from numerous DRA photoreceptors are likely to integrate on single interneurons, as discussed for crickets (Labhart et al. 2001). Thus light sensitivity of the pathway might be enhanced even further.

Both neuron types show specific background activities, which is a certain rate of action potentials that can be measured, even if no light stimulus is applied. Considering the sensitivity shift mentioned above, DRA photoreceptors, as well as LoTu1 and TuTu1 interneurons have their threshold of absolute light sensitivity at roughly 10^7 photons $cm^{-2}s^{-1}$. As discussed above, this is sensitive enough for nocturnal light conditions.

Even though the thresholds of DRA receptors. LoTu1 and TuTu1 are similar, the two later interneurons reach saturation at about 10^9 photons $cm^{-2}s^{-1}$, and by this at much lower intensities than the photoreceptors. This is mainly caused by the interneurons high background activities. Logically a saturated receptor cannot distinguish between light intensities above its saturation level. Light intensities during the day strongly exceed the light levels necessary for saturation in the here discussed neurons (see fig. 12). In conclusion, this observation underlines that information about light intensity is basically lost in the polarization vision pathway and only spectral and polarized information remain to be processed. Only at the low light levels during night saturation in the polarization pathway diminishes. Projection patterns of the LoTu1 neurons reach to the tubercles but also to the lobula, where they could be connected to the DRME via medulla tangential neurons (Homberg and Würden 1997). Arborizations of the TuTu1 neurons are only

found in the two tubercles. LoTu1 neurons could resemble a more peripheral part of the polarization pathway and the TuTu1 neurons a more central part. Therefore it appears that the loss of information about light intensity increases from the periphery of the posterior polarization pathway to its central stations.

However, a confusing fact is that LoTu1 interneurons are actually maximally excited by unpolarized light instead of polarized light and are inhibited at very high light intensities. They also show no polarization opponency. The prerequisite of polarization opponency is the antagonistic interaction of the two microvillar orientations in a DRA ommatidium. Its absence might imply that information from only one retinula cell block of an ommatidium is used here (either R7 or R1-6 and R8, see Schmeling et al. 2014, 2015). The strong response to unpolarized light implies input from the main eye, possible from the line tangential neurons. These connect the DRME with the anterior optic lobes, some showing polarization opponency and some do not (el Jundi et al. 2011). These interneurons run through the medulla where spectral and polarized light information could be collected.

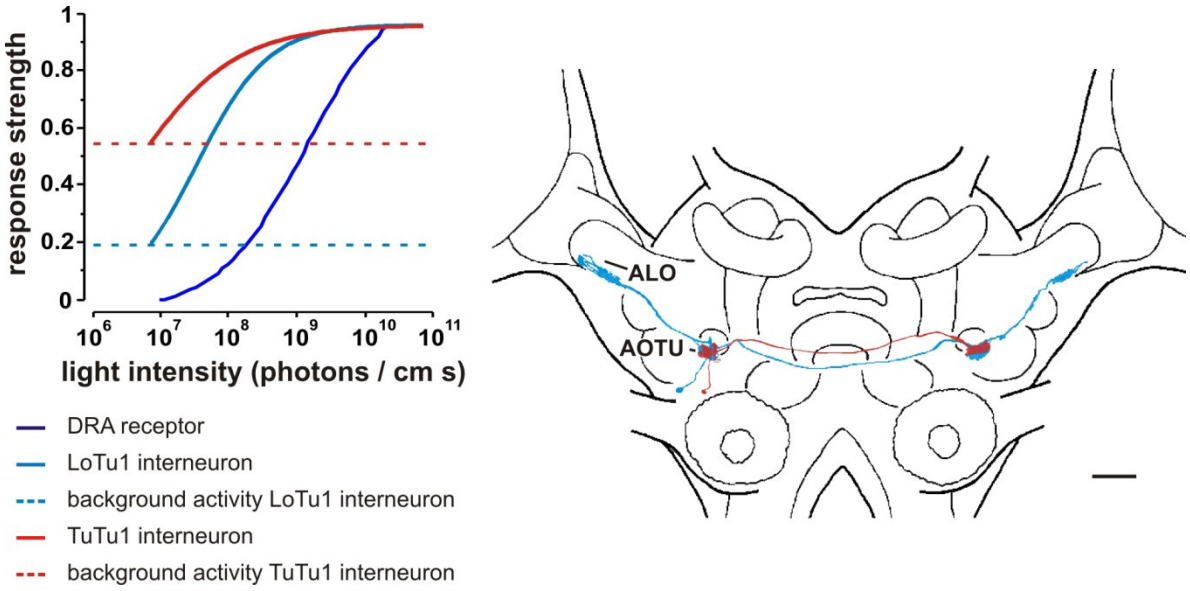

Fig.10: Comparison of V-logI curves and of arborization patterns between DRA photoreceptors and two interneuron types in the polarization pathway of the desert locust. The intensity response curve (V-logI) of DRA receptors is calculated from electrophysiological measurements in gregarious locusts (Schmeling et al. 2014). Because the visual field of DRA receptors is about 180 times larger than that of receptors of the main eye, the curve was shifted correspondingly to lower light intensities (Schmeling et al. 2015). Interneuron data are averaged measurements from the anterior optic tubercle (Kinoshita et al. 2007) and are shifted like the photoreceptor curve. It must be pointed out that measurements from receptors were performed with unpolarized light, while interneurons were stimulated with polarized light. Therefore the receptors might be even more sensitive (discussed in Schmeling et al. 2014). LoTu1 neurons connect the two posterior optic tubercle (POTU) but also the ventral layer of the anterior optic lobes (ALO). TuTu1 neurons only connect the POTU. Physiological and anatomical information adapted and changed from Pfeiffer et al. (2005) and Kinoshita et al. (2007). Scale bar indicates 200 µm.

Even though TuTu1 interneurons are located more distantly to the DRME, they are maximally excited by polarized light of a preferred *E*-vector and show polarization opponency. A mechanism considered to be directly linked to the interactions of DRA photoreceptors and their subsequent interneurons.

What functions it serves that the one interneuron type shows polarization opponency and the other does not remains unclear.

POTENTIAL PARTICIPATION OF THE MAIN EYE IN POLARIZATION VISION

LoTu1 und TuTu1 neurons are sensitive to UV and green light stimuli, although polarization vision in the locust is considered to rely exclusively on blue receptors of the DRA. The obvious assumption is that there is input from the main eye. Only there, additional UV and green sensitive receptors do occur (Schmeling et al. 2014). An integration of visual signals from the DRA and main eye likely occurs in polarization sensitive medulla tangential neurons. Most of these neurons have ramifications in layer 4 of the medulla but two types, TML1 and MeMe2, also arborize in layer 3 (el Jundi and Homberg 2010, el Jundi et al. 2011). All long visual fibers from the main eye terminate in medulla layer 3 (Schmeling et al. 2015). In conclusion medulla layer 3 might be the first station in which information from the main eye and the DRA are combined.

An influence of the locust main eye to polarization vision is also suggested by the fact that sensitivity to ventrally applied polarized light has been demonstrated (Shashar et al. 2005, el Jundi and Homberg 2010, Beetz 2013). The locust DRA has a visual field limited to signals above the horizon of the animal (Schmeling et al. 2015) and, therefore, cannot contribute to ventral polarization vision. In flies responses to ventrally polarized light are indeed mediated by the main eye (Wernet et al. 2012). The authors suggest that convergence of a high number of weak polarized light analyzers in the main eye allows for adequate detection of *E*-vector patterns outside the range of the flies DRA. All insect photoreceptors are weakly polarization sensitive as demonstrated for the desert locust main eye (Schmeling et al. 2014). Because microvilli are not arranged in orthogonal blocks in the ommatidia of the main eye, polarization opponency is unlikely to be found in this part of the vision pathway.

Ventral polarization sensitivity in insects is mainly associated with the detection of water surfaces, often to find an adequate habitat to lay eggs (e.g. Wildermuth, 1998). Whether the detection of water plays any role for the desert locust, for instance as an indicator of suitable feeding area, is unclear.

POLARIZATION VISION IN THE TWO LOCUST PHASES

Neither this work nor the study by el Jundi and Homberg (2010) found differences in anatomical or physiological features of the polarization vision pathway between gregarious and solitarious desert locusts. This is remarkable, since the two phases strongly differ in their behavior and the light conditions they are exposed to. Even though polarization vision has been examined mainly in the diurnal gregarious phase, there are hints that the desert locust polarization vision pathway is actually adapted to nocturnal conditions and thus to the life style of the solitarious phase.

As discussed above, during night it is advantageous to detect celestial *E*-vector patterns in the blue spectrum. In this spectrum these patterns might be relatively weak, but light levels, which are likely to be a more critical factor, are relatively high. The DRA of both phases contains exclusively blue receptors and seems to be adapted to detect lower light intensities (see paragraphs above). Furthermore, peak activity of solitarious desert locusts is specifically at dusk (Rao 1960, Roffey 1963, Roffey and Popov 1968, Ely et al. 2011), a time when light conditions are most favorable to detect polarized light. At dusk, when the sun stands close to the horizon, the percentage of polarized light is at its maximum, because the highest degree of polarization occurs 90° from the sun. This is the time when *E*-vector patterns are at their highest intensities and therefore a more reliable compass cue than during most of the day.

Hitherto long range migration and the role of polarized light orientation has been linked to the day active gregarious phase and is considered to be less prominent in the nocturnal solitarious phase. Why do both phases possess a highly specialized polarization vision system, and why is this system adapted to light conditions at night? Without providing a final conclusion, certain considerations can be made.

The importance of polarized light as an orientation cue might be differently weighted in the two phases. It could be hypothesized that diurnal gregarious locust rely predominantly on the sun position or chromatic gradients in the sky. In contrast, solitarious locusts are mainly active after sunrise, when the sun is not visible and the skies chromatic gradient vanished. Under these conditions polarized skylight might play a more dominant role for the animals. Therefore it seems reasonable to assume that locust polarization vision has adapted to the most limiting environment both locust phases are exposed to: that of nocturnal light conditions. And finally, it still has to be shown whether long range migration actually plays a minor role in solitarious locusts. Evidence for migratory flights of solitarious locusts is based on field observations, but has not been rigorously analyzed on a quantitative level (Rao 1936, 1942, 1960, Waloff 1963, Roffey 1963).

THE ROLE OF POLARIZED LIGHT FOR DESERT LOCUST ORIENTATION

The existence of a highly specialized polarization vision system in the desert locust brain can be considered as confirmed. In laboratory experiments, tethered flying locusts responded with periodic changes in yaw torque, when illuminated from above through a slowly rotating polarizer (Mappes and Homberg 2004). This response vanished after painting the DRAs black, indicating its role in mediating this behavior. Laboratory experiments also confirmed that sun position and chromatic gradients are integrated in the polarization vision pathway (Pfeiffer and Homberg 2007, el Jundi et al. 2014). Despite these investigations, the role of polarized light vision in locust long range migration is still poorly understood.

In an attempt to understand desert locust migrating behavior, Draper (1980) examined the data set obtained from a gregarious locust swarm. He claims that any orientations cues are absent in this case. The only factor influencing locust flight direction would be the wind current and all deviations from wind direction would be within statistical norms.

Therefore, flying locust swarms would simply ride on the wind without a specific target. That locust swarms can follow the current wind direction has also been reported by other researchers (Haskell et al. 1962, Steedman 1988). It has been argued that flying downwind saves energy, therefore being favorable. Using this strategy locusts are likely to be taken to regions where air masses collide, resulting in rainfall and the possibility of a new sustainable feeding area (Uvarov 1977, van Huis et al. 2007, Simpson and Sword 2008). Actually, several publications addressing locust plague prevention have acknowledged the importance of wind currents to forecast swarm occurrences (e.g. Symmons 1992, Showler 2002). Nevertheless, in a review on the desert locust life style, Symmons and Cressman (2001) argue that migration directions of gregarious swarms often cannot be explained by wind direction alone. Uvarov (1977) as well points out that desert locust swarms can maintain flight directions deviating from current wind directions.

Unlike bees or ants, desert locusts are not aiming for a certain nest or feeding site, but it seems that regional breeding areas exist. Solitarious locusts migrate between these areas in a seasonal pattern (Uvarov 1977, Symmons and Cressman 2001). At least during summer, seasonal winds support these directional migrations, but they might be not reliable enough for aiming. Due to fluctuations they could be temporally misleading or be absent for some time. Especially after the summer season locust swarms are leaving their recent breeding sites clearly flying upwind and are maintaining flight when wind currents are absent (review: Uvarov 1977, Symmons and Cressman 2001). Therefore celestial orientation cues would provide necessary stability in navigation.

Desert locusts nymphs do not fly at all and in conclusion wind directions might play a minor role in this stage. Bands of these nymphs are known to walk in distinct directions, apparently using a sky compass, and are able to detect polarized light (Kennedy 1951, Steedman 1988, Eggers and Weber 1993). So, in conclusion, orientation mechanisms like polarization vision could be more important in larval stages.

Migrating behavior of gregarious swarms does not follow the seasonal patterns mentioned above. They are not heading toward specific breeding sites, but are spreading over the boundary of the former inhabited areas (Symmons and Cressman 2001). Therefore, it seems more likely that the solitarious phase is more relying on compass cues than the gregarious phase. This fits to the impression that spectral and absolute sensitivity of the DRA appear to be adapted to nocturnal light conditions under which solitarious locusts are active (see paragraphs above).

In conclusion, polarization vision might be found in all stages and phases of the desert locust, but could have its major purpose in the solitarious phase.

COMPARISON WITH OTHER POLARIZATION-SENSITIVE INSECT SPECIES

As mentioned above, the biological significance of desert locust orientation behavior is not fully understood. Therefore it is difficult to make statements about how migration behavior and accuracy of orientation mechanisms correlate. Honeybees and desert ants, in contrast, are species in which a highly accurate polarization compass has been demonstrated. These insect species navigate toward their nest or feeding sites, which

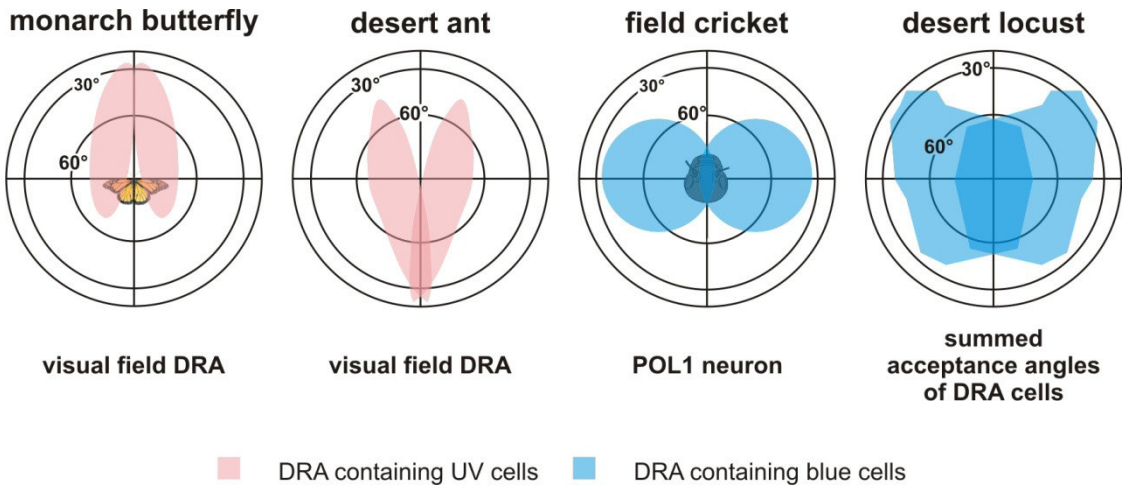

Fig.11: Receptive fields of DRA mediated polarization vision systems in different insect species. Because data is only available for different neuronal levels, some considerations have to be taken into account. (1) The information from the field cricket are found at interneuronal level and therefore might be considered relatively representative for the whole pathway. (2) It is not clear whether the whole visual field of the insect DRA is effectively used for *E*-vector detection. Therefore the patch of sky used by the monarch butterfly and the desert ants could be smaller than implied by their DRAs visual fields. In the case of the desert locust the acceptance angle was chosen for illustration, because the visual field of this parameter shows similarities to that of polarization-sensitive interneurons (el Jundi and Homberg 2010). Thus it might represent the effective region of polarization vision. Information drawn from Labhart(1986), Labhart et al. (2001), Heinze (2014), Schmeling et al. (2015).

are very distinct and commonly small areas. Even small course deviations would make the insect miss its target.

E-vector based orientation in honey bees relies on sky patches of down to 0.1°, what covers roughly 2.5% of the sky hemisphere (Zolotov and Frantsevich 1973). Crickets, detecting polarized light in the blue spectrum, need a patch of at least 1° (Henze and Labhart 2007). This might illustrate how accurate orientation after polarized light is, when using UV light. In fact it seem to be so reliable that UV *E*-vector patterns have been claimed to be the major orientation cue in the desert ant (Wehner and Müller 2006).

DRA size, its receptors angular sensitivity and its overall visual field seem to correlate positively in several insects species (Labhart 1980, Labhart 1986, Blum and Labhart 2000, Labhart et al. 2001, Stalleicken et al. 2006, Heinze 2014). The large visual fields of desert locust DRAs, as well as those of its polarization sensitive interneurons (el Jundi and Homberg 2010, Schmeling et al. 2015), might be considered similar to those in the cricket. All three parameters named above occur to be linked to the insect's life style and the spectrum in which polarized light is detected (Fig.11). Concluding from Fig.11, it seems that there can be distinguished between diurnal insects detecting polarized light in the UV over a relatively small part of the sky, and nocturnal insects detecting polarized light in the blue over a large part of the sky.

What is the reason that diurnal insects seem to generally use smaller parts of the sky for *E*-vector based orientation and nocturnal insects larger parts? As discussed above, sky

patches smaller than a DRAs visual field are still sufficient to detect a celestial *E*-vector pattern. Nevertheless, disturbances of this pattern could make it necessary to interpolate information over a wider part of sky. This way incorrect orientation, possibly caused by a localized irregularity in the sky, would be avoided. The stronger the disturbances of the *E*-vector pattern, the larger the part of the sky over which should be interpolated. Thus, the small visual fields of DRAs in diurnal insects might be considered sufficient to detect *E*-vector patterns in the UV, since there are only few disturbances in this spectrum. In contrast, nocturnal insects with larger DRA visual fields would have to interpolate over a wider part of the sky to compensate the unstable patterns of the blue spectrum.

Although detecting *E*-vector pattern in the UV spectrum has its clear advantages, the levels of UV light are low during the night and therefore might not be visible, while blue light levels are comparably high (Johnsen et al. 2006, see also Fig.12). And indeed, in the diurnal honey bee the light level threshold for polarization vision was measured to be 10^{10}-10^{11} photons $cm^{-2}s^{-1}$ in the UV (von Helversen and Edrich 1974). This threshold is too high for night conditions, but is sufficient for times between sunset and sunrise. The threshold is much lower in nocturnal crickets and lies here at about 2.5×10^7 photons $cm^{-2}s^{-1}$ in the blue spectrum (Herzmann and Labhart 1989). As discussed above, desert locust DRA receptors might have a threshold of about 10^7 photons $cm^{-2}s^{-1}$ in the blue spectrum. Blue light intensity of the night sky is usually above this level. This further underlines the adaptation of the polarization vision system in nocturnal insects to light levels at night. Diurnal insects with no such adaption pressure can rely on much lower absolute sensitivity because during the day light levels are high enough anyway.

THE MAIN EYE

SPECTRAL SENSITIVITY

Examinations on opsin expressions, ERGs and intracellular recordings showed that the main eye of the desert locust contains UV-, blue- and green sensitive photoreceptors (Schmeling et al. 2014). This is the most common set of spectral types found in insects (review: Briscoe and Chittka 2001). In contrast to most other insects, a fourth type of locust photoreceptor was found, containing blue as well as green absorbing opsins. Such combinations of several opsin types in a single photoreceptor are relatively new findings and were also confirmed for some other insect species (discussed in Schmeling et al. 2014). In addition, overall spectral sensitivity, measured with ERGs, differed between the dorsal and ventral half of the locust main eye and between the two phases (Schmeling et al. 2014). The main trend is that green sensitivity becomes more dominant in the main eye of solitarious locusts, particularly in the ventral half of the eye. A similar trend of dorsal eye regions being more sensitive for short wavelengths and ventral eye regions having additional long wavelength sensitivity is present in some other insects (dragonfly: Mazokin-Porshniakov 1959, Ruck 1965, Horridge 1969; owlfly: Gogala 1967, Hamdorf et al. 1971; mayfly: Horridge and McLean 1978).

A gradient of UV versus green sensitivity along the dorsoventral axis of insect eyes has been discussed in particular in the migratory locust (Osorio 1986). There it was considered to play a role for body orientation and flight stability through the dorsal light

response and optomotor responses. UV light appears stronger in the sky compared to the ground and is thereby perceived mostly by the dorsal eye. According to Osorio (1986), dorsal UV light is used by the locust to determine up and down. On the other hand, the ground reflects a relatively high amount of green light, which would be perceived by the ventral eye. Taking this into account, high green sensitivity of the locust ventral main eye seems reasonable, since the ground provides structures and objects necessary for precise optomotor responses. However, spectral receptor types are distributed randomly in the eye and the shifting spectral sensitivity in the main eye must be achieved a different way. This could happen either by changes of spectral sensitivity in the same photoreceptor classes or at later stages of information processing in the visual pathway. Three mechanisms have been observed in arthropod photoreceptors that could explain shifts in spectral sensitivity in identical sets of receptor types. (1) It has been shown that the expression ratio of opsin types within an insect eye can change over the day, controlled by a circadian clock (Oba and Kainuma 2009, Yan et al. 2014). In this case absolute sensitivity would be influenced by the current amount of pigments. In ERGs this would result in shifts of relative spectral sensitivity, as measured in Schmeling et al. (2014). (2) In the horseshoe crab *Limulus* the ratio of different opsins, co-expressed in single photoreceptors, changes in a diurnal rhythm, controlled by a circadian clock (Katti et al. 2010). (3) Another mechanism does not change the total amount of expressed opsin within a photoreceptor cell, but transports the visual pigments in or out of the receptors photosensitive site, the microvilli (Arikawa et al. 1987). A dynamic change in the blue and green opsin ratio in the photosensitive site of locust broadband photoreceptors could be a way to shift the receptors spectral sensitivity without influencing its absolute sensitivity.

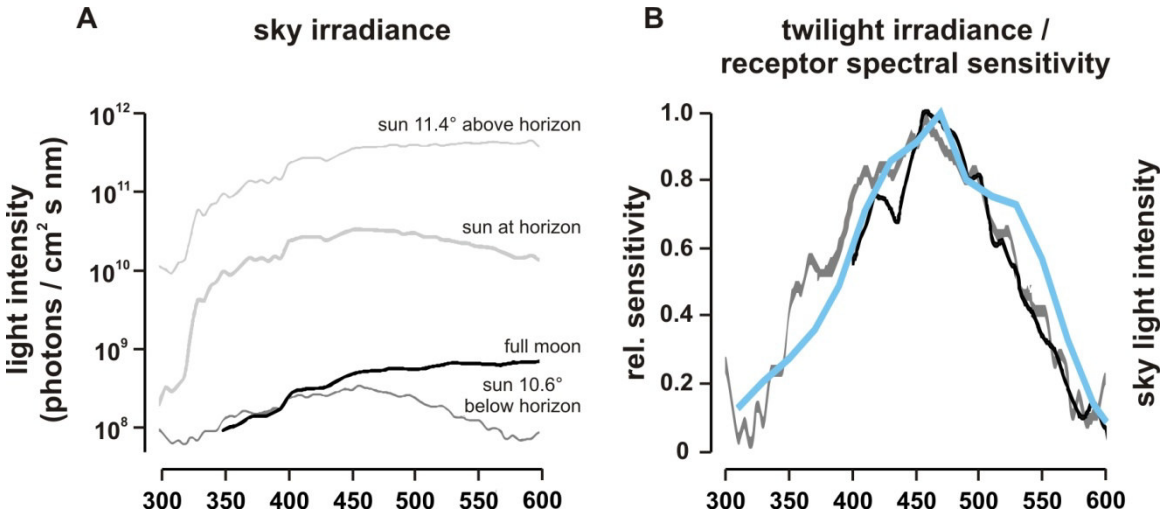

Fig.12: Composition of skylight compared to the spectral sensitivity of desert locust photoreceptors. A: Intensity of color spectra in the sky at different times of the day (adapted from Johnsen et al. 2006). B: Sky color spectra at dusk compared to spectral sensitivity measured in locust broadband photoreceptors. Light measurements are indicated by a black (Lythgoe 1979) and grey (Johnsen et al. 2006) line. The grey line resembles the measurement in A, with the sun 10.6° below the horizon. The blue line indicates the averaged spectral sensitivity of blue/green broadband receptors in the main eye of solitarious locusts (Schmeling et al. 2014). For a better comparison light intensity curves were adjusted manually to meet the same height as the spectral sensitivity curve.

POSSIBLE FUNCTION OF THE SHIFT IN SPECTRAL SENSITIVITY

Overall spectral sensitivity of dorsal eye regions of solitarious locusts are slightly shifted to longer wavelengths of the blue spectrum. Interestingly, the resulting spectral sensitivity curve shows strong similarity to the spectral composition of the evening sky after sunset, not only in wavelength peak, but also in the overall shape of the curve (Johnsen et al. 2006, Lythgoe 1979, see also Fig.12). Light levels before and after sunset are low and it is advantageous to be adapted to that part of the spectral skylight that has still relatively high intensity. These findings fit to the fact that solitarious locusts start their flight activity just after sunset (Rao 1960, Roffey 1963, Roffey and Popov 1968, Ely et al. 2011). A similar precise adjustment of spectral peak sensitivity is found in photoreceptors of fireflies, which are perfectly adapted to detect the light flashes of other fireflies (e.g. Cronin et al. 2000).

ABSOLUTE SENSITIVITY OF PHOTORECEPTORS COMPARED TO LIGHT INTENSITIES AT NIGHT

Light intensities during the evening and at night barely reach 10^9 photons $cm^{-2}s^{-1}$, even under full moon conditions (Johnsen et al. 2006, see also Fig.12). Actual intensity response curves, measured in the main eye of the desert locust, do not show distinct photoreceptor responses to light stimuli at this level (Schmeling et al. 2014). This might imply that the main eye of the desert locust is not sensitive enough for the dim light conditions during the night. However, several mechanisms can be assumed in the locust's visual system to increase absolute sensitivity.

As discussed above for DRA receptors, receptive fields strongly influence the number of photons captured by a receptor and thus the receptor’s light sensitivity. Larger visual fields lead to higher absolute sensitivity. Receptive fields of photoreceptors measured in the migratory locust varied in different studies from 1.4° to 6.6° (Tunstall and Horridge 1967, Wilson 1975, Williams 1983) and similar changes could to be present in the desert locust’s main eye, depending on environmental light conditions. A very likely cause for this variability is light adaption through moving screening pigments. An endogenous and perhaps circadian controlled change in locust rhabdom diameter could also influences absolute sensitivity (Williams 1982). Such diurnal changes in rhabdom size have been proven for other arthropods as well (review: Blest 1988). Furthermore, in some insects, concentrations of photopigments in a receptor cell underlie similar daily changes (Isono et al. 1986, Hariyama and Tsukahara 1992, Oba and Kainuma 2009). Taking these mechanisms into account, desert locust intensity response curves, as measured in Schmeling et al. (2014), could vary accordingly to environmental conditions and circadian rhythms. A daily change in photoreceptor absolute sensitivity has already been proven in other insects (Bennett 1983, Lall 1993, Kral and Stelzl 1998) and seems to be present in the desert locust as well (unpublished data of the Prof. Homberg working group). Nevertheless, it must be pointed out that V/log I functions in solitarious desert locusts were actually examined during their night period and thus should already be considered at a more sensitive state. Nevertheless, no significant differences in their receptor response curves were found compared to gregarious locusts during their day period.

An answer to this problem might be the co-expression of blue and green opsins within five single photoreceptors in each ommatidium (Schmeling et al. 2014). Spectral sensitivity of the receptor is broadened by this combination of photopigments. The ability to absorb photons over a broader spectrum increases the total number of detected photons per receptor. That would result in an overall higher sensitivity. A trade-off would be the lost ability for color discrimination in these receptors. Because receptor response curves were measured with monochromatic light, this effect might have been missed in the experiments of Schmeling et al. (2014).

A further possible mechanism for enhancing total light sensitivity could be receptor coupling. In the cases in which a blue/green broadband photoreceptor was dye marked after recording, it appeared that not only one, but all five cells of this type were stained in the corresponding ommatidium. A possible explanation is electrical coupling, as discussed in Schmeling et al. (2015). In this case all five cells would work together as a single receptor with higher absolute sensitivity. The fact that this postulated higher sensitivity was not measured by Schmeling et al. (2014), could be explained by convergence of light information on axonal level of the receptor cells. When recording from the more distal microvillar part of the cell, this increase in sensitivity would be missed. Shaw et al. (1989) already discussed electrical coupling of fly photoreceptors in the lamina.

In addition, it is likely that information from several receptors converges at the level of the lamina. Certain types of locust lamina monopolar cells possess arborizations which reach towards neighboring cartridges (Nowel and Shelton 1981, Wernitznig et al. 2015, see also Fig.13), thereby collecting light information from numerous ommatidia.

All of the mechanisms named above could cause an increase in overall light sensitivity of the locust main eye to an extent which cannot be estimated yet.

THE POSSIBILIY OF AN ACHROMATIC VISUAL PATHWAY IN THE DESERT LOCUST

Like in humans, a chromatic and an achromatic visual system seem to occur in several insect species. For instance, under dim light conditions, a green based achromatic vision replaces the otherwise trichromatic vision in honey bees (Menzel 1981, Giurfa et al. 1996). In the desert locust, a visual pathway with high absolute sensitivity but no color coding might be represented by the receptors co-expressing opsins absorbing blue and green light. Possible electrical coupling between these receptors would underline this function (see former paragraph).

Another noteworthy aspect is the separation of the locust ommatidia into two types with either one UV- or one blue receptor. It is more common in insects that each ommatidium contains one UV- and one blue sensitive receptor, both with long visual fibers, and two green receptors, both with short visual fibers (Zufall et al. 1989, Briscoe et al. 2003, White et al. 2003, Spaethe and Briscoe 2005). Different types of ommatidia within the eye have been reported for other insect species (moth: White et al. 2003, bumblebee: Spaethe and Briscoe 2005, honeybee: Wakakuwa et al. 2005), although the function of this separation is not always completely clear. In desert locusts, the small number of UV-

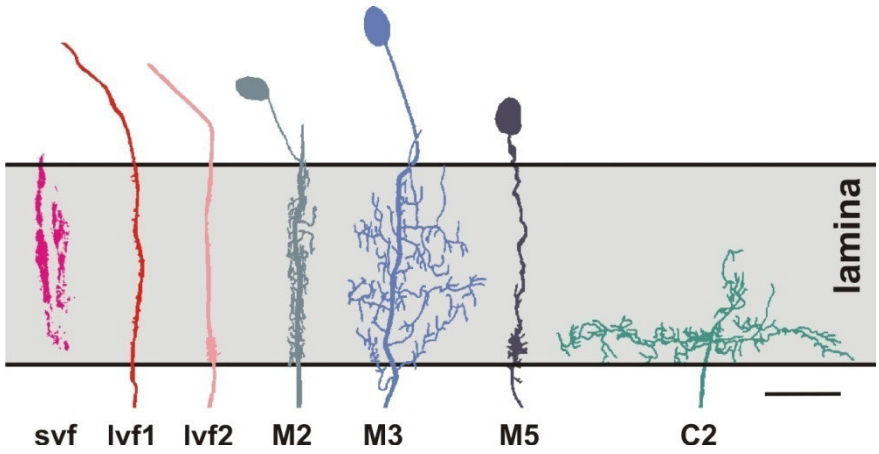

Fig.13: Comparison of short visual fiber terminations with ramifications of interneurons of the lamina of the desert locust. Stained short visual fibers (svf) of photoreceptor cells R2,3,5,6 and 8 are set in scale with histological drawings of the proposed two morphological types of long visual fibers (lvf) of photoreceptor cell R7, with lamina monopolar cells 2, 3 and 5 (M2, 3 and 5), and with lamina centrifugal neuron 2 (C2). Adapted from Nowel and Shelton (1981) and Schmeling et al. (2015). Scale bar: 20 µm.

and blue receptors in the main eye weakens the chromatic vision, in particular its spatial resolution, but this might be a necessary trade-off for advanced vision under low light conditions.

In conclusion, locusts appear to have a chromatic visual system, comprising UV, blue, and green receptors, and an achromatic system, consisting of receptors co-expressing blue and green opsins. The chromatic system consists of a relatively small number of receptors, the achromatic of a higher number. In addition the achromatic system might enhance absolute sensitivity by electrical coupling of its receptors.

PHOTORECEPTOR TERMINATIONS IN LAMINA AND MEDULLA

In the main eye the only successful stainings of short visual fibers are from broadband photoreceptors, co-expressing blue and green opsin, and these recpetors were alsways stained together. However, the numbers of stainings are low, so interpretations have to be made with caution. Fig.13 shows that the terminations of these receptors are separated into two bundles with different lengths. One bundle reaches the inner margin of the lamina, the other barely extends to the proximal third of the neuropil. Interestingly, there are lamina interneurons, whose anatomy fits quite well to this pattern (Nowel and Shelton 1981). There are interneurons with arborizations restricted to the proximal part of the lamina (M5). Such neurons would perceive information solely from the longer of the short visual fibers. Another type (C2) spreads throughout several lamina cartridges with fibers running close to the lamina's inner margin, but shows a single branch reaching distally. This way information from both visual fiber bundles of one cartridge might be combined with information of the deeper reaching visual fiber bundles from several neighboring cartridges. As discussed above, convergence of photoreceptor information from multiple ommatidia on few subsequent interneurons can be considered a major

mechanism for adaptation to dim light conditions. However, what functions the different lengths of the short visual fibers have is not clear, since they proceed the same broadband color information. Other interneurons (M2 and M3) might rather communicate with the long visual fibers (lvf1 and 2), implied by their similar arborization patterns throughout the whole depth of the lamina.

The terminations of the long visual fibers in medulla layer 3 strongly suggest a role of this layer in color vision. Medulla layer 3 is also innervated by polarization sensitive neurons, possibly representing the first stage in which color gradients of the sky are processed with polarization information.

FINAL CONCLUSIONS

In the desert locust, photoreceptor physiology strongly differs between the dorsal rim area and the main eye, and so do details of photoreceptor morphology and projections (Fig.14). It appears that dorsal rim area photoreceptors are mainly adapted to detect *E*-vector patterns during the difficult light conditions at night, while the main eyes function is color vision and a higher spatial resolution. There is also evidence for achromatic vision in the main eye.

All eight dorsal rim area receptors are highly polarization sensitive, pointing out their role to detect *E*-vector patterns of the sky. The fact that all these receptors are exclusively blue sensitive can be understood as an adaptation to nocturnal light conditions, because the blue spectrum dominates in the sky during this time. Wide angular sensitivities make it possible for a single receptor to collect a higher amount of photons compared to receptors with smaller angular sensitivities, like in the main eye. That might increase dorsal rim area receptor sensitivity at night. Furthermore, *E*-vector patterns can be integrated over a larger region of the sky. This is an advantage, since *E*-vector patterns in the blue spectrum are relatively disturbed.

In one dorsal rim area ommatidium microvilli orientations of the receptor cells R1-6 and R8 are arranged parallel to each other, thus detecting the same *E*-vector. All these cells have projections to the dorsal rim lamina. Receptor cell R7 has microvilli oriented orthogonal to those of the other cells. It projects through the dorsal rim lamina, where it has small arborizations, but it terminates in the dorsal rim medulla. A main feature of insect polarization vision pathways is the phenomenon of polarization opponency. It presupposes convergence of antagonistic *E*-vector information from the two orthogonal receptor microvilli block on subsequent interneurons. Because all dorsal rim area receptors have arborizations in the dorsal rim lamina, information exchange at this level cannot be completely excluded. Nevertheless, it still might be suggested that the first stage at which polarization opponency occurs in the dorsal rim medulla. In this case, hitherto not indentified interneurons would connect receptor terminations in the dorsal rim lamina with the dorsal rim medulla.

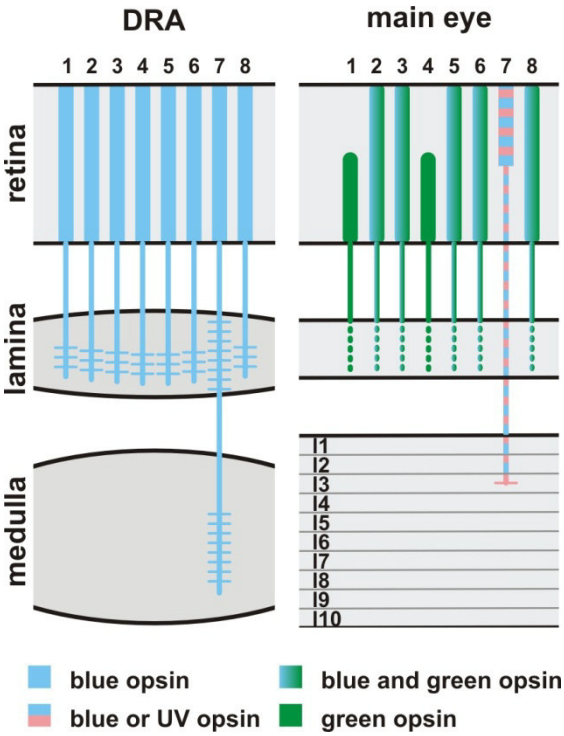

Fig.14: Schematic overview of photoreceptor spectral sensitivity, their length within the corresponding ommatidium and their termination sites in main eye and DRA of the desert locust. Numbers indicate receptor identity (receptor cell 1-8) and layers in the medulla (I1-I10). Dashed lines indicate that the exact length of the visual fiber in the lamina is unknown. Scales in the drawings do not necessarily represent actual size.

The retinotopic arrangement of the dorsal rim area shows main similarities to *E*-vector tuning in interneurons of the central complex. However, this topographic arrangement of polarization information is not present in the whole polarization pathway. It remains an open question whether topography in the central complex evolved secondarily.

Photoreceptors in the main eye show low polarization and smaller angular sensitivity, and can be grouped into four spectral types. One receptor cell per ommatidium is either UV or blue sensitive (R7), two are green sensitive (R1 and R4) and five receptor cells contain blue and green light absorbing pigments (R2, R3, R5, R6 and R8). The two visual pigments in the latter five receptors result in a broadened spectral sensitivity. It might be suggested that because of the broader spectral range, the total number of detected photons increases, thus increasing total sensitivity of these receptors. A trade-off would be a loss of spectral accuracy. Regular colabeling implies electrical coupling between these five receptors and their possible role as a functional unit. In contrast to the other three chromatic receptor types, a parallel, achromatic and more sensitive visual system might be suggested.

The microvillar site of the green sensitive photoreceptors is restricted to the proximal region of the ommatidia, while microvilli of the UV/blue receptor were found exclusively in the distal region of ommatidia.

Except for R7 all receptors terminate in the lamina, but at different depth. How deep each individual receptor type reaches is not clear. R7 projects further and terminates in layer 3 of the medulla. In this layer, interactions with polarization sensitive interneurons can be assumed. Hence information of spectral gradients in the sky is processed with polarization information, layer 3 of the medulla might be the connection stage between

the polarization and color pathway. The main eye could also contribute to polarization vision, since the visual field of the dorsal rim area is limited above the horizon of the animal, but certain locust interneurons also respond to polarized light below the horizon.

The general physiology of the desert locust eye implies an adaption to nocturnal conditions (blue sensitive dorsal rim are with high absolute sensitivity and large visual fields, and a possible achromatic pathway in the main eye with proposed high absolute sensitivity). This is the case in both locust phases, even though only the solitarious phase is nocturnal. No differences were found between the two phases, except a shift in overall spectral sensitivity in the main eye. The eye of solitarious locusts seems to be more sensitive to longer wavelength than in gregarious locusts. Since the photoreceptor set of both phases is identical, further, more dynamic mechanism of spectral adaptation might be assumed.

REFERENCES

Anderson H (1978a) Postembryonic development of the visual system of the locust, *Schistocerca gregaria* I. patterns of growth and developmental interactions in the retina and optic lobe. J. Embryol. Exp. Morph. 45:55-83

Anderson H (1978b) Postembryonic development of the visual system of the locust, *Schistocerca gregaria* II. An experimental investigation of the formation of the retina-lamina projection. J. Embryol. Exp. Morph. 46:147-170

Arikawa K, Kawamata K, Suzuki T, Eguchi E (1987) Daily changes of structure, function and rhodopsin content in the compound eye of the crab *Hemigrapsus sanguineus*. J. comp. Physiol. A 161:161-174

Beetz MJ, el Jundi B, Heinze S, Homberg U (2015) Topographic organization and possible function of the posterior optictubercles in the brain of the desert locust *Schistocerca gregaria*. J. comp. Neurol. in press

Beetz MJ (2013) Electrophysiological and morphological characterization of visually sensitive interneurons of the posterior protocerebrum from the desert locust *Schistocerca gregaria*. Master thesis, Philipps-University Marburg

Bennett RR(1983) Circadian rhythm of visual sensitivity in *Manduca sexta* and its development from an ultradian rhythm. J. comp. Physiol. 150:165-174

Blest AD (1988) The turnover of phototransductive membrane in compound eyes and ocelli.Adv. Insect Physiol. 20:1-53

Blum M, Labhart T (2000) Photoreceptor visual fields, ommatidial array, and receptor axon projections in the polarisation-sensitive dorsal rim area of the cricket compound eye. J. comp. Physiol. A 186:119-128

Briscoe AD, Chittka L (2001) The evolution of color vision in insects. Annu. Rev. Entomol. 46:471-510

Briscoe AD, Bernard GD, Szeto AS, Nagy LM, White RH (2003) Not all butterfly eyes are created equal: Rhodopsin absorption spectra, molecular identification, and localization of ultraviolet-, blue-, and green-sensitive rhodopsin-encoding mRNAs in the Retina of *Vanessa cardui*. J. comp. Neurol. 458:334-349

Cronin TW, Järviletho M, Weckström M, Lall AB (2000) Tuning of photoreceptor spectral sensitivity in fireflies (Coleoptera: Lampyridae). J. comp. Physiol A 186:1-12

Dearborn R Jr, He Q, Kunes S, Dai Y (2002) Eph receptor tyrosine kinase-mediated formation of a topographic map in the *Drosophila* visual system. J. Neurosci. 22:1338-1349

Draper J (1980) The direction of desert locust migration. J. Animal Ecol. 49:959-974

Eggers A, Weber T (1993) Behavioral evidence for polarization vision in locusts. In: Elsner N, Heisenberg M (eds.) Gene-Brain-Behaviour. Thieme, Stuttgart pp 336

el Jundi B, Homberg U (2010) Evidence for the possible existence of a second polarization-vision pathway in the locust brain. J. Insect Physiol. 56:971-979

el Jundi B, Pfeiffer K, Homberg U (2011) A distinct layer of the medulla integrates sky compass signals in the brain of an insect. PLoS ONE 6:e27855

el Jundi B, Pfeiffer K, Heinze S, Homberg U (2014) Integration of polarization and chromatic cues in the insect sky compass. J. comp. Physiol. A 200:575-589

Ely SO, Njagi PGN, Bashir MO, El-Amin Slah El-T, Hassanali A (2011) Diel behavioral activity patterns in adult solitarious desert locust, *Schistocerca gregaria* (Forskål). Psyche(doi:10.1155/2011/459315)

Gebhardt S, Homberg U (2004) Immunocytochemistry of histamine in the brain of the locust *Schistocerca gregaria*. Cell Tissue Res. 317:195-205

Giurfa M, Vorobyev M, Kevan P, Menzel R (1996) Detection of coloured stimuli by honeybees: minimum visual angles and receptor specific contrasts. J. comp. Physiol. A 178:699-709

Gogala M (1967) Die spektrale Empfindlichkeit der Doppelaugen von *Ascalaphus macaronius Scop.* (Neuroptera, Ascalaphidae). Z. vergl. Physiol. 57:232-243

Hamdorf K, Gogala M, Schwemer J (1971) Beschleunigung der Dunkeladaption eines UV-Rezeptors durch sichtbare Strahlung. Z. vergl. Physiol. 75:189-199

Hardie RC (1987) Is histamine a neurotransmitter in insect photoreceptors? J. comp. Physiol. A 161:201-213

Hardie RC (1989) A histamine-activated chloride channel involved in neurotransmission at a photoreceptor synapse. Nature 339:704-706

Hariyama T, Tsukahara Y (1992) Endogenous rhythms in the amount of 11-cis retinal in the compound eye of *Ligia exotica*(Crustacea Isopoda). J. exp. Biol. 167:39-46

Haskell PT, Paskin MWJ, Moorhouse JE (1962) Laboratory observations on factors affecting the movement of hoppers of the desert locust. J. Insect Physiol. 8:53–78

Heinze S (2014) Polarized-light processing in insect brains: recent insights from the desert locust, the monarch butterfly, the cricket and the fruit fly. In Horváth G (ed.) Polarized light and polarization vision in animal sciences. 2nd edition. Springer, Heidelberg, New York, Dordrecht, London

Heinze S, Homberg U (2007) Maplike representation of celestial *E*-vector orientations in the brain of an insect. Science 315:995-997

Heinze S, Reppert SM (2011) Sun compass integration of skylight cues in migratory monarch butterflies. Neuron 69:345-358

von Helversen O, Edrich W (1974) Der Polarisationsempfängerim Bienenauge: ein Ultraviolettrezeptor. J. comp. Physiol. 94:33-47

Henze MJ, Lahart T (2007) Haze, clouds and limited sky visibility: polarotactic orientation of crickets under difficult stimulus conditions. J. exp. Biol. 210:3266-3276

Herzmann D, Labhart T (1989) Spectral sensitivity and absolute threshold of polarization vision in crickets: a behavioral study. J. comp. Physiol A 165:315-319

Homberg U, Paech A (2002) Ultrastructure and orientation of ommatidia in the dorsal rim area of the locust compound eye. Arthropod Struct. Dev. 30:271-280

Homberg U, Würden S (1997) Movement-sensitive, polarization-sensitive, and light-sensitive neurons of the medulla and accessory medulla of the locust, *Schistocerca gregaria*. J. comp. Neurol. 386:329-346

Homberg U, Hofer S, Pfeiffer K, Gebhardt S (2003) Organization and neural connections of the anterior optic tubercle in the brain of the locust, *Schistocerca gregaria*. J. comp. Neurol. 462:415-430

Homberg U, Brandl C, Clynen E, Schoofs L, Veenstra JA (2004) Mas-allatotropin/Lom-AG-myotropin I immunostaining in the brain of the locust, *Schistocerca gregaria*. Cell Tissue Res. 318:439-457

Horridge GA (1969) Unit studies on the retina of dragonflies. Z. vergl. Physiol. 62:1-37

Horridge GA, McLean M (1978) The dorsal eye of the mayfly *Atalophlebia* (Ephemeroptera). Proc. R. Soc. B. 200:137-150

Isono K, Hariyama T, Kito Y, Tsukahara Y (1986) Exogenous and diurnal rhythms of chromophore turnover of visual pigment in the locust analysed by HPLC. Neurosci Res. (Suppl.) 4:S1-S10

Johnsen S, Kelber A, Warrant EJ, Sweeney AM, Widder EA, Lee Jr. RL, Hernández-Andrés J (2006) Crepuscular and nocturnal illumination and its effects on color perception by the nocturnal hawkmoth *Deilephila elpenor*. J. exp. Biol. 209:789-800

Katti C, Kempler K, Porter ML, Legg A, Gonzales R, Garcia-Rivera E, Dugger D, Battelle B-A (2010) Opsin co-expression in *Limulus* photoreceptors: differential regulation by light and a circadian clock. J. exp. Biol. 213:2589-2601

Kennedy JS (1951) The migration of the desert locust (*Schistocerca gregaria* Forsk.). I. Behaviour of swarms. II. A theory of long-range migrations. Phil. Trans. R. Soc. Lond. 235:163-290

Kinoshita M, Pfeiffer K, Homberg U (2007) Spectral properties of identified polarized-light sensitive interneurons in the brain of the desert locust *Schistocerca gregaria*. J. exp. Biol. 210:1350-1361

Kral K, Stelzl M (1998) Daily visual sensitivity pattern in the green lacewing (*Chrysoperla carnea*) (Neuroptera: Chrysopidae). Eur. J. Entomol. 95:327-333

Labhart T (1980) Specialized photoreceptors at the dorsal rim of the honeybee's compound eye: Polarizational and angular sensitivity. J. comp. Physiol. A 141:19-30

Labhart T (1986) The electrophysiology of photoreceptors in different eye regions of the desert ant, *Cataglyphis bicolor*. J. comp. Physiol. A 158:1-7

Labhart T, Petzold J, Helbling H (2001) Spatial integration in polarization-sensitive interneurons of crickets: A survey of evidence, mechanisms and benefits. J. exp. Biol. 204:2423-2430

Lall AB (1993) Nightly increase in visual sensitivity correlated with bioluminescent flashing activity in the firefly *Photinus versicolor* (Coleoptera: Lampyridae). J. exp.Zool. 265:609-612

Luo L, Flanagan JG (2007) Development of continuous and discrete neural maps. Neuron 56:284-300

Lythgoe JN (1979) The ecology of vision. Clarendon Press, Oxford

Mappes M, Homberg U (2004) Behavioral analysis of polarization vision in tethered flying locusts. J. comp. Physiol A 190:61-68

Mazokin-Porshniakov GA (1959) Colorimetric study of vision in dragonflies. Biophysica 4:327-436

Menzel R (1981) Achromatic vision in the honeybee at low light intensities. J. comp. Physiol. A 141:389-393

Nässel DR (1999) Histamine in the brain of insects: a review. Microsc. Res. Tech. 44:121-136

Nowel MS, Shelton PMJ (1981) A Golgi-electron-microscopical study of the structure and development of the lamina ganglionaris of the locust optic lobe. Cell Tissue Res. 216:377-401

Oba Y, Kainuma T (2009) Diel changes in the expression of long wavelength-sensitive and ultraviolet-sensitive opsin genes in the Japanese firefly, *Luciola cruciata*. Gene 436:66-70

Osorio D (1986) Ultraviolet sensitivity and spectral opponency in the locust. J. exp. Biol. 122:193-208

Pfeiffer K, Kinoshita M, Homberg U (2005) Polarization-sensitive and light-sensitive neurons in two parallel pathways passing through the anterior optic tubercle in the locust brain. J. Neurophysiol. 94:3903-3915

Rao YR (1936) The locust incursion of 1935 in North-West India-its significance in the study of the locust problem. Indian J. agr. Sci. 6:1031-1053

Rao YR (1942) Some results of studies on the desert locust (*Schistocerca gregaria* Forsk.). Bull. Entomol. Res. 33:241-265

Rao YR (1960) The desert locust in India. Indian Coun. agric. Res. New Delhi

Roffey J (1963) Observation on night flight in the desert locust *Schistocerca gregaria* (Forskål). Anti-Locust Bulletin38:1-32

Roffey J, Popov G (1968) Environmental and behavioral processes in a desert locust outbreak. Nature 219:446-450

Ruck P (1965) The components of the visual system of a dragonfly. J. gen. Physiol. 49:289-307

Schmeling F, Tegtmeier J, Kinoshita M, Homberg U (2015) Photoreceptor projections and receptive fields in the dorsal rim area and main retina of the locust eye. J. comp. Physiol. A 201:427-440

Schmeling F, Wakakuwa M, Tegtmeier J, Kinoshita M, Bockhorst T, Arikawa K, Homberg U (2014) Opsin expression, physiological characterization and identification of photoreceptor cells in the dorsal rim area and main retina of the desert locust, *Schistocerca gregaria*. J. exp. Biol. 217:3557-3568

Shashar N, Sabbah S, Aharoni N (2005) Migrating locusts can detect polarized reflections to avoid flying over the sea. Biol. Lett. 1:472-475

Shaw SR, Fröhlich A, Meinertzhagen IA (1989) Direct connections between the R7/8 and R1-6 photoreceptor subsystems in the dipteran visual system. Cell Tissue Res. 257:295-302

Showler AT (2002) A summary of control strategies for the desert locust, *Schistocerca gregaria* (Forskål). Agric. Ecosyst. Environ. 90:97-103

Simpson SJ, Sword GA (2008) Locusts. Curr. Biol. 18:R364-R366

Spaethe J, Briscoe AD (2005) Molecular characterization and expression of the UV opsin in bumblebees: three ommatidial subtypes in the retina and a new photoreceptor organ in the lamina. J. exp. Biol. 208:2347-2361

Stalleicken J, Labhart T, Mouritsen H (2006) Physiological characterization of the compound eye in monarch butterflies with focus on the dorsal rim area. J. comp. Physiol. A 192:321-331

Steedman A (1988) Locust Handbook. Overseas Development Natural Resources Institute, London

Symmons PM, Cressman K (2001) Desert locust guidelines 1. Biology and behaviour. Food and Agriculture Organization of the United Nations, Rome

Symmons P (1992) Strategies to combat the desert locust. Crop Protection 11:206-212

Tunstall J, Horridge GA (1967) Electrophysiological investigation of the optics of the locust retina. Z. vergl. Physiol. 55:167-182

Uvarov B (1977) Grasshoppers and locusts. Vol. 2. Centre for overseas pest research, London

van Huis A, Cressman K, Magor JI (2007) Preventing desert locust plagues: optimizing management interventions. Entomol. Exp. Appl.122:191-214

Vitzthum H, Müller M, Homberg U (2002) Neurons of the central complex of the locust *Schistocerca gregaria* are sensitive to polarized light. J. Neurosci. 22:1114-1125

Wakakuwa M, Kurasawa M, Giurfa M, Arikawa K (2005) Spectral heterogeneity of honeybee ommatidia. Naturwissenschaften 92:464-467

Waloff Z (1963) Field studies on solitarious and transient desert locusts in the red sea area. Anti-Locust Bull.40:1–93

Wehner R, Müller M (2006) The significance of direct sunlight and polarized skylight in the ant's celestial system of navigation. Proc. Natl. Acad. Sci. 103:12575-12579

Wendt B, Homberg U (1992) Immunocytochemistry of dopamine in the brain of the locust *Schistocerca gregaria*. J. comp. Neurol. 321:387-403

Wernet MF, Velez MM, Clark DA, Baumann-Klausener F, Brown JR, Klovstad M, Labhart T, Clandinin TR (2012) Genetic dissection reveals two separate retinal substrates for polarization vision in *Drosophila*. Curr. Biol. 22:12-20

Wernitznig S, Rind FC, Pölt P, Zankel A, Pritz E, Kolb D, Bock E, Leitinger G (2014) Synaptic connections of first-stage visual neurons in the locust *Schistocerca gregaria* extend evolution of tetrad synapses back 200 million years. J. comp. Neurol. 523:298-312

White RH, Xu H, Münch TA, Bennett RR, Grable EA (2003) The retina of *Manduca sexta*: rhodopsin expression, the mosaic of green-, blue and UV-sensitive photoreceptors, and regional specialization. J. exp. Biol. 206:3337-3348

Wildermuth H (1998) Dragonflies recognize the water of rendezvous and oviposition sites by horizontally polarized light: a behavioural filed test. Naturwissenschaften 85:297-302

Williams DS (1982) Ommatidial structure in relation to turnover of photoreceptor membrane in the locust. Cell Tissue Res. 225:595-617

Williams DS (1983) Changes of photoreceptor performance associated with the daily turnover of photoreceptor membrane in locusts. J. comp. Physiol. A 150:509-519

Wilson M (1975) Angular sensitivity of light and dark adapted locust retinula cells. J. comp. Physiol. 97:323-328

Yan S, Zhu J, Zhu W, Zhang X, Li Z, Liu X, Zhang Q (2014) The expression of three opsin genes from the compound eye of *Helicoverpa armigera* (Lepidoptera: Noctuidae) is regulated by a circadian clock, light conditions and nutritional status. PLoS ONE 9:e111683

Zolotov V, Frantsevich L Orientation of bees by the polarized light of a limited area of the sky. J. comp. Physiol. 85:25-36

Zufall F, Schmitt M, Menzel R (1989) Spectral and polarized light sensitivity of photoreceptors in the compound eye of the cricket *(Gryllus bimaculatus)*. J. comp. Physiol. A 164:597-608

Erklärung

Ich versichere, dass ich meine Dissertation

Polarized light vision in the eye of the desert locust, *Schistocerca gregaria* - An electrophysiological and histological approach

selbständig, ohne unerlaubte Hilfe angefertigt und mich dabei keiner anderen als der von mir ausdrücklich bezeichneten Quellen und Hilfen bedient habe. Die Dissertation wurde in der jetzigen oder einer ähnlichen Form noch bei keiner anderen Hochschule eingereicht und hat noch keinen sonstigen Prüfungszwecken gedient.

Marburg, 02.07.2015 _____